REPUBLIC OF TURKEY

YILDIZ TECHNICAL UNIVERSITY

GRADUATE SCHOOL OF NATURAL AND APPLIED SCIENCES

EVOLUTIONARY OPTIMIZATION METHODOLOGY FOR RESONANT CONVERTER DESIGN CONSIDERING PHOTOVOLTAIC SYSTEMS

Mohammed Sami Mohammed MOHAMMED

DOCTOR OF PHILOSOPHY THESIS

Department of Electrical and Communication Engineering
Electronic Program

Advisor

Assist, Prof. Dr. Revna ACAR VURAL

REPUBLIC OF TURKEY

YILDIZ TECHNICAL UNIVERSITY

GRADUATE SCHOOL OF NATURAL AND APPLIED SCIENCES

EVOLUTIONARY OPTIMIZATION METHODOLOGY FOR RESONANT CONVERTER DESIGN CONSIDERING PHOTOVOLTAIC SYSTEMS

A thesis submitted by **Mohammed Sami Mohammed MOHAMMED** in partial fulfillment of the requirements for the degree of **DOCTOR OF PHILOSOPHY** is approved by the committee on 29.06.2020 in Department of Electrical and Communication Engineering, Electronic Engineering Program.

Assist. Prof. Dr. Revna ACAR VURAL

Yildiz Technical University

Advisor

Approved By the Examining Committee	
Assist. Prof. Dr. Revna ACAR VURAL, Advisor Yildiz Technical University	
Assoc. Prof. Dr. Burcu ERKMEN, Member Yildiz Technical University	
Assist. Prof. Dr. Derya Ahmet KOCABAŞ, Member Istanbul Technical University	
Prof. Dr. Tülay YILDIRIM, Member	
Yildiz Technical University	
Assoc. Prof. Dr. Aysel ERSOY YILMAZ, Member	
Istanbul University-Cerrahpaşa	

I hereby declare that I have obtained the required legal permissions during thesis preparation and simulation procedures, that I have made the in-text citations and cited the references properly, that I haven't falsified and/or fabricated research data and results of the study and that I have abided by the principles of the scientific research and ethics during my Thesis Study under the title of "EVOLUTIONARY OPTIMIZATION METHODOLOGY FOR RESONANT CONVERTER DESIGN CONSIDERING PHOTOVOLTAIC SYSTEMS" supervised by my supervisor, Assist. Prof. Dr. Revna ACAR VURAL. In the case of a discovery of false statement, I am to acknowledge any legal consequence.

Mohammed Sami Mohammed MOHAMMED
Signature

To my loving parents and my wife.

ACKNOWLEDGEMENTS

I would like to thank my loving parents, my father, mother and my sister whose words of encouragement ring in my ears. My Wife whose never left my side. I dedicate this work my wonderful son Asir for being there for me. All of you have been my best supporters.

Undertaking this PhD has been a truly life-changing experience for me and it would not have been possible to do without the support and guidance that i received from many people. I would like to first say a very big thanks to my supervisor Assist. Prof. Dr. Revna ACAR VURAL for all the support and encouragement she gave me, during both the long years i spent undertaking my field work in Turkey and also the time i spent at Yildiz Technical University. Without her guidance and constant feedback this PhD would not have been achievable.

I also want to send my special thanks to thesis steering committee members Assoc. Prof. Dr. Burcu ERKMEN and Assist. Prof. Dr. Derya Ahmet Kocabaş. I can never thank you enough for all the advices and notes that you done for me. Your constant effort to make me on the straight working way is highly appreciated and unforgettable. Thank you!

Many thanks also to all of electronic department staff in Yildiz Technical University who helped me during my many questions that i requested and who made it possible for me to understand system procedures.

I am also grateful to the encouragements that i have received from College of Education for Pure Science, University of Diyala and special thanks to the computer departments as well.

Mohammed Sami Mohammed MOHAMMED

TABLE OF CONTENTS

L	IST OF SYMBOLS	vii
L	IST OF ABBREVIATIONS	X
L	IST OF FIGURES	xii
L	IST OF TABLES	xv
A	BSTRACT	xvi
Ö	ZET	xviii
1	INTRODUCTION	1
	1.1 Literature Review	1
	1.2 Objectives of the Thesis	18
	1.3 Hypothesis of the Thesis	18
2	OPTIMIZATION TECHNIQUES	19
	2.1 Genetic Algorithm (GA)	19
	2.1.1 GA Operators and Selection Process	19
	2.1.2 GA limitations	20
	2.1.3 GA Problem Domain	20
	2.2 Differential Evolutionary Algorithm (DEA)	22
	2.2.1 DEA Operators and Selection Process	23
	2.2.2 DEA limitation	25
	2.2.3 DEA problem domain	25
	2.3 Non-dominated Sorting Genetic Algorithm (NSGA-II)	26
	2.3.1 NSGA-II Operators and Selection Process	28
	2.3.2 NSGA-II limitation	29
	2.3.3 NSGA-II problem domain	30
	2.4 Finite Element Method (FEM)	31
3	PV- ARRAY SHADED & NON-SHADED CONFIGURATION OPTIMIZATION	35
	3.1 Introduction	35
	3.2 PV Selected Model	37
	3.3 Climate Conditions of Selected Area	38
	3.4 PV Optimization Techniques	42
	3.5 PV Simulation Design Steps	44

	3.6 Simulation Results	45
	3.7 Summary	50
4	SINGLE & THREE PHASE TRANSFORMER STRUCTURE DESIGN	51
	4.1 Introduction	51
	4.2 Single & Three Phase Transformer Model	54
	4.3 Optimization Tools	55
	4.3.1 Genetic Algorithm	56
	4.3.2 Differential Evolution Algorithm	57
	4.3.3 Non-Dominated Sorting Genetic Algorithm	58
	4.3.4 Finit Element Method	60
	4.4 Proposed Mathematical Combinational Model	60
	4.5 Experimental Results	62
	4.5.1 Single Phase Transformer Optimization Design using GA and NSGA with FEM	
	4.5.2 Three Phase Transformer Optimization Design using GA, DEA and NSGA-II with FEM	68
	4.5.3 Determination of EA Own Parameters	74
	4.5.4 Calculation of Total Efficiency and Cost	75
	4.6 Summary	78
5	SERIES RESONANT CONVERTER AUTOMATED DESIGN	79
	5.1 Introduction	79
	5.2 PV Module	84
	5.3 Multi-objective Optimization of Overall Loss and Output Voltage Variation	n 84
	5.4 Equivalent SRC Circuit	87
	5.5 Operating Modes	89
	5.6 Calculation of SRC Overall Losses	90
	5.7 Calculation of Output Voltage Variation	90
	5.8 Cost Function and Efficiency	91
	5.9 Simulation and Optimization Results	91
	5.10 Summary	.105
6	RESULTS AND DISCUSSION	107
R	EFERENCES	113
P	IIRLICATIONS FROM THE THESIS	129

LIST OF SYMBOLS

 r_{eq} Apparent equivalent resistor of SRC equivalent circuit, (Ω) .

 R'_{load} Apparent load resistor of SRC equivalent circuit, (Ω).

 V'_0 Apparent output voltage of SRC equivalent circuit, (V).

 V_{req} Apparent voltage of SRC equivalent resistor, (V).

η DC/DC converter efficiency.

F DEA controlling number.

v DEA initialized vector.

U DEA new generation vectors.

 T_{dt} Dead time.

P_{D,Cond} Diode conduction loss power, (W).

V_f Diode forward voltage, (V).

D Duty cycle.

 E_L Eddy current losses, (W/m³).

K_e,k_h Eddy current/ hysteresis constant.

G Evolutionary algorithm generation number.

C₁-C₉ Flux density evaluating coefficients.

 H_L Hysteresis losses, (W/m³).

i/j Individuals/new individuals sets.

I_{av} MOSFET average current, (A).

V_{DS} MOSFET drain-source voltage, (V).

V_{SW} MOSFET gate voltage, (V).

P_{MOSFET,Cond} MOSFET-conduction loss power, (W).

 R_{ds} MOSFET-drain-Source resistance, (Ω) .

P_{MOSFET,Switch} MOSFET-switching loss power, (W).

A₁,A₂ No load/load cost (TOC) evaluating coefficients.

 F_1,F_2 No-load(NLL)/load(LL) loss objective functions.

K₁,K₂ No-load/load objective function coefficients.

R No-load/load ratio.

M Number of objective function/functions.

 S_1,S_2 Objective function constraint ratio.

 O_L Ohmic losses, (W/m^3) .

VoutActual Output SRC actual voltage, (V).

VoutDesired Output SRC desired voltage, (V).

V_{out_var} Output voltage variation, (V).

 R_{pv} Photovoltaic cable resistor, (Ω) .

 N_{pop} Population number for EAs.

f_r Resonant frequency of SRC, (Hz).

C_r Resonant tank capacitor, (F).

 I_{Lr} Resonant tank current, (A).

L_r Resonant tank inductor, (H).

f_S Selected switching frequency, (Hz).

N Single phase transformer turn ratio.

V_{Cr} SRC capacitor voltage, (V).

 R_{load} SRC Load resistor, (Ω) .

 C_0 SRC output filter capacitor, (F).

 V_0 SRC output voltage, (V).

P_{Overall Losses} SRC-overall output losses power, (W).

F_X Switching frequency to resonant frequency ratio.

V_{ab} Switching stage voltage, (V).

 T_{SWoff} Switching turn off time, (s).

 T_{SWon} Switching turn on time, (s).

X₇ Transformer bobbin's depth, (mm).

X₆ Transformer bobbin's height, (mm).

 X_8 Transformer core area, (mm²).

 X_1 Transformer core thickness, (mm).

 η_T Transformer efficiency.

B Transformer flux density, (T).

P_{Tin} Transformer input power, (W).

 V_{Tin} Transformer input voltage (V).

I_{Tout} Transformer load current, (A).

f Transformer operating frequency, (Hz).

P_{Tout} Transformer output power, (W).

V_{Tout} Transformer output voltage (V).

X₄ Transformer primary Conductor area, (mm²).

X₂ Transformer primary turn number.

X₅ Transformer secondary Conductor area, (mm²).

I_{Sec} Transformer secondary current, (A).

X₃ Transformer secondary turn number.

 R_W Transformer winding resistance, (Ω) .

X₉ Transformer window's width, (mm).

LIST OF ABBREVIATIONS

ABC Artificial Bee Colony algorithm

ANN Artificial Neural Network

BOS Balanced of System

BTS Base Transceiver Station

CD Combined Dispatch

DEA Differential Evolution Algorithm

DT Decision Tree

EAs Evolutionary Algorithms

ECTP Eddy Current non-destructive Testing Probe

EMI Electromagnetic Interferences

EMU Electrical Multiple Units

FEM Finite Element Method

FEMM Finite Element Method Magnetic

GA Genetic Algorithm

HFT High Frequency Transformer

ICS Interference Cancellation System

LF Load Following

LL Load Loss

MIC Module Integrated Converter

MO Multi Objective

MPPT Maximum Power Point Tracking

NLL No-Load Loss

NSGA-II Non-dominated Sorting Genetic Algorithm

PAES Pareto-Archived Evolutionary Strategy

PEV Plug-in-Electric Vehicle

PSC Partial Shadow Condition

PSO Particle Swarm Optimization

PTO Power Take Off

PV Photovoltaic

PWM Pulse Width Modulation

RF Radio Frequency

RMSE Root Mean Square Error

SA Simulated Annealing

SPEA Strength Pareto Evolutionary Algorithm

SRC Series Resonant Converter

SRHC Series Resonant Harmonic Compensator

TEG Thermoelectric Generators

TOC Total Owning Cost

ZCS Zero Current Switching

ZVS Zero Voltage Switching

LIST OF FIGURES

Figure 1.1	Magnetization curves for soft magnetic materials.	3
Figure 1.2	Dc-Dc converter main structures.	6
Figure 1.3	$lem:multiple switching circuit design for megawatt wind turbine system. \ 1$	4
Figure 2.1	Differential evolutionary algorithm (DEA) basic steps for optimization a specific problem	2
Figure 2.2	Differential mutation applied on three selected vectors	3
Figure 2.3	Pseudo code for the classical DEA algorithm2	4
Figure 2.4	The main algorithm of NSGA-II procedure2	7
Figure 2.5	Low and high sensitive solutions using NSGA-II for minimizing two cost functions	1
Figure 2.6	Piezoelectric transformer (a) structure design and (b) equivalent circuit. 3	2
Figure 2.7	Flux density pattern using FEM for two cases: (a) one short circuit winding and (b) both short circuit windings	
Figure 3.1	Annually temperature range of the selected area (a)temperature range and (b) dry bulb with humidity relation	
Figure 3.2	Monthly diurnal average of the selected area4	0
Figure 3.3	Wind wheel chart using climate consultant v6.0 for Turkey/Istanbul 4	0
Figure 3.4	Sun shading chart between east and west of the selected area4	1
Figure 3.5	Monthly 3D temperature chart according to days light4	1
Figure 3.6	Psychometric data using climate consultant v6.0 for Turkey/Istanbul4	2
Figure 3.7	Simulation area for PV-module design (Yildiz Technical University) 4	2
Figure 3.8	Non-dominated sorting genetic algorithm NSGA-II working principles 4	3
Figure 3.9	PV panel's dimension and related angle for NSGA-II design4	3
Figure 3.10	Flow chart of PV simulation design using two program with applying weather conditions4	5
Figure 3.11	Building design area with 6 array of selected PV module (a) top view and (b) side view4	6
Figure 3.12	PV module simulation results for TSM-200PC05-6 array connected (a) monthly production of the module designed and (b) system main losses sources	8
Figure 3.13	Simulated building using design builder software in 3 dimensions4	9
Figure 3.14	Solar array on the roof of the selected building 4	g

Figure 4.1	Commercial prototype transformers architecture of (a) single phase transformer (b) three phase transformer	4
Figure 4.2	Flux density distributions of FEM calculations of single phase transformer	4
Figure 4.3	Flux density distributions of FEM calculations of three phase transformer	
Figure 4.4	Detailed flow chart of GA+FEM optimization model57	7
Figure 4.5	Detailed flow chart of DEA+FEM optimization model58	3
Figure 4.6	Detailed flow chart of NSGA-II+FEM optimization Model59)
Figure 4.7	Computational results of GA for single phase transformer	3
Figure 4.8	NSGA-II based results of NLL relationship with specific parameters of single phase transformer	
Figure 4.9	NSGA-II based results of LL relationship with specific parameters of single phase transformer	4
Figure 4.10	Results of (a) no-load-losses(NLL) and (b) load-losses(LL) box-and-whisked plot for GA and NSGA-II of single phase transformer design	
Figure 4.11	Results of total loss by using box-and-whisker plot for GA and NSGA-II of single phase transformer design	7
Figure 4.12	Flux density of GA for the FEM calculations6	7
Figure 4.13	Flux density of NSGA-II for the FEM calculations6	7
Figure 4.14	Computational results of GA for three phase transformer	3
Figure 4.15	EA based results of NLL relationship with some specific parameters of three phase transformer (a) DEA and (b) NSGA-II60	
Figure 4.16	EA based results of LL relationship with specific parameters of three phase transformer (a) DEA and (b) NSGA-II70	
Figure 4.17	NLL and LL relationship using NSGA-II for the last iteration7	1
Figure 4.18	Box-and-whisker plots of (a) no-load-losses (NLL) And (b) load-losses (LL) using GA, DEA and NSGA-II73	
Figure 4.19	Flux density calculation with FEM for GA based design73	3
Figure 4.20	Flux density calculation with FEM for DEA based design73	3
Figure 4.21	Flux density calculation with FEM for NSGA-II based design73	3
Figure 4.22	(a) Total efficiency and (b) cost for the prototype and EA based models of single phase transformer under design	5
Figure 4.23	(a) Total efficiency and (b) cost for the prototype and EA based models of three phase transformer under design	7
Figure 5.1	PV system configuration84	4

Figure 5.2	Multi-objective optimization methodology for SRC design	86
Figure 5.3	SRC loss analysis model	87
Figure 5.4	Series resonant converter topology	88
Figure 5.5	Series resonant converter equivalent circuit	89
Figure 5.6	Waveforms of resonant inductor current and capacitor voltage	89
Figure 5.7	Diode conduction loss variation according to SRC design parameter variation	93
Figure 5.8	MOSFET conduction loss variation according to SRC design parameter variation	93
Figure 5.9	MOSFET switching loss variation according to SRC design parameter variation	94
Figure 5.10	Efficiency of EA based designs at varying input voltages	98
Figure 5.11	Single phase transformer flux density calculation using FEM method1	02
Figure 5.12	The efficiency variation of SRC versus load current for input voltages of 100V, 170V and 240V1	.03
Figure 5.13	Vab, Vout, ILr @ Vin = 240 V for full load condition1	04
Figure 5.14	Vab, Vout, ILr @ Vin = 100 V for full load condition1	04
Figure 5.15	ZVS condition for NSGA-II based SRC design @ Vin = 240V	04

LIST OF TABLES

Table 1.1	Typical comparative data of soft magnetic materials2
Table 3.1	Electrical & mechanical characteristics of the PV-TSM-PC0537
Table 3.2	PV-TSM-PC05 calculated total used area and current-voltage/temperature coefficient
Table 3.3	Helioscope applied parameters for PV simulation after NSGA-II optimization 46
Table 3.4	The summary of the annually building performances using NSGA-II47
Table 3.5	The summary of the annual building utility performance using design builder for 8760 hours on 2019-02-05 at 02:58:13 after optimization
Table 4.1	Specifications of single and three phase transformer55
Table 4.2	Design parameter and loss calculations of single phase transformer65
Table 4.3	Total loss values for varying NSGA-II calculated design parameters of single phase transformer
Table 4.4	EA based design parameter estimations and loss calculations71
Table 4.5	Optimized design parameter and total loss values obtained with NSGA-II 72
Table 4.6	Own parameter values of EA methods for single phase transformer design .74
Table 4.7	Own parameter values of EA methods for three phase transformer design $\dots 75$
Table 4.8	Total efficiency and total cost calculated for single phase transformer under design
Table 4.9	Total efficiency and total cost calculated for three phase transformer under design
Table 5.1	Optimal own parameter values of EA methods91
Table 5.2	Optimization results for GA based method94
Table 5.3	Optimization results for DEA based method95
Table 5.4	Optimization results for NSGA-II based method96
Table 5.5	Transformer NLL&LL and flux density evaluation for 5P and 9P models 99
Table 5.6	Output voltage regulation using EA techniques for 25 runs100
Table 5.7	SRC design parameters optimized with NSGA-II101
Table 5.8	Comparison of sensitivity to transformer design parameters between 5P-model and 9P-model using NSGA-II102

EVOLUTIONARY OPTIMIZATION METHODOLOGY FOR RESONANT CONVERTER DESIGN CONSIDERING PHOTOVOLTAIC SYSTEMS

Mohammed Sami Mohammed MOHAMMED

Department of Electrical and Communication Engineering

Doctor of Philosophy Thesis

Advisor: Assist. Prof. Dr. Revna ACAR VURAL

Series Resonant Converter (SRC) design parameters are calculated by evaluating circuit characteristics of resonant tank circuit, transformer and rectifier circuit that constructs SRC. Evaluation of these characteristics helps to investigate various effects of parameters on the overall system performance and optimizes converter parts to be more efficient and compatable with each other. Transformer is the main isolation part of SRC and optimal design of this part leads to reduce transformer losses as well as cost and circuit size. In order to provide more accurate design, 5-parameter and 9-parameter transformer models are suggested and compared to minimize transformer no-load loss (NLL) and load loss (LL). Moreover, reduction of transformer cost and size are also studied as another objective function by providing better circuit performance. Optimization is carried out utilizing three evolutionary algorithms (EAs): Genetic Algorithm, Differential Evolutionary Algorithm and Nondominated Sorting Genetic Algorithm for transformer loss minimization according the suggested two models. Flux density is calculated using Finite Element Method (FEM) after transformer design parameters are optimized. Total owning cost is used as a measurement tool by taking into account of no-load and load loss values.

SRC is designed for photovoltaic (PV) system which is a renewable energy system. First, PV array is constructed for 6 modules in series connection taking into account of weather

conditions. Array characteristics are collected according to selected region (Yildiz Technichal University – Dept. of Electronics and Communication Building Roof) and according to non shaded or shaded configuration functions. Annual generated power and output voltage variation are gathered from this design to provide better performance when designing a converter topology. Azimuth angle, tilt angle, distances between two panels and tracking types are the main optimization parameters for photovoltaic data collection process. Helioscope and Design Builder program are used to simulate the real photovoltaic design module.

Keywords: Series resonant converter, zero voltage switching, differential evolutionary algorithm, non-dominated sorting genetic algorithm, photovoltaic system

REZONANS DÖNÜŞTÜRÜCÜ TASARIMI İÇİN FOTOVOLTAİK SİSTEMLER DİKKATE ALINARAK EVRİMSEL OPTİMİZASYON METODOLOJİSİ

Mohammed Sami Mohammed MOHAMMED

Elektronik Ve Haberleşme Mühendisliği

Doktora Tezi

Danışman: Dr. Öğretim Üyesi Revna ACAR VURAL

Seri Rezonans Dönüştürücü (SRC) tasarım parametreleri, SRC'yi oluşturan rezonans tank devresi, transformatör ve doğrultucu devrenin devre karakteristiklerini değerlendirilerek hesaplanır. Bu özelliklerin değerlendirilmesi, parametrelerin genel sistem performansı üzerindeki çeşitli etkilerinin araştırılmasına yardımcı olur ve dönüştürücü parçalarını daha verimli ve birbirleriyle daha uyumlu olacak şekilde optimize eder. Transformatör, SRC'nin ana izolasyon kısmıdır ve bu parçanın optimum tasarımı, transformatör kayıplarının yanı sıra maliyet ve devre boyutunun azaltılmasını da sağlar. Tasarım doğruluğunu arttırmak için, 5 parametreli ve 9 parametreli transformatör modelleri önerilmiştir ve transformatör yüksüz kaybını (NLL) ve yük kaybını (LL) en aza indirmek için bu modellerin performansları karşılaştırılmıştır. Ayrıca, trafo maliyetinin ve büyüklüğünün azaltılması başka bir amaç fonksiyonu olarak çalışılarak daha iyi bir devre performansı sağlanmıştır. Optimizasyon üç evrimsel algoritma (EA) kullanılarak gerçekleştirilmiştir: Önerilen iki modele göre transformatör kaybının en aza indirilmesi için Genetik Algoritma (GA), Diferansiyel Evrimsel Algoritma (DEA) ve Hakim Olmayan Sıralama Genetik Algoritma-II (NSGA-II). Tek ve üç

fazlı transformatörler için tasarım parametrelerinin NLL ve LL üzerindeki etkilerini araştırmak için de optimizasyon süreci uygulanır. Akı yoğunluğu, transformatör tasarım parametreleri optimize edildikten sonra Sonlu Elemanlar Yöntemi (FEM) kullanılarak hesaplanır. Toplam edinim maliyeti, yüksüz kayıp ve yük kaybı değerlerinin dikkate alındığı bir ölçüm aracı olarak kullanılır.

SRC yenilenebilir bir enerji sistemi olan fotovoltaik (PV) sistem için tasarlanmıştır. İlk olarak, PV dizisi, hava koşulları dikkate alınarak seri bağlantılı 6 modül için inşa edilmiştir. Dizi karakteristikleri seçilen bölgeye (Yıldız Teknik Üniversitesi - Elektronik ve Haberleşme Binası Çatı Bölümü) ve gölgesiz veya gölgeli konfigürasyon fonksiyonlarına göre toplanır. Dönüştürücü topolojisi tasarlanırken daha iyi performans sağlamak için yıllık üretilen güç ve çıkış gerilimi değişimi bu tasarımdan elde edilir. Azimut açısı, eğim açısı, iki panel arasındaki mesafeler ve izleme türleri fotovoltaik veri toplama işlemi için ana optimizasyon parametreleridir. Helioscope ve Design Builder programı, seçilen bölgenin gerçek fotovoltaik tasarım modülünü simüle etmek için kullanılır.

Anahtarlar: Seri rezonans dönüştürücü, sıfır gerilim anahtarlama, diferansiyel evrimsel algoritma, hakim olmayan sıralama genetik algoritma, fotovoltaik sistemler

1 INTRODUCTION

1.1 Literature Review

The abilities of power electronic systems are dominated by different design parameter selection of electronic devices. Restrictions and characteristics of design process are the key of conversion effectiveness. Power handling capacity of converters represents a critical feature in such design. On the other hand, power dissipation occurs for different reasons such as switching and conducting losses has a significant impact on the efficiency of the circuit and therefore has to be minimized. Switching between different operations modes effects the dissipated power of DC-DC converters. Converter components like inductors and capacitors can be smaller and lighter when working under high switching frequencies. However, high switching frequencies increase the electromagnetic interference (EMI) and lead to significant turn on and turn off losses during switching transients. Searching of different power converter systems that able to work at higher frequencies while maintaining reduced losses, minimized EMI by working under zero voltage switching (ZVS) conditions is an active research area.

Calculation of DC-DC converter characteristics assist to investigate different parameters affection on various converter parts to be more effective and compatible with each other. They are calculated by evaluating each specification such as resonant inverter gain performance, transformer overall loss and switching conditions. The most effective method to design DC-DC converter circuits that fulfill the requirements under a set of limitations has been clarified through using solid models. The challenges of a determined power for home or small market where single phase voltage is accessible are getting complicated. On the other hand, three phase voltage is also available by factories and facilities. Therefore converters should be designed according to grid conditions. Transformer design plays a significant role in power converter design. Transformer materials are not the only affection features on the overall system

performance. Transformer dimensions and winding values are also considerable on transformer quality as well as overall power electronic system performances [1]. Searching of materials to build transformer core with high induction and low switching losses ought to be clarified correctly. Ferrite magnetic core is still the popular selection due to wide range of operating frequency. Two main levels of core are employed for transformer: first, level is built from iron and mixed with a specific amount of different materials such as Nickel (Ni), Cobalt (Co) and Silicon (Si). While the second level is built from iron with a magnetic element such as Zinc due to its high resistivity privilege. Table 1.1 shows comparison between different magnetic materials utilized for transformer design [2].

Table 1.1 Typical comparative data of soft magnetic materials [2]

Parameters	Steel iron		alloys	Ferrite		
	silicon	powder	carbonyl	anoys	Mn-Zn	Ni-Zn
Frequency range, Hz	20-1k	400-10k	50k-1M	40-70k	400- 250k	200k-10M
Temperature range, °C	-55 to 300	-55 to 125	-55 to 105	-55 to 200	-30 to 105	-55 to 250
Initial permeability	500	90	35	160	2700	100
flux density @ 25°C, T	1.75	0.86	0.86	0.63	0.47	0.24
Remanence, T	1.2	0.2	0.001	0.02	0.2	0.12
Intrinsic mmf strength, A/m	440	2560	9120	1448	40	350
Resistivity, Ωcm	0.1	-	-	-	100	10 ⁵ - 10 ⁶
Curie temperature, °C	300	200	150	500	200	450

Ferrite core type can be considered as the appropriate selection based on relevance between permeability and flux density as shown in Table 1.1. However, this type is suffering from high eddy current and hysteresis losses. Figure 1.1 shows relations between magnetic force and flux density according to different type of transformer materials [2]. It is also shown that, increment in flux density means more transferring voltage per each transformer turn.

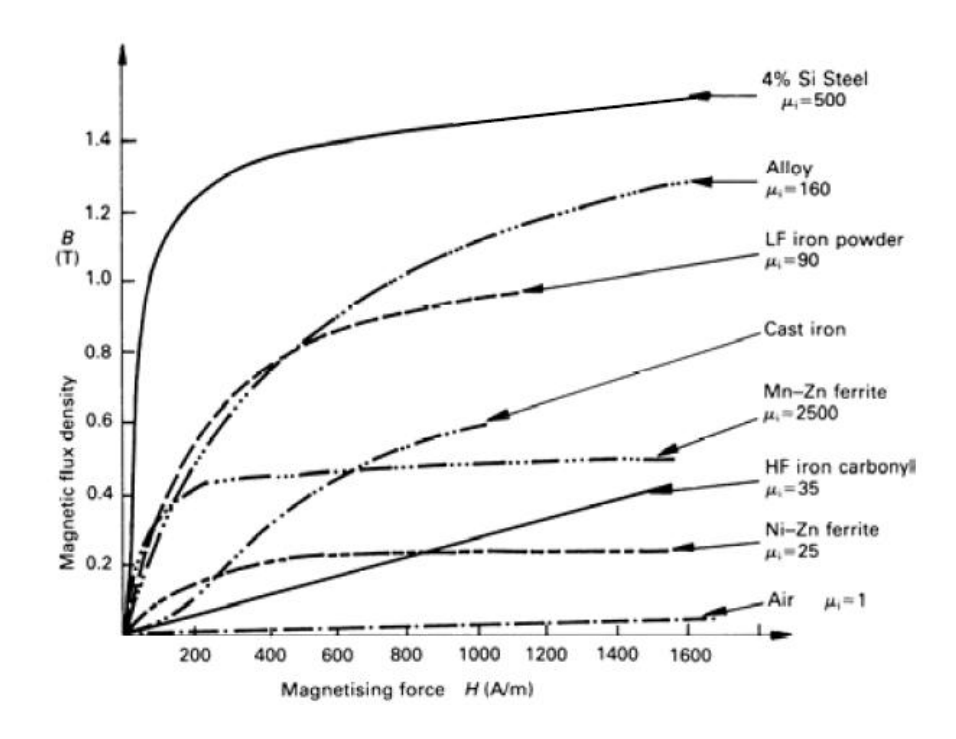


Figure 1.1 Magnetisation curves for soft magnetic materials [2]

A converter design is proposed based on rated power, resonant tank inverter stored power and inductor value as explained in [3]. The goal was to find an optimal value of inductance according to a specified load condition and switching frequency of 70 kHz. This model was tested for a wind shield load with 12V and 24 V as input and output voltage, respectively. Magnetic components minimization such as inductors and transformers with a fine balance between delivered power and overall design performances has taken more interest recently. In [4], a step down transformer of piezoelectric type is intended to work under DC-DC converter specific conditions. This type of transformer has ability to dissipate thermal energy and provides low output impedance due to its multi-layer ring structure. It also operates under high switching frequency for low power applications. Using wide air gap structure to design a low coupling contactless transformer type is presented in [5]. The main objectives for this study is to reduce transformer size, minimize overall system cost and provide higher

efficiency compared to prototype design. Volume reduction, weight and losses minimization of transformer which is embedded in resonant converter are significant issues for modern aircraft design. Operating under high frequency zone is an important factor to minimize inductor component size with a noticeable reduction in magnetic integration. In [6], various topologies are introduced for such applications. Full bridge phase shifted topology is reported to be suffering from drawback points such as center tapped complexity and larger size than regular transformer. Full bridge topology is also prone to hard switching and it is similar to dual active bridge topology. For that reason, Series Resonant Converter (SRC) provides the best solution to this application. Series connection of transformer in the primary side with a parallel connection in the secondary side is presented for this study to keep similar conversion ratio. Connection structure is also introduced in some studies for a specific application of DC-DC converters. Three phase-delta connection is proposed with a SRC topology for capacitor charger application in [7]. Transformer in this study has been designed with two rectifier circuits to be compatible with different charging voltage values. Transformer has been investigated for different DC-DC converter application according to handling and dissipated power. Two photovoltaic (PV) module topologies are considered for LLC resonant converter design as in [8] with Multi Power Point Tracking (MPPT) system. Serial and cascaded connection with insulated DC-DC converter is compared according to transformer design performances. Searching for reliable transformer type made authors select planner type by considering winding and core losses evaluation due to high frequency applications. High frequency is effective on both weight and overall design performances; due to this reason two different transformer designs are proposed for two PV connection types. In this study, authors clarified that transformer turning number ratio affected transformer loss distribution. It means that for higher secondary turning number, coil losses will be increased compared to core losses. Moreover, this relation is quite different when primary and secondary turning numbers are equal. It also displayed that coil losses can be reduced by reshaping core structure, but core reshaping process can cause a weight increment as explained. Researchers provided a size or weight minimization by using different algorithms; most of these algorithms were by trial and error process which requires high computation time. In addition,

transformer that implemented by industrials and companies has limited applications or operating frequency. Also, it is a hard task to discover a compatible transformer for a specific application of DC-DC converter. Due to all of these reasons, this study has focused on minimization in transformer losses types and cost while optimizing transformer dimensions. This design is also guided according to a specified application to fit system requirements without additional cost. Single and three phase transformers are designed according to 5 and 9 parametric (5P, 9P) models using evolutionary algorithms (EAs). These two models are applied according to core type-single phase transformer and shell type-three phase transformer at high operating frequency.

Improvement in DC-DC converter performance is not only related to transformer reshaping but is also carried out with optimal parameter combinations of different resonant converter topologies. In [9], LLC topology is combined with an additional capacitor connected to the output. The proposed model keeps efficiency with wide input voltage range as (100 - 400 V) and power of 240W. LLC is able to work at high input voltage while, LLC + C is capable to work at low input voltage. Comparisons between prototype and proposed model showed that, the proposed model exceeded prototype at every checked point. In addition, ZVS and Zero Current Switching (ZCS) provided a soft switching process for the switching circuit at the primary side and the rectifier circuit at the secondary side, respectively. In general, a low profile application such as notebook adaptors requires a minimization in size by collecting both high performances and safety regulations with low design cost. In order to reduce switching losses and EMI, converters generally utilize an auxiliary circuit. In [10], researchers suggested to merge an auxiliary circuit with some specified elements to LLC converter. The main objective of this work was to reduce both voltage and current stress. Some parameters were clarified like optimal inductance ratio of LLC resonant converter and the maximum delivered voltage when full load is applied. In addition, switching frequency variation according to output voltage requirements is verified to achieve ZVS condition. Moreover, maximum MOSFET current under full load case are calculated to fulfill the design requirements. Output voltage is adjustable at its maximum value when input voltage is low under no load case. In the other hand, minimum value of output voltage is acquired under no load and load cases. Conventional LLC converter showed better results at minimum output

current which is improved by LLC-LC when output current value is increased. The high value of resonant inductor was the main reason of increasing performances of LLC at low output current. Transformer copper and core losses are mainly increased by harmonic signal due to non-sinusoidal primary and secondary current such in PWM converters. In SRC, a sinusoidal signal at each transformer side is achieved easily at full load condition especially when working near to resonant frequency region. Auxiliary circuit is added to compensate the output voltage or to reduce the stress condition in current and voltage which occurred in both sides. In [11], an auxiliary circuit was proposed for a SRC to compensate hold up time when it's required to get a higher gain and to improve converter performances. Multi output application systems can be adapted for resonant converter topologies with an auxiliary circuit which connected in the secondary side with symmetrical structures of resonant topology. In [12], dual rectifier circuit are connected for SRC as full and half wave rectifier topology with a different structure for low and medium output power applications. Matching network in DC-DC converter system can be connected with transformer to reduce the undesirable primary leakage inductance which ring with the secondary capacitance value as explained in [13]. This issue increases the switching losses at high switching frequency, especially if operating under the same of resonant frequency value (where gain = 1). Matching network can absorb the transformer primary leakage inductance and secondary capacitance effect which in turn eliminates the switching losses. In [14], active double rectifier is suggested for parallel resonant converter design at the secondary side, which doubles the output voltage and minimize the transformer turning ratio. To achieve ZVS for this topology, leakage inductance and capacitance of primary transformer side are considered. The main four DC-DC converter parts are shown in Figure 1.2 [14].

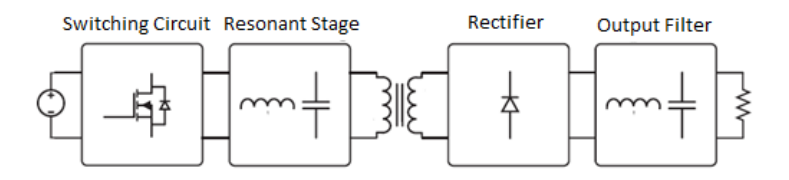


Figure 1.2 DC-DC converter main structures [14]

Multiple converters are connected also either in primary or secondary side or even both sides as design solutions to some issues. A high power application where the target is to overcome SRC high stress current by connecting two parallel converters with load is investigated in [15]. Output voltage is regulated by the meaning of switching frequency changing while maintaining ZCS. Proposed model offered 12 modes of operations according to the two parallel converter designs for 960W system application. Two power converters might be connected to the primary and secondary side of transformer as main and auxiliary converters, respectively as in [16]. Auxiliary converters are proposed to add its output voltage to the main converter to compensate the changing in output load voltage. In this paper, five design parameters are optimized according to system specifications as minimization of output power, input and output voltage. Resonant design parameters like inductance value are determined according to required power minimization level which keeps system working in a stable region. Resonant capacitor was calculated functionally, but resonant inductance is related to maximum resonant capacitor voltage which has to be smaller than input minimum voltage.

Shift operation between two converters, A at the primary side is working alternatively with converter B at the secondary side was proposed in many studies for various types of power conversion applications. Bidirectional LLC resonant converter was studied in [17] to be applied for battery charging process. In this work authors tried to fit the overall system requirements which ought to be compatible for different charging operations. Such a design is able to adapt different voltage levels to be controlled for various applications like Thermoelectric Generators (TEG) and PV. Matrix connection of bidirectional SRC is derived also for plug-in electric vehicle (PEV) battery charging process in [18]. This design consists of three phase line connected to 3x1 matrices SRC resonant converter with a high frequency transformer and rectifying circuit. Three phase voltage lines are connected to these matrices by using LC filter. Magnetizing inductor of high frequency transformer is not affected by the resonance process but has a significant impact on transformer primary voltage. Trying to transfer more power to the secondary side, DC-DC converter is connected with three parallel secondary half bridge sides which in turns connected to the same load as suggested in [19]. This sharing parallelism process reduced number of MOSFETs and number of design

parameters by sharing only a single switching circuit rather than three. This can also lower the stress occurred in current for each power devices by supplying one-third of overall power to the required load for medium power applications. For some applications, pair of multiple resonant tanks can be utilized by arranging transformer in different sides such in [20]. Selection of resonant topology needs some considerations such as: transformer parasitic elements identifying that can be occurred at high operating frequency and transformer losses. LLC and CLL are selected for this study as an equivalent topology that can substitute between each other. In LLC or CLL, resonant inductor can be intentionally added by implementing an air gap in transformer magnetic core part. In LLC, design parameters are all located at the primary side which makes transformer connect directly to the rectifier circuit and only transfers the active power. While in CLL topology, design parameters are located at both transformer sides which causes both active and reactive power to be transferred to the load. Reactive power occurs because of secondary inductance and for this reason SRC is usually preferred for low power applications that has a significant loss dependency. Hybrid configurations of series and parallel converters are equivalent to LCC topology. In high voltage applications, transformer is usually suffering from leakage inductance and reflected capacitance from the secondary side. Reflected capacitance is due to high secondary turning ratio compared to primary value. While, leakage inductance is increased mainly for a wide gap transformer type. Adding parameters or circuits to enhance DC-DC converters have some issues like: high cost, high power consumption due to additional elements, current and voltage stress increments and thermal issues. Designing DC-DC converter without additional components is a rough task and requires accurate design and calculations.

Wide voltage range applications requires a DC-DC converter design having features like hold up operation and/or wide range of input or output voltage. Telecommunication systems require hold up process for providing reliable and continues supplying power. In these types of applications, resonant converter needs to keep output voltage near to the desired value and should fit any input voltage changing state, so equipment is insured to work properly and efficiently. Renewable energy sources like PV are usually focused on constant output voltage for wide input voltage range. For this reason,

designing a converter for such applications requires not only the analysis of operation modes but also all input voltage range regarding the converter performance. The same scenario is applied for wide output voltage range with a fixed input voltage such in battery charging systems. However, designing resonant converters for one of the scenarios mentioned above requires the increment in switching frequency range to overcome any sudden voltage changes in the different sides of transformer. Moreover, widening the switching frequency leads a restriction in ZVS and ZCS region, reshaping core size of transformer according to lowest value of switching frequency and involving more in light load condition problem. To solve all of these issues, studies illustrated different enhancements to conventional resonant converter topologies for either fitting range requirements or performance evaluations such in [21-23]. A wide output voltage is often used for LED driver as in [24]. SRC design optimization is proposed to cover wide output voltage with high quality for 140W power requirement. Resonant frequency, resonant tank parameters, transformer turning ratio and the resonant to magnetizing inductance ratio are the design parameters to be optimized in [24]. MOSFET switching loses; MOSFET and diode conduction losses constitute the cost function to be minimized with availability of ZVS condition. Trade-off between resonant tank values and core losses are analyzed because smaller resonant capacitor compared to high resonant inductor assists to narrow the range of switching frequency but to increase transformer losses as well. Another design in [25] is also introduced to optimize LLC resonant converter for wide output range. Maximum output voltage in addition to high load and minimum switching frequency causes a high resonant capacitor voltage and increase stress on converter parameters. Ratio between switching frequency to resonant frequency ought to be close to unity, so component stress and switching range can be reduced. For improving light load condition, small value of additional capacitor is connected in parallel with MOSFET to assist discharging of MOSFET gate-source capacitor and turn it off before rising of drain-source voltage again. In [26], SRC was selected for wide input voltage range application at 300 W. Wide input voltage become a worse case for different types of converters at light load state, which forces resonant converter to increase switching frequency and leads to increase the range of operating switching frequency.

Front-end converters are usually designed for PV module array to supply DC voltage to different bus lines. These types of converters require a good isolation for wide input voltage range with a high gain value. In [27], a hybrid model is suggested for wide input voltage range to be operated under multiple modes such as boost and buck converter for both low and high input voltages, respectively. A step down isolated converter is proposed for PEV in [28]. Comparative study between three DC-DC converter topologies (SRC, buck and delay time LLC) is presented in terms of efficiency and power density enhancement. Buck topology among these types, provided the highest performance when input voltage is increased. This reduces root mean square value of resonant current as well as conduction and transformer losses. Dual bridge configuration can also be introduced to adapt wide range of input voltage, reduce the conduction losses and achieve soft switching process for the overall conversion as in [29]. Each switching cycle contains both full and half bridge modes, which provides benefits to regulate the output voltage for a bidirectional DC-DC converter. Other studies related to transformer sizing and reshaping for different topologies are more analyzed in [30]. In the other hand, wide output applications is sort of difficult to overcome converter operation near to resonant frequency region. In [31], SRC topology is introduced for this type of application based on voltage quadruple rectifier. It is achieved by modulating duty cycle to overcome the wide output voltage range and working under the same resonant frequency which is preferred to decrease the circulating energy and minimize the conduction loss. According to input and output voltage levels, four configurations of SRC operation modes are illustrated for wide range applications in [32]. A dual structure of primary side bridge with a configurable full bridge at the secondary side is proposed. The proposed model contains a low voltage switching circuit connected in the middle point between normal SRC switching circuit and parallel capacitors. One diode at the secondary side is replaced with a switching device working under low frequency. This can provide four circuit configurations as mentioned for this study.

Improving optimization methods to increase resonant converter performance is explored in recent studies. In [33], researchers suggested an improvement selection based on operation modes and overall transfer function. Resonant and magnetizing currents are mainly affected by resonant tank parameters which mean proper selecting

of these parameters can minimize conduction losses. Therefore; high ratio between resonant and magnetizing inductor leads to increasing normalized inductor current and conduction losses as well. In SRC, the normalized current is inversely related to inductors ratio while output voltage and resonant frequency is identified. In turn, low inductors ratio provides a lower gain which makes designers pick a trade-off selection between conduction losses and keeping a fixed gain value for high system performances. To demonstrate this approach, high transformer turning ratio is utilized for minimum input voltage range and required high output voltage. Another design of circuit parameter optimization is illustrated in [34] based on peak gain evaluation and DC-DC converter application modes. Conduction losses were the main objectives function in this study that have to be reduced for a small input voltage value and medium application system. Operation mode P is denoted when resonant and switching frequencies are equal, while resonant inductor and capacitor are only entered to the resonant conversion regardless of magnetizing inductor value. While operation mode 0 is denoted when switching frequency is less than resonant frequency and rectifier diode is turned off with sharing magnetizing inductor the resonant conversion process. Another operation mode N might also be referred to high load application or minimum utilizing of switching frequency which forces rectifier circuit to turn on and magnetizing inductor voltage increase as well. Two main aspects are clarified for LLC optimal design. First, the estimation of voltage gain should be low at maximum input voltage with a high switching frequency and light load case. Second, the estimation of voltage gain should be higher for low input voltage with low switching frequency and full load case. Converter is expected to achieve some advantages regardless of its topology, like achieving ZVS condition of MOSFET switching circuit, regulate wide range of output voltage especially for high output voltage range and reducing switching or conductance losses for both MOSFET and diode. In [35], a design view of LLC resonant converter circuit has been utilized for front end DC-DC voltage application. In this work, researchers attempt to minimize each of switching and conduction losses for both MOSFET and diode components. Resonant frequency, load range and magnetizing to resonant inductors ratio are the main design parameters to be optimized. Complexity of resonant converter characteristics due to its various parametric relations has forced authors to discover another method rather than traditional trial and error methods. Rapid parameter calculations are suggested for SRC of LCLC topology with arbitrary transformer turning ratio for identical primary and secondary core as in [36]. In DC-DC converter, transformer architecture should be determined according to system requirements and turning number ratio. Inductor value is also effective on transformers window size which also restricts core selection. Higher value used for inductor in the primary or secondary side increases transformer window size. At the same time, working under high switching frequency can reduce the transformer size. All these mentioned reasons make transformer characteristics have a significant key effect to assist soft switching in DC-DC converter circuit. For the similar applications, [37] proposed an unregulated SRC with a buck converter for fast charging electric vehicle (EV) requirements. High power applications acquire a fault detection and protection as a significant aspect to avoid increasing of cost failure issue. System failure is often occurred at high or unbalanced stress in voltage and current, which weakens resonant converter and damages other components.

Recently soft switching is more desired to enhance resonant converter circuits' performance, especially with increasing rates of industrial applications that mainly depends on resonant converter efficiency. Conventional converters suffered from hard switching operation. In addition, capabilities of minimizing converter losses by working under higher switching frequencies make it a significant choice for multiple types of applications. Performances of DC-DC converter topologies are compared in [38], which explain converter utilization for PEV charging process. To achieve stable battery performances without any degradation in its characteristics, authors applied constant current and voltage for charging process. Circulated conduction losses and switching losses are the related metrics. In [39], authors localized load conditions and its impact on PEV battery charger process for LLC resonant converter optimal design. Unlike previous studies where authors concentrated only on wide input voltage range or hold up time, this study deals with this two states. Constant voltage is illustrated for low load performances by determining the range of switching frequency. Interference is also occurred using this type of converter for such an application between output DC voltage and the external storage units. These issues need a higher power density converter with

a better isolation for the bidirectional charging process. In [40], researchers introduced a comparison between four converter types to evaluate the compatibility for such applications. Transportation applications are also one of commonly studied devices for DC-DC converter circuits. Power take-off (PTO) in different places such as automotive devices has to be highly efficient and providing lower fuel consumption. In [41], a step up converter topology is proposed with a low ripple current and stress under full load condition. Resonant current dependent design of the suggested model makes light and no-load conditions suffered from small value of flowing resonant current. Thus, circuit will significantly different in behavior from the suggested model. In addition, low turning on and off MOSFET energy should be selected for this model due to hard switching process. Smart transformer applications are also one of the popular SRC usages due to its high efficiency and good reliability. In [42], the most failure devices are studied with an effect analysis and a failure mode evaluation according to SRC design. Referred to this work, semiconductors and resonant inverter capacitors are the main susceptible devices in SRC topology that suffered from a failure chance. Other researchers are focused on selecting appropriate topology, switching frequency and resonant tank parameters with some considerations for specific application as proposed in [43]. SRC is also proposed for low and high power applications in [44] for Electrical Multiple Units (EMU) train sets purpose. Different applications of SRC are also introduced due to its high efficiency, low circulated power compared to other types and working softly under ZVS conditions such in [45] and [46]. Renewable energy systems are stated to be a long power term solution for various applications such as portable device charging systems. The advantages of applying resonant converter for renewable energy are simply clarified in some studies such as in [47]. Three resonant frequencies are observed for LCLC suggested topology. LCLC topology is considered as SRC when high load is applied. While, light load make LCLC moves towards parallel resonant frequency region.

Due to fast changing of PV delivered power and various regulation conditions, PV requires a reliable and accurate resonant converter design. Multiple or dual input sources such as PV suppliers from two different models can be connected as one source to a single resonant converter to share the same resonant inverter parameters as

explained in [48]. Wind turbine is also considered as one of popular applications that require accurate resonant converter design due to voltage variation and high generated power. In [49] and [50], researchers suggested SRC for megawatt and kilowatt wind turbine applications, respectively. In order to avoid transformer excessive size and losses issues, pulse removal technique is applied by placing resonant inverter component at secondary side. Design steps are analyzed as followed: At the first step input voltage characteristics are specified to determine the converter ratings as well as parameters and topology selection by considering the worst case of full load conditions. Second step involves device selection of DC-DC inverter tank and rectifier circuit in the secondary side. Also, transformer shapes and architecture are selected according to leakage inductance which is used as a resonant inductor in the same time. Third step: performances should be defined by losses and temperature estimation for all design parts according to the selected transformer thermal model. Then transformer volume will be evaluated as final step. Placing inverter tank parameters like inverter capacitor in the secondary side brings higher voltage with a chance of temperature breakdown issue. Diode selection limits operating frequency by diode losses consideration. SRC topology is able to turn off diode naturally at ZCS state which decreases diode losses in turn. For this aspects, two comparisons are done between primary resonant tank of SRC placement and secondary placement with pulse removal technique to rate the converter selection priority. Figure 1.3 shows wind turbine suggested SRC for a megawatt generated power with multiple switching circuit connections [49].

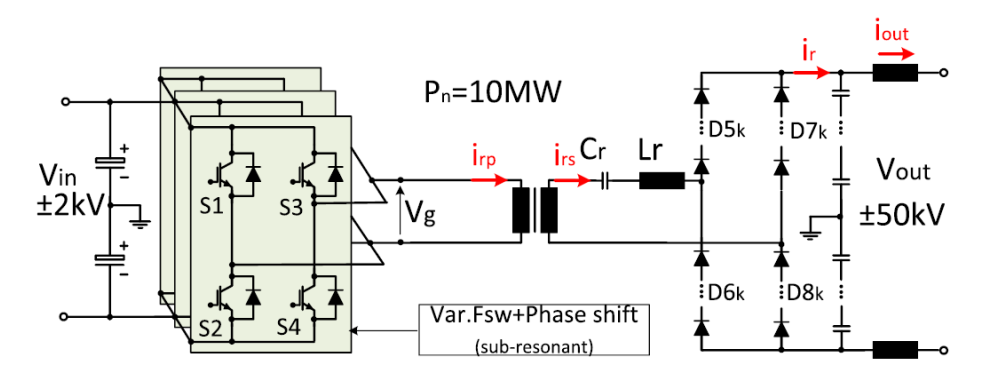


Figure 1.3 Multiple switching circuit design for megawatt wind turbine system [49]

Different parameters influenced DC-DC converter performances and have a significant impact on losses calculations as well. Resonant inverter components, transformer turning ratio, duty cycle time, resonant and switching frequency, load variation and input and output voltage range represented the most affected parameters. Each element has a specific impact on a different DC-DC converter losses types, for example: resonant inverter components affected mainly switching loss and transformer turn ratio affected No-Load and Load losses. Some elements like duty cycle influenced on many losses types like switching and conductance losses due to its affection on overall switching process. Compatible selection of these elements leads to achieve several important points for the full design like: achieving ZVS condition, regulating output voltage easily, reducing different losses values and operating under different load range efficiently. Researchers such in [51-54] offering a step by step parametric selection using trial and error process. This operation required more time due to feedback calculations of each changing elements required for any single step. In addition, single solution can be provided for a specific application which is not reliable for designer. For all of these mentioned reasons, an evolutionary optimization methodology for resonant converter design considering photovoltaic systems is proposed.

Parametric automation is able to achieve reliable solutions of various designs at different stages of system requirements. However, automated parameters at early stages make designer capable to adjust design demands with a quicker change that might be existed due to different reasons. At the same time, these automation processes require an observation to determine system complexity according to design objectives and scopes. Automated design based on optimizer reflection that supplied a quality to each set of parameters according to cost functions and the overall system response. Also, automated design provided a comprehensive opinion about the relationships between parameters and estimate the outcome or consequences of these set combinations. At the end of each automation stage, one or multiple parameters can be corrected to provide a proper option for the design improvements unlike ordinary techniques that depends on trial and error process. Parametric automation also has the ability to instantly modify system performances according to design constraints. Unlike popular selection process, automation is able to extract useful parameters from invalid set of parameters which

keep searching area near to optimal solutions line. Linking of optimization parameters is a significant priority to electrical circuit design to implement an efficient system which fit project requirements. Automation in general is primarily associated with parameter numbers, constraints limitations and solution boundaries. Increment in design parameter numbers offers a rough challenge to the designer due to inconvenient calibration that might be raised compared to lower parameter number version of the same design. Moreover, automated design provided a harmonious preparation for upcoming requirements according to various conditions. Recently, multi objective optimization techniques are more utilized for power electronic circuit design due to high frequency applications and compact elements size. By considering designs reliability for a set of parameters as weighted measurements, artificial automated design is proposed for power electronic circuit as in [55]. In this study, an efficient relationship between system's reliability and parameters are introduced to obtain an optimal design. It's provided two relevant training models using Artificial Neural Network (ANN) to offer a simple plan of design parameters according to several constraints. First model is to deal with a lower version set of parameters which is considered as a replacement converter model. The second model is based on first model out coming data and employed it for larger version set of parameters. The main objectives of this study were to achieve a compatible design between element size and system reliability. It's shown that these issues are more relevant to switching frequency and other suggested parameters such as inverter parameters.

Automated design is preferable for power converter design to obtain a clear sight of nonlinear input/output parameter borders. Designer probably concerned in a multiple number of solution sets instead of a single set. This issue is an essential part without applying multi objective optimization techniques; therefore, authors recently are more focused on utilizing these techniques such in [56]. While in [57], authors presented an optimization techniques combined with a mathematical tool to evaluate three phase transformer performances. In this study, five parameters are optimized using three different techniques to minimize transformer No Load and Load losses as well as transformer cost. Multiple solutions are supplied based on this study and provided promising results which proper for different fields and application area.

The significant advanced of automated process is discussed widely such in [58]. Based on charging time and switching frequency, SRC is adopted in capacitor charging applications due to its constant characteristics at various load conditions. Several applications are required to be operated in continues and discontinues modes with a high switching frequency range identifications which is done easily using SRC converter topology. While automated design of SRC above resonant frequency is illustrated in [59] depending on considerable features such as harmonic reduction and operated under ZVS conditions. In addition, multi layered printed board is used to implement converter transformer section to fit high switching frequency utilization for this design. In [60], an optimization technique is developing to evaluate power loss model of boost converter. Parameters optimization in this study established to minimize system average power loss with keeping ZVS condition. Applications such as charging capacitor and photovoltaic required multiple individual parameters to fit output modification. In addition, numerous design needed multiple solutions in a reasonable amount of time which easily acquired by applying automated process. Loss analysis model, component cost evaluations and voltage regulations are the major rules to automated DC-DC converter in this study. SRC is suggested to achieve these approaches due to its operating flexibility under wider voltage range and high switching frequency utilization. Moreover, lower SRC circulating energy compared to other topologies due to soft switching process granted SRC a valuable advantage among similar topologies.

Maximum power tracking for 6-PV module tracked to collect information according to specified area and based on shaded and non-shaded configurations [61]. Weather conditions are identified, while module affected vertical and horizontal angles are taken into considerations as optimization parameters for this design. This design is simulated using two programs: Helioscope online program to specify main power loss consumption part and Design Builder to collect annual data of overall system generated power. Due to wide range of PV generated power, SRC is adopted to deal with these conditions and regulated output voltage accurately at the same time. Previous study is suggested an optimization model to automated single and three phase transformer based on No Load and Load evaluations as in [57]. While in this study, an advanced model with four additional parameters is suggested and analyzed for SRC converter

circuit design. Optimization process was according to 17 different parameters: 9 parameters for the new single phase transformer model and 8 parameters related to SRC converter own parameters to evaluate overall losses types.

1.2 Objectives of the Thesis

SRC has to be designed carefuly to be compatable with the general requirements of PV array. Automated design is required for extensive search space of the values of SRC design parameters such as resonant tank passive component values, transformer turning ratio, dead time and switching frequency. Optimization is carried out to reduce overall SRC circuit losses: MOSFET switching loss, MOSFET and diode conduction losses and transformer NLL and LL. This thesis proposes an evolutionary optimization methodology for SRC design considering PV systems. The proposed design methodology is evaluated under various conditions: load variation, wide input voltage range and different operation modes. Output voltage regulation is also introduced as an objective function together with the minimization of SRC overall losses. A comparison is also performed between 5 parameters and 9 parameters transformer models used within automated SRC design according to PV grid requirements. Genetic Algorithm, Differential Evolutionary Algorithm and Non-dominated Sorting Genetic Algorithm are used for optimizing the objective functions which are the output voltage regulation and minimization of total loss.

1.3 Hypothesis of the Thesis

The importance of evolutionary algorithm (EA) based automated design in power electronics is growing as the design parameter selection for complicated circuits requires enormous search space. Moreover, parametric automation of circuit design provides faster optimization than trial and error methods. Reduction of overall losses, achieving ZVS condition with robust circuit performance and regulation of output voltage for various loads are the major challenges of this study. Multi-objective optimization of SRC design is carried out with EAs and FEM, where the evaluation performances of EAs are validated comprehensively. Other contributions of this study can be listed as the investigation of loss value dependency on particular SRC design parameters, selection of optimum operation mode for robust performance, and validation of optimization performances of EAs for different aspects and conditions.

OPTIMIZATION TECHNIQUES

2.1 Genetic Algorithm (GA)

Genetic Algorithm (GA) is a meta-heuristic evolutionary algorithm influences by natural selection process which widely used to reproduce new generation of solutions that has a higher quality for optimization and searching issues. GA is built depending on biological operators by John Holland in 1960 such as cross over, mutation and selection process. In GA, population of nominated solutions to a specific optimization problem is improved to new better solutions using various mentioned operators. Each solution has its own representation as a binary coding or other possible coding types. Optimization process often started with random solutions with an objective function evaluation that need to be minimized or maximized. Each generation of individual's solutions has the ability to be selected and mutated to share next generations with new solutions. GA like other EAs stopped when iteration number or generation number are exceeded, or when providing the required minimized/maximized cost value. Solutions should be represented correctly with a fixed size for each solution to simplify crossover and mutation process.

2.1.1 GA Operators and Selection Process

According to problem kinds, population size could be determined. In general, first generations are usually generated randomly which increase the availability of searching space area. While solutions are filtered by the fitness (sometimes called cost function) and then selected as reproduction new generation of solutions. Parents are selected as pairs from each previous generation to produce new "child" solutions that share different or similar characteristics of parent solutions. Next generations are now different from previous generations because the average quality of cost function is increased and better solutions are kept to move forward with it. GA is terminated to produce new generations when abort conditions are occurred like: maximum generation number reached, solutions are established with cost function satisfaction.

2.1.2 GA limitations

GA like other EAs has different limitations should be clarified to be aware of GA ability to handle a specific cost function and solutions. At each generation, cost function is calculated to overall solutions which mean more time consumption when complex cost functions with a high number of parameters are used. This is force designer to approximate cost function which may affect the overall solutions and drift it towards another line which may or may not provide any cost function satisfactions. In the other hand, mutation operator is often suffering when large number of optimization parameters are utilized, which may lead to raise the searching area for next generations. Also, stopping conditions are different from each other for the same problem because solutions are compared with previous randomly created solutions only. Moreover, GA searching area moving towards non beneficial solutions when "cost" function contained a different group of parameters [62].

2.1.3 GA Problem Domain

GA is often utilized when computational simulation is time dependent process to get a better solutions faster than manual or trial and error process like microwave devices modeling improvement [62]. In this study, discrete model has been presented as a cost function to be compatible with multi variables and simple structures. While parameters in this work are determined as a sequence of real values to represent lumped elements without any coding process. GA recently applied to address the rising challenges to design the next generations of semiconductor devices. In this specific field, another work has been introduced in [63] to use GA as a multi objective optimization method for double gate semiconductor MOSFET type to measure its electrical performances. The main goal of this work is to obtain the best solutions which referred to MOSFET dimensions and electrical performances to enhance circuit strategy for CMOS digital and analogue applications. In this work, several objective functions are presented to be deled with GA simultaneously to simplify finding required solutions and to assist designer selections for different application. This work has been done according to two steps: first, obtaining the optimal related solutions according to selected multiple cost

functions; then, selecting the appropriate solutions for a specific design by applying higher level of related information.

In [64], high power application optimized also using GA to reduce flux density of field coil that utilized for renewable wind turbine energy generators. Three cost functions are selected to be minimized for several field coil parameters while other related parameters have been identified as constant values. Variables represented as follow: field coil width and height with a magnetic field error and transport current as optimizer constraints. GA is also considered as an optimizer approach for functions that consists nonlinear elements. GA is also moving towards new levels of optimization when mixed with mathematical parallel tools especially where cost functions evaluations are much important. In this work, GA is used for different types of electrical circuit to optimize its affected parameters and illustrated the impact on transient response of this design. Four parameters are selected for this optimization with maximum voltage, current and fault clearance time as a constraint for this design. Threshold current which high power transformer need to start with, time period that required for transferring current between its part, inductance value and arrester circuit voltage are the four optimized parameters in this work. GA is applied for this design several times as a multi stage computing which is independent evaluation with different input parameters. Utilizing of GA is required for fast evaluation when a huge data need to be illustrated as in power system problems. Multi stage of GA is proposed in many articles and studies but it has a simple implementation of master and slave global population. In this type a single population can be stored in master processor and then divided into some groups to be evaluated by slave processor with a noticeable speed up process without any further instructions. While other researchers combined between sub domain model and multi stage of GA to increase optimization performances of GA for multi objective goal such as in [65]. This study introduced for permanent design with eight selected parameters that influence the solution or cost function quality. In [66], authors selected sum of squares for differences between output and desired waveform error as a cost function to be optimized for two types of discharge drivers. Triggering times which represent about 16-20 variables for each driver parts and driver parts voltages also are selected as an optimized parameters. In this work, huge number of parameters is used for a single cost

optimization function and this may lead to a large significant error if multi objective has been applied as well. GA from this historical review has been applied for different fields due to its simplicity and low time consumptions and these are the main reasons to apply GA for this work as well.

2.2 Differential Evolutionary Algorithm (DEA)

Differential Evolutionary Algorithm (DEA) is also meta-heuristic evolutionary algorithm which also suggested optimizing a problem by candidate solutions improvement. DEA utilized for valued cost functions without requiring any problem gradients. Which is detailed and presented by Price & Storm in 1995, Figure 2.1 shows DEA basic fundamental steps for optimizing a specific problem/problems [67].

```
Algorithm 2 Differential Evolution
  P_t: Population at time t
  TP: Transient population
  t \leftarrow 0;
  Initialize P_t;
  Evaluate P_t;
  while not termination condition do
      TP \leftarrow \emptyset:
      for \forall indiv_i \in P_t do
          Offspring \leftarrow TrialVectorGeneration(indiv_i);
          Evaluate Offspring,
          if Offspring is fitter than indiv_i then
              Put Offspring into TP;
              Put Parent into TP;
          end if
      end for
      t = t + 1;
      P_t \leftarrow TP;
  end while
```

Figure 2.1 Differential evolutionary algorithm (DEA) basic steps for optimization a specific problem [67]

In each generation, DEA basically selected three solutions or set of solutions to produce a vector called trial vector. One of these solutions consider as a basic vector which added to the differences between two other selected solutions to perform the required trial vector [67]. DEA used a scaling factor which its value larger than 0 to control population improvement rates. Population number, crossover and mutation operators in addition

to the scaling factor are the main DEA own parameters which are carefully need to be adjusted. DEA has some differences than GA and also differences than other classical EAs of selecting child using crossover without random decision requirements. Set of solutions in DEA are listed to rank the position of each individuals without affection on the required cost function measurements. Iterations number of DEA started with mutant vector creation and then randomly selection from that vector to choose three individuals. At this step, base mutated vector and perturbation vector are performed to create the trial vector. Trial vector is created by crossover operator utilization for both mutant and perturbation vector [68].

2.2.1 DEA Operators and Selection Process

Like classical EAs such as GA, initial population of DEA has to be defined for each required optimization parameters with a limited range. Then according to the range limitation, randomly parameters are generated for the first generation individuals. DEA treats individuals as a real numbers, so it should be considered and generated as real values for various optimization problems. DEA has a scaling factor (its value is real and greater than zero) to control mutation and recombination of trial vector creation. Three vectors of the first and next generations are selected randomly to perform trial vector using mutation or it's called in DEA as differential mutation. Figure 2.2 shows the new target vector after applying differential mutation on three randomly selected versions and the crossover possibilities that inherited from mutation step or not [69].

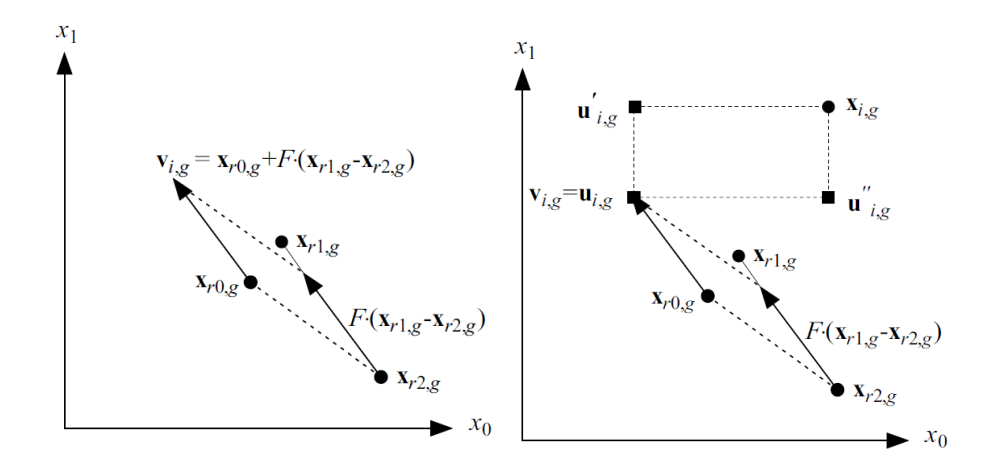


Figure 2.2 Operators and selection process of DEA (a) differential mutation and (b) uniformly crossover probability [69]

Uniform crossover is also applied in DEA to accomplish the differential mutation step. Crossover is also defined by user to control mutant parameter solutions that taken from two different versions of generation vectors. A uniform random number is often generated randomly and compared to crossover value, if crossover higher or equal to this number the trial vector will be taken from mutation step to the next step and vice versa. While selection process depends on comparing trial vectors with another generation trial vectors if they have equal or lower cost function value so it will be replaced. DEA provided a robust recombination and selection process compared to classical EAs and this can prevent these individuals from being replaced twice. Figure 2.3 represented classical DEA by indicates all operators and different vectors than the target solutions [69].

Figure 2.3 Pseudo code for the classical DEA algorithm [69]

DEA is quite different than GA in some points such as:-

- DEA is much easier to use especially that it does not require any coding and encoding process because DEA deals with optimization parameters as a real values regardless of design parameter types.

- Work better in large number of parameters due to mutation, crossover and selection operator that prevent premature issue which is normally occurred in GA.
- For the same observation, DEA provided faster convergences to finding solutions and closer to global minima target.

2.2.2 DEA limitation

Real value representation for DEA has an exponent limitation which forced designer to define minimum and maximum value of each selected parameters to be optimized. When "cost" function consists of large parameters with huge differences of about 7 digits or greater between two or more parameters makes contribution of these smaller values to be neglected. This issue led to error on cost function evaluation steps as well as trial vector creation process. DEA became harder to operate under these conditions due to that DEA is a trial vector dependent. Due to creating more than one vector and calculating differences and then addition process is applied as well, time is considered as DEA main limitation points. Also, DEA suffered from far initialization issues when parameters bounds (minimum and maximum values) are quite of far away from the target solutions. This issue is also made DEA sometimes creates duplicated solutions especially with large number optimization process.

2.2.3 DEA problem domain

DEA utilized easily as an optimizer algorithm for different applications due to simple operating under specific hard limits and constraints which match design parameters and performances. Combination between DEA and other multi objective functions is helpful to provide the ability of changing number of variables and also to change easily cost function numbers as explained more in [70]. In addition, coupled DEA with a mathematical tool like FEM can improve optimization performances and provided sufficient information of related design deleted.

Difficulties in searching space of power electronic circuit design require plenty efforts and researchers attempted to utilize EAs to solve this problem. In [71], authors suggested a modified DEA algorithm to provide more simplification in power electronic

circuit design and better improvements in finding solutions. Typically power electronic system consists of power transferring part and feedback network stage. These two parts have different parameters to be considered and at the same time to be controlled but feedback network parameters have a huge impact on system performances and ought to be accurately optimized. Output voltage steady state error, transient response, output steady state ripple and dynamic system behavior are the aim cost function to be optimized according to different selected parameters. Seven parameters are selected for this work to controlling the optimization of feedback network stage. While buck converter main parameters are considered as fixed known elements. DEA compared to different EAs such as GA and PSO according to some metrics like average cost function value that gained from selected EAs and standard deviation of the optimization process....etc. strongest searching ability is obtained after applying DEA. In addition, high quality of finding optimal solutions with faster searching schema supplied a better reliability when applying DEA as well compared to other selected EAs. DEA is easy to build and powerful algorithm in single or multi objective functions due to useful parent selection which leads to better child production process. According to this incident, DEA applied for different area such as Microwave circuit design which explained in [72], electromagnetic design such in [73] and also for integrated circuit design in [74] which promising a good results compared to different EAs.

2.3 Non-dominated Sorting Genetic Algorithm (NSGA-II)

Multi Objective problems have methods limitations due to complexity expression definition and number of optimized parameters. Improvement of classical optimization techniques lead to simplify the difficulties with better performances by changing or enhancing one of the classical optimization operators. Non-dominated Sorting Genetic Algorithm (NSGA) is one of the improved optimization techniques which introduced by Deb in 2000. NSGA second generation is different by: searching process of solutions that are closer to the optimal solution line, increase solutions diversity in the optimized solutions. The main algorithm of NSGA-II is shown in Figure 2.4.

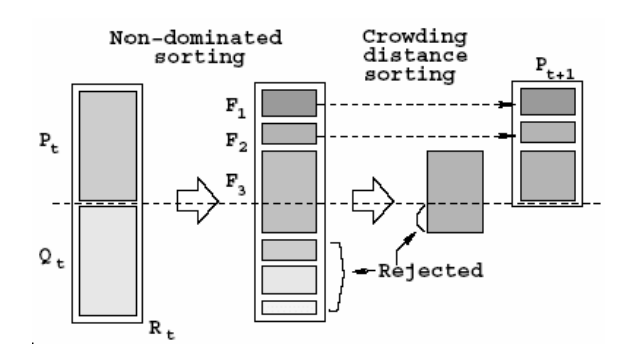


Figure 2.4 The main algorithm of NSGA-II procedure [75]

NSGA-II implemented according to parent and child combination process to make a dominated and non-dominated sorting solutions from the two groups. It is also has fast sorting process, fast calculation of solution distance and a simple process for comparing solutions between various Pareto front lines. Several problems have been demonstrated that NSGA-II provides a better diversity in cost function optimization such in [75]. NSGA-II in general has some difficulties which can be summarized in: complexity in computational mechanism, non-elitism solutions and sharing parameters that have to be specified and defined carefully. In order to alleviate the mentioned issues, faster mechanism depending on the same previous schema with a non-dominated sorting ranking is presented in [76]. In this work, author presented an improved version of NSGA which has a better solution searching speed for larger size optimization problems. This is also led to support more complex future applications and encourage utilizing it for real world problems such as power electronic devices and renewable energy systems. Conventional algorithm identified better solutions by comparing the same generations (with size N_{pop}) solutions with each other based on number of objective required functions (M). This process need of about (MN_{pop}) computation number to compare solutions, which are led to (MN_{pop}²) comparison number for the first level of non-dominated generation number. Moving to the next population numbers, the same process required also (MN_{pop}²) by repeating the same comparison approach. Suppose one solution is found to be optimal among a specific number of generations which mean (N) operations, in total optimization process required (MN_{pop}^{3}) as overall computation approaches. While non-dominated comparison process needs to lessen computation numbers by following faster NSGA approach [76]. In the beginning, calculate number of dominated solutions for the same population level and number of solutions which are dominated by other solutions in a group definition. This operation required (MN_{pop}^2) of comparisons as mentioned previously at the same level of population. By applying this process, each solution has a group of dominated solutions which reduced computation number needed before by one. These dominated solutions will be grouped in a different space also to repeat the same approach and the second level of solutions will also has a group of dominated solutions reduced by one. By repeating this process, solutions will never go around again, so total computation number will be (MN_{pop}^2).

2.3.1 NSGA-II Operators and Selection Process

Next optimization group of solutions are not designed to be closer to Pareto front only but also solution diversity specified as an important additional EAs requirements. A possible diversity of solutions is guaranteed using NSGA by applying sharing function with a convenient tuning of related parameters. A sharing parameter that used in NSGA to frame sharing problems area is related to distance between two different solutions. Sharing parameter are set by user with specific guidelines and suffered from two issues: first, sharing function is sharing parameter dependent; second, computational complexity is increased to compare each solution with other solutions. These difficulties can be alleviated using crowding distance comparison, which is proposed for faster and elitism optimization in NSGA-II [76]. NSGA-II has no defined sharing parameter such as previous version with an easier computation issues. Crowding distance represented the nearest neighbor between two solutions along desired cost function. Each solution as shown previously in Figure 2.4 has an average length between the nearest solutions of the same front line. To achieve this approach, population has to be sorted by magnitude in an ascending order. The edge solutions will be taken as an infinite average crowding distance to be compared with and continued to the next generations. Other solutions lie in the same front line has an average calculated distance which also related to its objective function values. Hence, complexity in NSGA-II simplified and each member at the same population front line has an assigned distance. The most crowded solutions (in other words- the smallest distances between two different individuals) will be selected as better solutions which create more crowding in solutions at the same area with a better diversity in next generations. To accomplish the priority mechanism, each solution has a rank and crowding distance value. Solutions with lower rank (which means better and closer to optimal line) will be selected. Otherwise, if two solutions have the same rank value when they allying at the same front line, a lower crowding distance will be make the selection priority [76]. First populations in NSGA-II is also created randomly and sorted according to domination and non-domination groups based on cost/costs function values. This is meant that Pareto front line with a lower rank is better than higher one. NSGA-II in first generation has the same classical operators and will be changed after this step. New created populations will be combined with previous population to ensure elitism process. All solutions of the first front line will be selected to combine with the overall first population if it's smaller in size. That's mean if the size of the first front line is not enough to cover the next generations. Then sub-sequent non-dominated solutions for example the second front line, will be also selected to combined for the same conditions and so on until required net generation length is reached. Binary tournament selection is used for NSGA-II depending on crowding distance comparison. Sorting procedure of solutions will be stopped as soon as next population are size sufficient and ready for operators to performed again [76].

2.3.2 NSGA-II limitation

In spite of closeness solutions area using NSGA-II compared to different EAs, but still has some minor limitations. NSGA-II procedure selected non dominated solutions from all fronts lines, but last front lines usually deleted while it consists of good individuals and it may be helpful to generate a new offspring better than normal approach. Therefore; some authors provided a niching selection from all front lines to be different and keep closing to optimal solution as much as possible such explained in [77] which explained in more detailed in the next section. NSGA-II like other heuristic algorithm required accurate selection of its own parameters because it has a high impact on finding optimal solutions. This issue has to be solved by designer to tune NSGA-II parameters which expend more time than searching process itself; some authors explained a tuning technique for NSGA-II such in [78]. This makes designer aware when using NSGA-II for a non-linear and dynamic problems like electromagnetic field issues. As mentioned, these

issues forced designer to try and accumulate error knowledge of changing parameters until reaching better results. In the other hand, some solutions have relatively low sensitivity to changing NSGA-II own parameters which has more information when it kept for next generations. Due to this reason, reaching optimal solution near or closer to the searching space area require more time if these solutions are not considered or selected such explained in [79]. Improvement version of NSGA-II has been explained and suggested in [80] but still close to the second version in searching accuracy.

2.3.3 NSGA-II problem domain

Deb original research in 2000, selected ten studies as testing problems to compare NSGA-II performances with Pareto-Archived Evolutionary Strategy (PAES) and Strength Pareto Evolutionary Algorithm (SPEA). In this study, different testing problems are presented according to author objective names, number of optimized parameters and objective function specifications. Among all of the tested techniques, NSGA-II provided the best optimization compared PAES with randomly selected iteration of NSGA-II [77]. In this study, author suggested to increase number of optimization population to 500 instead of 250 to study different parameter affection on NSGA-II overall performances. Compared studying between 250 and 500 number of populations was to clarify solution convergences and diversity. While other researchers suggested a learning tools such as reinforcement technique to tune NSGA-II parameters as explained in [78]. To reach optimal solutions closer to Pareto required line parameters need to be tuned for a techniques such as NSGA-II especially for large number of parameters. This adds difficulties and more time requirement to user for tuning these parameters for faster optimization process. Shortage knowledge of dynamic behavior of such a problems force users to collect it by trial and error firstly. Many tests are done to collect such knowledge for dynamic system performances evolution. For this reason, NSGA-II has introduced to adjust parameters instead of trial and error that done hardly by users. Crossover, mutation and two indexes are the main four parameters to enhance NSGA-II performances. The collected information is done according to rank solutions and sorted in a memory. A reward function is given to all successful NSGA-II four parameters depending on cost function and solution continuity. Researchers such in [79], suggested a sensitivity model of circuit optimization using NSGA-II deals with multi objective functions in a simultaneously process not by weight measurement for each cost function such as many studied did. The variation ratio between cost function and related parameters are considered as first order computation of sensitivity. While in this paper, researchers used Richardson technique to evaluate the mentioned ratio which utilized as well for in-loop technique. After performing a Pareto front line using NSGA-II, generally low sensitive solutions will be identified and deleted from each dominated solutions. This approach makes a very small group of solutions spread along front line or zero sets sometimes if not found or not conditioner achieved. In this approach, low sensitive solutions will be kept to be used when next population are generated. Figure 2.5 shows the low sensitive NSGA-II and high sensitive solutions in [80].

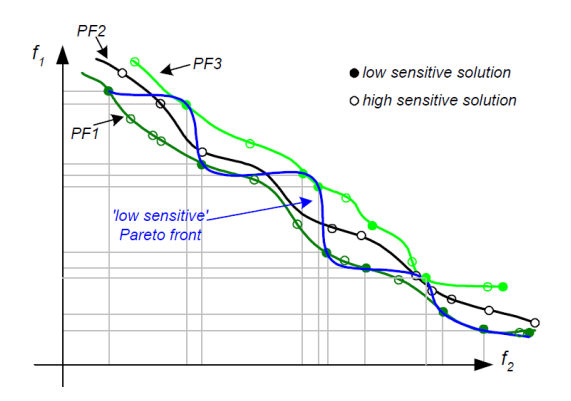


Figure 2.5 Low and high sensitive solutions using NSGA-II for minimizing two cost functions [80]

A sensitivity analysis is also applied by [81] to minimize space searching region for voltage regulator optimization using NSGA-II. Choosing less design parameters with a high sensitivity is the main goal for applying this sensitive analysis which led to reduce searching region or parameters. Parameter minimization is significant design property to fast reaching optimal solutions with less time exhausted.

2.4 Finite Element Method (FEM)

Physical problems which deal with essential design structure required useful mathematical tools especially for engineering analysis field. FEM is a numerical procedure that defined as a minimization formulated function to solve different physical problems. FEM among other mathematical tools provided a good precision and locality

of approximations such is explained in more details in [82]. Inductor design required a performances determination and upper frequency limitation which is done by applying different models such as stray capacitance model [83]. FEM is applied in this work to modulate stray capacitance distribution of a rod inductor type. This inductor is utilized as a noise reduction in Radio Frequency (RF) circuit and consists of a round wire made from copper which winded around ferrite core. At a specific resonant frequency, parasitic capacitance appeared between winding turns which forced inductive impedance to be capacitive type. In this work, authors described FEM technique to module single layer of rod inductor with its core definitions. FEM is utilized for various boundary conditions related to electrical design such as piezoelectric transformer analysis study in [84]. The main two components of this type are two electrodes and by the meaning of impedance transformation, voltage transmission is occurred. Transformer configuration and its equivalent circuit are shown in Figure 2.6.

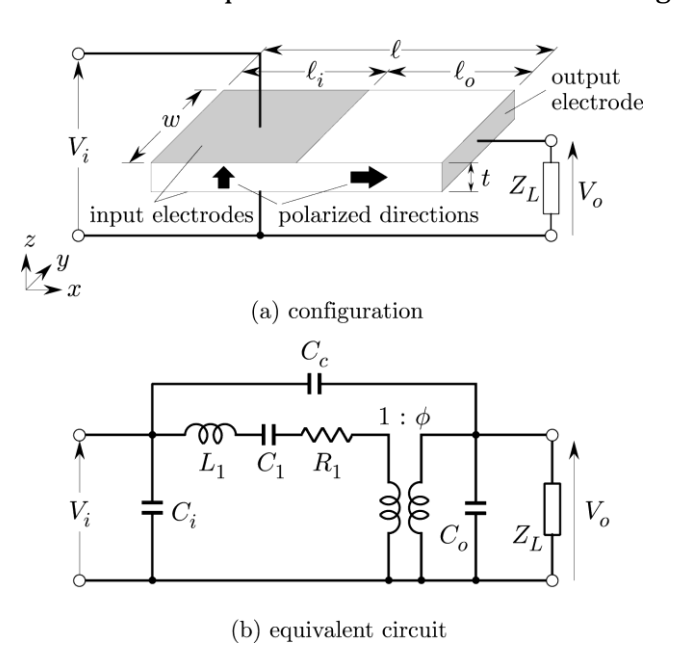


Figure 2.6 Piezoelectric transformer (a) structure design and (b) equivalent circuit [84]

As shown in Figure 2.6 (a), a ceramic plate consist of input electrodes pair by z direction placement and an output electrodes on the other side of this plate by x direction. Input electrodes are considered as a ground and input side. While Figure 2.6 (b), shows two damped capacitor related to both electrode sides and three additional lumped elements. Other researchers applied FEM to analyze piezoelectric devices according to output

power with a resistance load condition such in [85]. While others in the same field deals with power transformer design and study magnetic shunt affection on short circuit impedance with its field analysis as well such in [86].

Field calculation was done for this work using FEM combined a boundary element technique. One from three phase legs has been selected with three main components to simulate its magnetic field characteristics. Leakage field changes which occurred in this type of transformer are considered as a cost function and to be optimized according to its geometry elements. The transformer selected part has been divided into active section which represented by mesh FEM and second section for the overall area related to BEM work. Short circuit failure issues occurred in power transformer is another critical issue and causes an overall power system failure. Three phase transformer has unstable performances compared to single phase during this failure issue. In [87], researchers submitted a power transformer analysis during the worst case of three phase transformer for short circuit failure issue using FEM. FEM is applied for this research to analysis dynamic response in addition to electromagnetic field of power transformer winding by considering stress and other deformation transformer factors. These characteristics are measured in general using vibration signal that taken from tank.

This prediction or measurement is affected by stress and elasticity feature of spacer and copper disk. Researchers focused on studying dynamic deformation according to this features or spacer because it is small in copper disk section. In this paper, author considered the two body using FEM to analysis these property in various voltage winding. While other transformer types like split winding structure has been introduced in [88] for measuring leakage field distortion through short circuit condition. These types of transformers are widely used for power electronic applications due to space discrimination and low short circuit current property. FEM is employed to this type of transformer because it is sort of difficult to specify magnetic field value and its location need a flexible tool to handle these issues. Two cases are illustrated according to short circuit conditions. First, one of the two low voltage sides is in short condition and the other in open condition. Second case, both of low voltages are side are in short

condition. Results as shown Figure 2.7 is proved that flux density much higher for the first case with a high current following through secondary high voltage side.

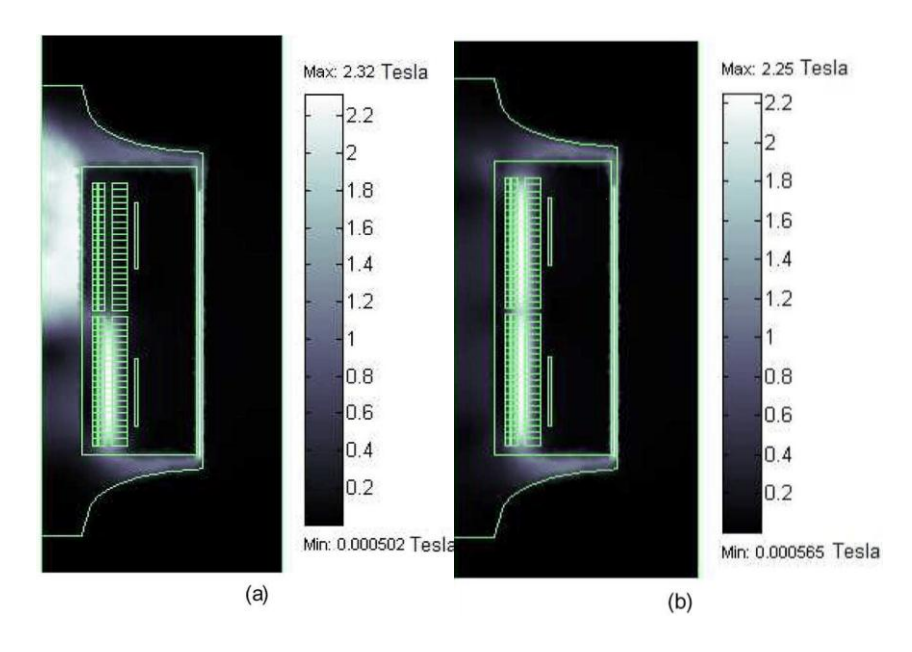


Figure 2.7 Flux density pattern using FEM for two cases: (a) one short circuit winding and (b) both short circuit windings [88]

PV- ARRAY SHADED & NON-SHADED CONFIGURATION OPTIMIZATION

Complexity of Photovoltaic (PV) design needs an optimization rule for providing better performances and utilizing accurate annually generated power. In this section, NSGA-II has been applied to optimize the shaded and non-shaded configuration for 6-array of Trina Solar PV module connected in series. Azimuth angle, tilt angle, distances between each panel as well as the racking type was the main parameters for the optimization technique and for the selected area. In addition, weather condition is applied after all of the picked parameters have been optimized. This technique showed 92% of annual efficiency for Azimuth angle 207° and Tilt angle of about 10° with Total On-Site and Utility Electric Sources of about 1.101043 kWh. It's also pointed to the system main losses sources for more accurate to be applied with a high frequency switching topologies.

3.1 Introduction

Challenges of PV load variation in day-hours are more different to be considered without optimization of PV main parameters. Expected PV generated power is mainly affected by various parameters like weather conditions, height of building, shading and non-shading factors. Moreover, other parameters give more challenges for the PV design as the tilt and azimuth angle which provide more accurate to the generated power. An analytical approximation of a large scale of PV arrays are studied and introduced as a simplified model in [89]. In this paper, evaluation period of yearly generated power are not related to the size of array design with a better error provided compared to the numerical simulation. Another optimization technique has been applied for a large scale of renewable energy like PV as explained and utilized in [90]. In this paper, and based on multistage and various/multi schemas like echo design principles with consideration of

weather conditions. In addition, the used model is mixed with MO as NSGA-II with a statistical algorithm for deleting the unnecessary objectives regardless the affecting of the main characteristics of the PV design. Due to the variety generated power of PV arrays which mismatch the load requirements are recovered and recouped by using ultra-capacitor as explained in [91]. It's showed that the total cost of a compensated power which made by using ultra-capacitor and fuel cell are reduced to about 40% of the main design in spite of load requirements.

A comparative study is presented for optimizing the generated power of a PV array using MATLAB as in [92]. In this paper, author provided an algorithm for generated power and PV voltage of 71 cell divided and connected differently in parallel and series. Partial Swan Optimization PSO provided an annual energy more than other used techniques with a reduction in PV distribution. PV performances are influenced with Partial Shadow Condition (PSC) which caused a losing of array desired power. According to this truth and according to weather changing elements a tracking model like Maximum Power Point is applied to avoid and solve this problem as showed in [93]. Utilizing of PSO for searching the global point to achieve high efficiency and more reliability using MATLAB to compare it with Incremental Conductance IC. An affection study is withal introduced for PV generated power calculation as a Bypass Diode in [94]. It's showed various configurations of diodes have been investigated with a different shading manner. It is also utilize that through a defined conditions of shading cases, the bypass diodes did not affect the total generated power of PV while this configuration didn't assure this on a Partial Condition of Shading. Same author also presented an impact of the Partial Shading Conditions on PV array maximum power as in [95]. These conditions are mainly related on the sensibility of shadow strongest and weakness points, while searching of a conclusive point which minimize the losses as well as increasing the PV generated power was the main approaches of this article. An ideal technology selection for calculating cost, size and various type of building with a different location and different structures are presented and studied as in [96]. This model is applied for the whole strategy system as PV cells, energy storage unit and the controlling mechanism of PV load. With a better optimization design and a good analytical calculation the Hybrid Energy System HES demonstrated to be a better sources comparing with the Single Energy System SES in reliability and economic as provided and illustrated in [97]. Considering of weather conditions with a multiple technique are used such as a Combined Dispatch (CD), Load Following (LF)... etc. and compared in this article. It's showed that CD provided lower cost per generated watt than other used technique leading to better performances as well. A modified of PSO algorithm are also provided for optimizing a tow objective function related to the generated power and the annual energy with a consideration of weather changing and masking limits as explained more in [98]. This approach utilized the minimum area needed for a specific load required in a selected area.

3.2 PV Selected Model

Needed to a component to have a Balanced of System (BOS) compatibility make Trina Solar Firm a best choice due to its withstanding against weather and environments conditions. In addition 11 GW of PV Trina Solar Module are sold until 2014 as a main supplier for many courtiers like India make it's more available. Withal, this firm is more fixating on amending PV Module efficiency which it is the main reason for this paper design. TSM-PC05 with a 60 cells and 200-220 W. are culled for this paper to be utilized as array of PV Module, its characteristics are shown and more described in Table 3.1 and IV-Curves are additionally expounded with Temperature/Voltage referring conditions in [99].

Table 3.1 Electrical & mechanical characteristics of the PV-TSM-PC05

Electrical & Mechanical Characteristics	Value
Power Rating	200 – 220 W
Power per unit of area	122.2W/m2
Number of Cells	60
Rated Current	6.97 A
Rated Voltage	28.7 V
Length	1,650mm
Width	991.9mm

Active area of picked PV Module has been calculated for this design and for 6 PV array of the same module. In addition Current / Temperature Coefficient and Voltage / Temperature Coefficient are withal calculated according available datasheet information as expounded in Table 3.2.

Table 3.2 PV-TSM-pc05 calculated total used area and current-voltage/temperature coefficient

	Value
Active PV Area (Ac)	1.63m2
Total Area of 6 PV array (Ac1) (connected each 3 in a raw)	4.99m2
Current/Temperature Coefficient (KC/T)	0.003875 A/K
Voltage/Temperature Coefficient(KV/T)	-0.1116 V/K

3.3 Climate Conditions of Selected Area

The chosen environment conditions ought to be characterized and confirmed also of this plan for more exact control incited calculation. For this reason, Climate Specialist v6.0 as a realistic based computer program are embraced and downloaded to hoard data of Common information of Turkey [100]. Assembled data and information which is more related to the plan for the chosen zone (Yildiz Technical University/ Turkey-Istanbul) showed some points to be viewed and concluded as follow:

• Temperature range of the chosen region is annually around (-12 to 43) °C and the leading conditions are primarily concentrated in 7 months from April to October as explained in Figure 3.1.

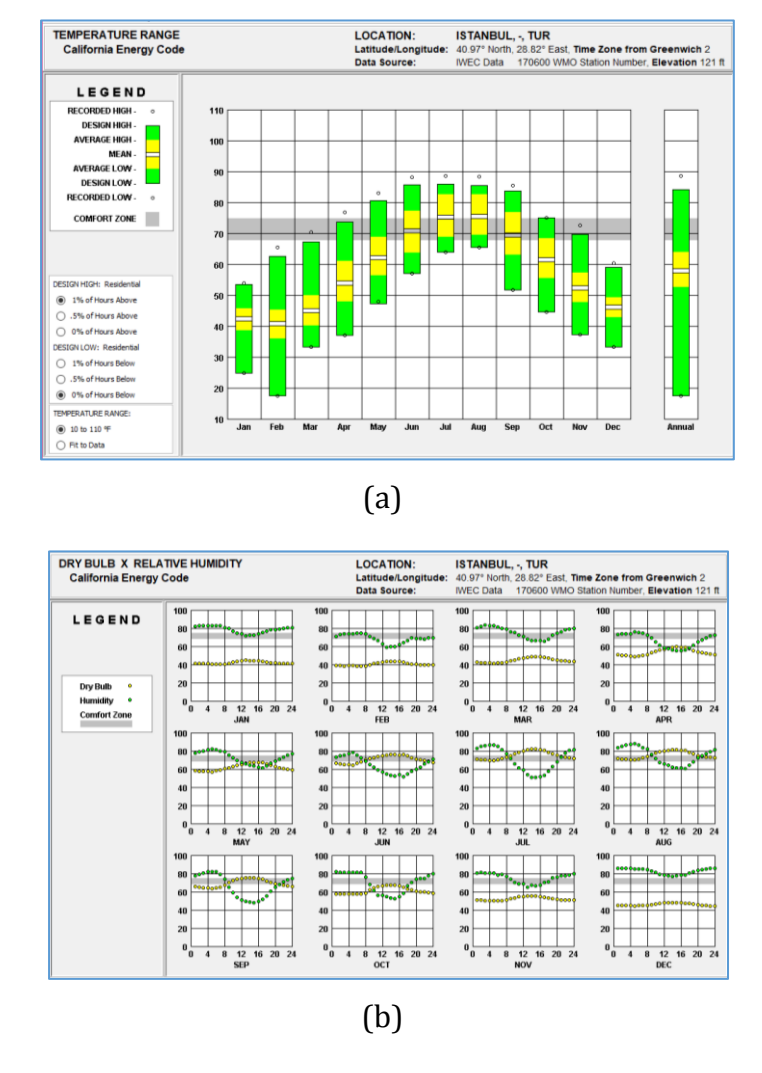


Figure 3.1 Annually temperature range of the selected area (a) temperature range and (b) dry bulb with humidity relation

 Monthly Diurnal Normal of this range appeared that around 8 months are in consolation zone of sun beams run with coordinate or ordinary radiation. As shown in Figure 3.2.

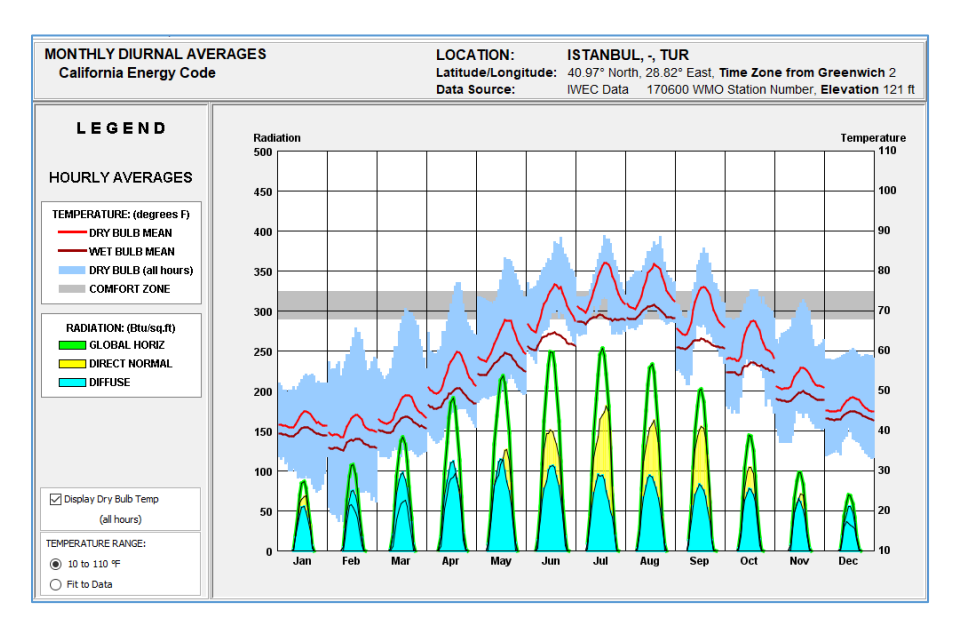


Figure 3.2 Monthly diurnal average of the selected area

Wind wheel chart is additionally pointed to the course of the affected wind which
ought to be connected and entered to the plan information to be considered and
studied. Wind wheel chart are shown in Figure 3.3.

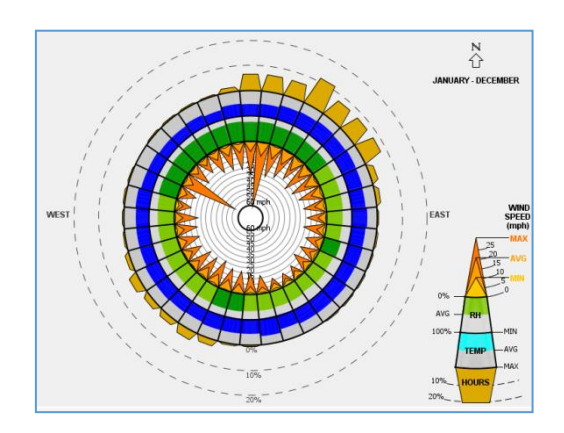


Figure 3.3 Wind wheel chart using climate consultant v6.0 for Turkey/Istanbul

• Shading data moreover appeared that between East and West Racking are the leading heading for the plan with a suitable angle choices. From the factual calculation, 40% of hours are within the comfortable zone with a tall rate of sun beam uncovered. This can be too make the chosen region so imperative to be uncovered to the sun light and within the comfortable zone to assemble more power as shown in Figure 3.4.

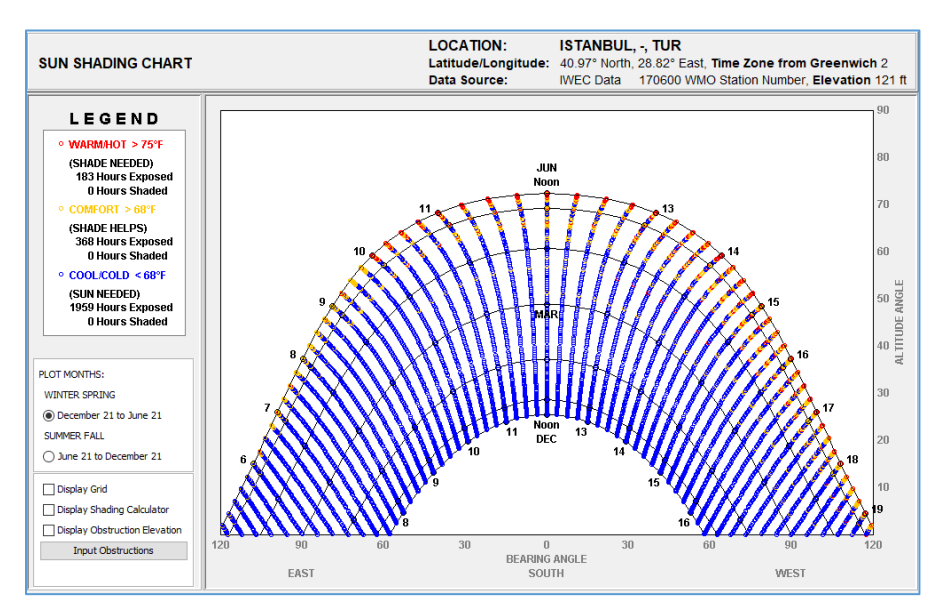


Figure 3.4 Sun shading chart between east and west of the selected area

• 3D chart are also showed that from 8:00 AM – 6:00 PM are reasonable for gathering data and created power as shown in Figure 3.5.

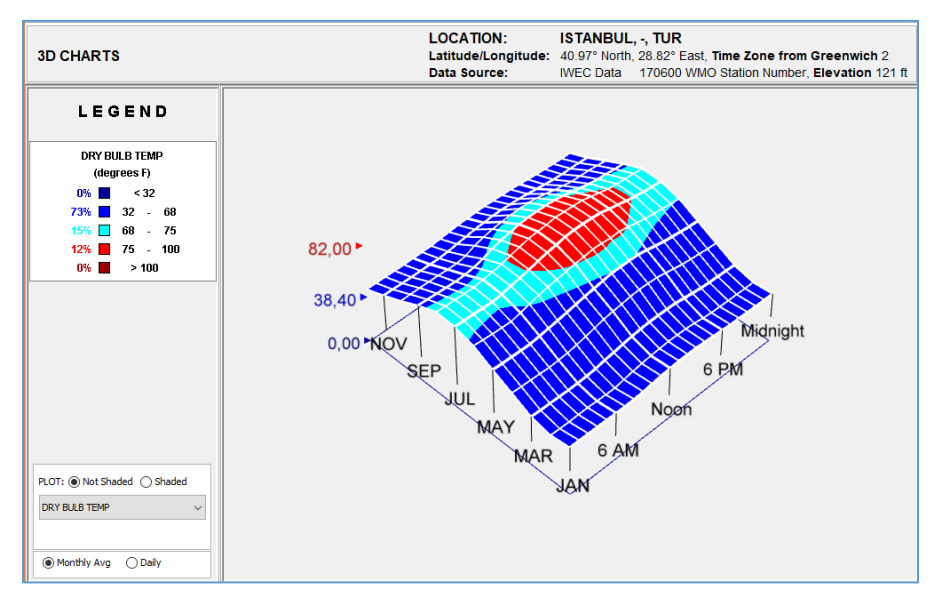


Figure 3.5 Monthly 3D temperature chart according to days light

 Relation with humidity of this range is sort of tall proportion compared to the dry bulb which lead to more challenges for the PV designer and chosen region to rummage around for a great heading and position. More related data are shown in Figure 3.6 about the psychometric data of Turkey.

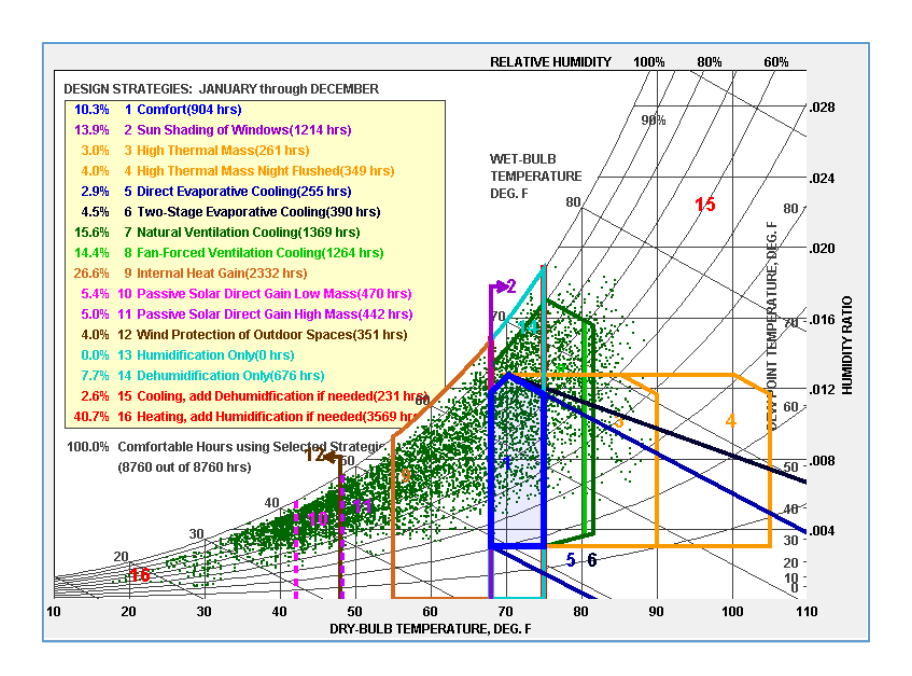


Figure 3.6 Psychometric data using climate consultant v6.0 for Turkey/Istanbul

The area related to the planning simulation is shown in Figure 3.7. This area is used for many reasons as mentioned before to be more exposed to the sun rays with a low ratio of humidity. In expansion, a few of the clarified information are entered manually to the utilized program to induce the most excellent calculation of the gotten power.



Figure 3.7 Simulation area for PV-module design (Yildiz Technical University)

3.4 PV Optimization Techniques

Number of required computational calculation in such a design like PV and different/multiple parameters need an accurate and fast algorithm for a multi objective and function optimization as NSGA-II which explained in more details in [101]. NSGA-II

provided a better spread of individuals solutions compared to another MOEA like GA, DEA... etc. as explained and discussed in many articles with a better performances for the parametric design as in [102]. Principles and algorithm of NSGA-II are shown in Figure 3.8 as presented in [103].

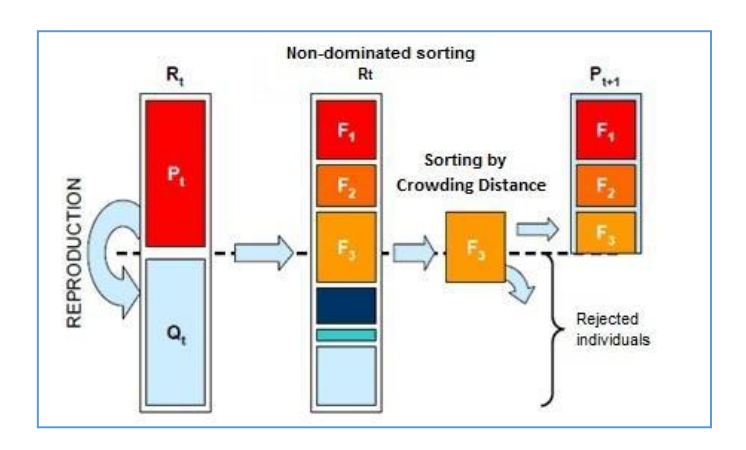


Figure 3.8 Non-dominated sorting genetic algorithm-II working principles [103]

NSGA-II is presented in this work for a three objective function: shaded, un-shaded configuration factors and efficiency of PV panel total system. PV panel optimization is more related to the distance between two panels L, tilt angle and the azimuth angle. By using NSGA-II as optimized technique for calculating multi objective function for configuration factor of shaded and un-shaded regions as in (3.1) and (3.2) respectively. In addition calculating the overall efficiency of the designed model according to panel's number, width and length. The height of the selected array D will be represented and evaluated according to tilt angle α . Figure 3.9 show the related optimized parameters using NSGA-II.



Figure 3.9 PV panel's dimension and related angle for NSGA-II design

$$F_1 = \cos^2(\alpha/2) \tag{3.1}$$

$$F_2 = F_1 - \{ (L/W + Sin^2(\alpha))^{1/2} - L/W \}$$
 (3.2)

Where F_1 for shaded configuration factor calculation, F_2 for un-shaded configuration factor and the limited of the azimuth/tilt angle according to the selected PV design are [20 - 30] / [160 - 230] respectively to get a highest optimization efficiency. The overall efficiency calculated after parametric optimization and according to the applied applications.

For an approximation calculations in West and East Racking Panel of PV array Design, L are so small so compared to the width and the second objective function are calculated according to (3.3).

$$F_2 = F1 - Sin(\alpha) \tag{3.3}$$

3.5 PV Simulation Design Steps

The simulation design of selected PV array with 6 Module are presented and studied for total power and losses calculation using two programs for more accurate results for the total output power to be applied to the automated converter design. The dependence mechanism of this simulation design is shown in Figure 3.10. The steps of designing and simulating PV-array are explained as followed:-

- Selecting PV module as explained in more details in Section 3.2.
- Specifying Area and other related parameters for the overall design as explained in Table 3.2.
- Defining the weather and environment conditions as well as the selected area as explained in section 3.3.
- Applying NSGA-II obtained parameters for the design for a better PV array Design performances as explained in 3.4 section.
- Comparing the two program results to obtain the exact output voltage from the two selected program and specify the main parameters.

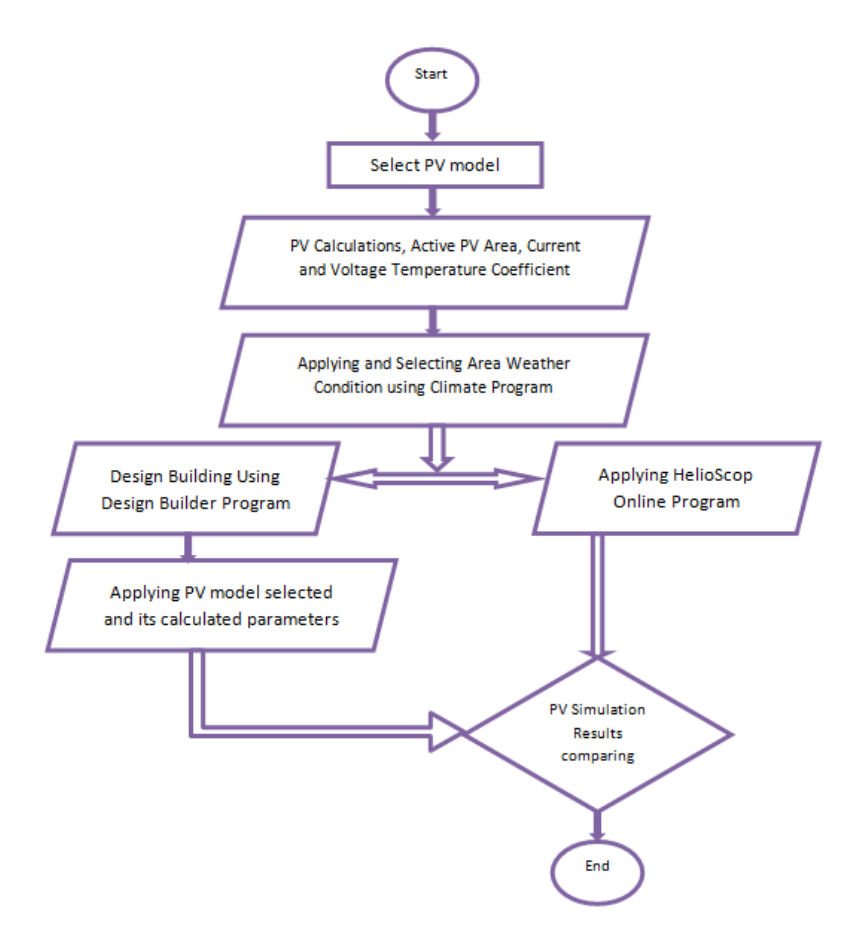


Figure 3.10 Flow chart of PV simulation design using two programs with applying weather conditions

3.6 Simulation Results

HelioScope and Design Builder are used as a 3D application and applied for simulating solar performances for a better optimizing for gathering information. Utilizing Helioscope is diminishing the plan time particularly it works as a PV test system and an AutoCAD program. All of the collected information from Climate Expert will be connected to accumulate the resultant generated power value from 6-array of TSM-PC05 Module. Indicating the Module parameters, height of chosen building, racking sort, azimuth and tilt point, number of Module to be outlined, add up to zone utilized for recreation as calculated before for 6-PV cluster associated Module. Figure 3.11 shows the chosen range with a little building for an indicated number of PV modules.

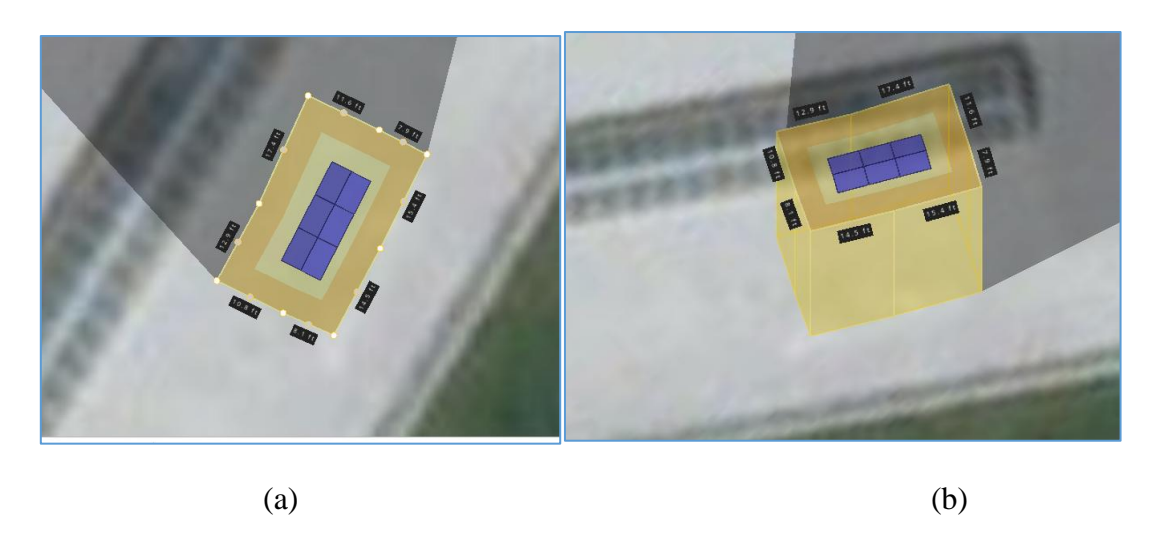


Figure 3.11 Building design areas with 6 array of selected PV module (a) top view and (b) side view

PV module and other parameters are entered manually with the required angle as shown in Table 3.3.

Table 3.3 Helioscope applied parameters for PV simulation after NSGA-II optimization.

Parameter	Value	
Height of Building	48 ft	
Azimuth angle	207	
Tilt Angle	10	
Racking Type East-West Racking		
Solar Module Type	Trina Solar TSM-200 PC05(200 watt)	

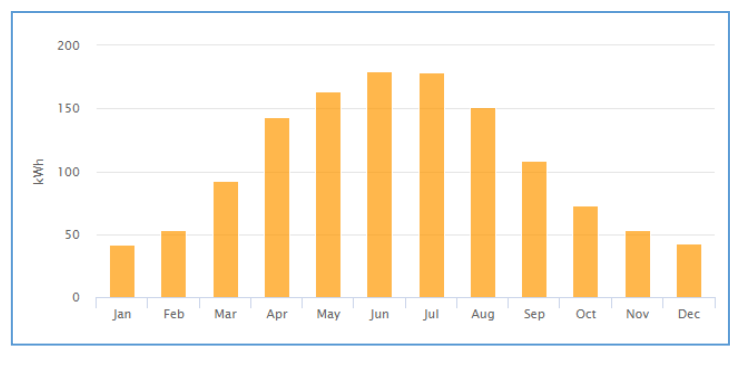
Optimization Parameters according to NSGA-II are shown and more utilized in Table 3.4 with objective function and overall efficiency calculation.

Table 3.4 The summary of the annually building performances using NSGA-II

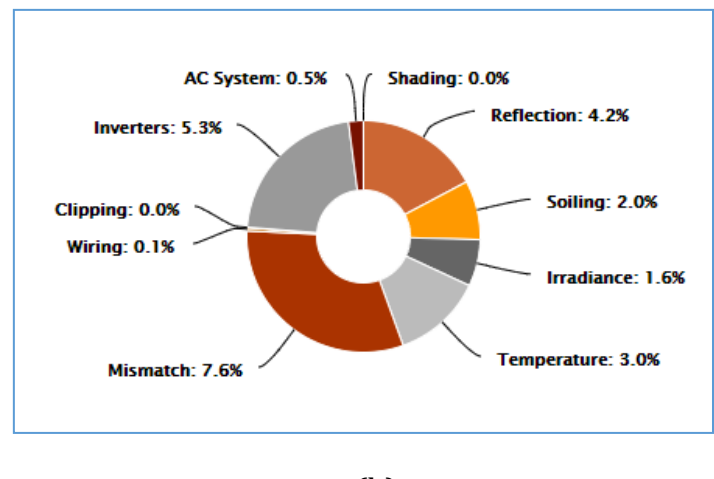
Azimuth	Tilt	F ₁	F ₂	Generated Power (kW)	Efficiency
214	19	0.994352	0.844475	1,005.00	84%
218	8	0.42725	-0.56211	1,007.00	84%
200	27	0.353931	-0.60245	994.00	83%
195	16	0.22117	0.309074	962.00	80%
207	10	0.080464	0.624485	1,101.00	92%
226	8	0.42725	-0.56211	923.00	77%
229	9	0.544435	-0.36768	927.00	77%

According to Table 3.4, the highest efficiency achieved is occurred when azimuth angle and tilt angle are 207 and 10 respectively. While the distances between two raw of panels are so small due to the racking type selected for PV module and other parameters are drawn and entered manually with the required angle.

Climate dataset for the chosen range are moreover connected to this program to gotten more exact simulation results, 78% of PV Module exhibitions are procured with the chosen conditions and almost 1.068 kW are picked up from this design. The program appeared that around 5.3% of losing power is basically due to the power inverter. In addition, the designer should attempt numerous times for matching between the inverter and the module to induce the highest performances. The expected power of such a Module is around 1.2kW, instead the procured appeared approximately 11% diverse by optimize the PV Module parameters. Figure 3.12 showed the monthly production of this design.



(a)



(b)

Figure 3.12 PV module simulation results for TSM-200PC05-6 array connected (a) monthly production of the module designed and (b) system main losses sources

A PV grid connected design are also simulated using more complicated software which need to draw the chosen area and then placed the selected PV Module on the building's roof. The main steps for this software and such an article design are explained as followed:-

• Drawing the selected area according to the exact shape extracted from the Google Earth as shown in Figure 3.13.

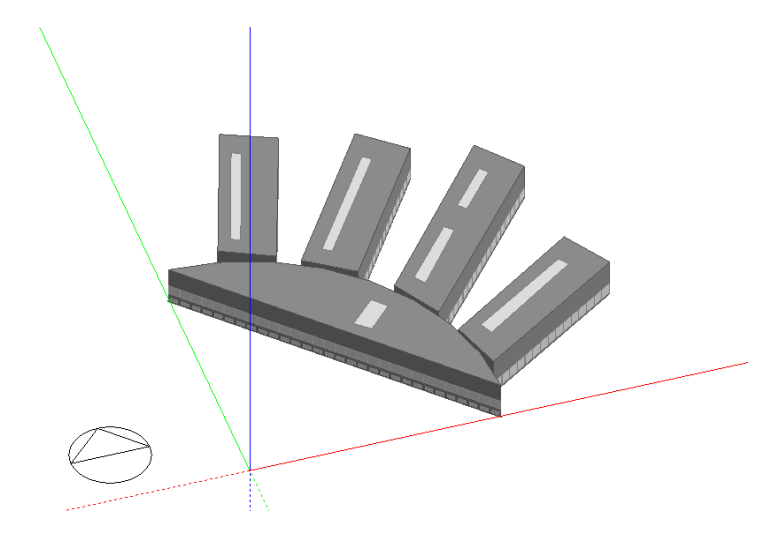


Figure 3.13 Simulated building using design builder software in 3 dimensions

 Place the solar array on the roof of the selected building according to total active area calculated in Table 3.2 for 6-PV Module with the desired connection type.
 Figure 3.14 showed the Solar Array of the design Module.

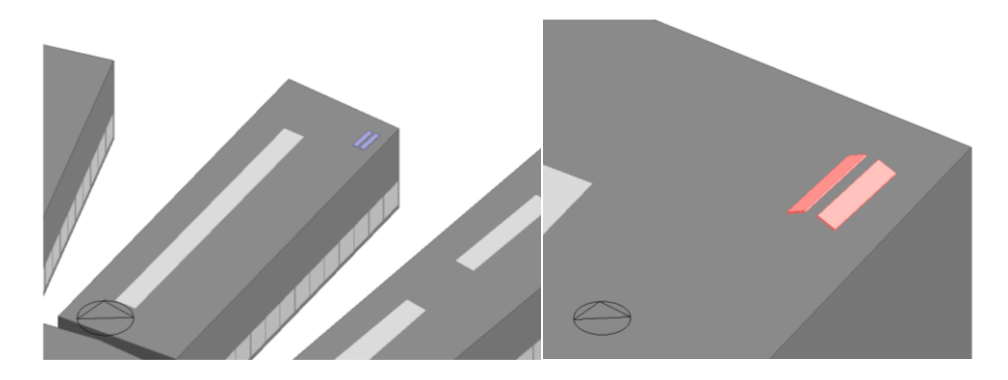


Figure 3.14 Solar arrays on the roof of the selected building

- Selected the PV Module from the software list.
- Gathering information about the simulated design as an annual building utility performances summary. Total generated power is 1.101 kW from the chosen PV-Module. About 8% of losses are gained from this software without even applying or using the inverter, which leads as well to the important of designing the power converter/inverter for such an application.

Table 3.5 showed the annual report over 8760 hours according to selected parameters and the PV Module as well.

Table 3.5 The summary of the annual building utility performance using design builder software for 8760 hours on 2019-02-05 at 02:58:13 after NSGA-II optimization.

	Electricity [kWh]
Photovoltaic Power	1.607
Total On-Site Electric Sources	1.607
Electricity Coming From Utility	1.099436
Net Electricity From Utility	1.099436
Total On-Site and Utility Electric Sources	1.101043
Total Electricity End Uses	1.101043

3.7 Summary

PV panel design is more complicated due to its relation with weather conditions based on shaded and non-shaded configuration and due to selected tilt angle and azimuth angle. Such a design needs an optimization for all related parameters before deploying PV module on the roof of any building. NSGA-II provides fast and accurate individuals solutions according to its crowding distance and non-dominated features of this technique compared to other Multi Evolutionary Optimization Algorithms. Spaces between two line arrays are also added to the design for more sun rays exposed and affection, azimuth angle showed a better results with 207° with tilt angle of about 10° for 6 array of PV selected Trina Solar module. Yildiz technical university in Istanbul/Turkey are selected for this PV design and east and west racking gave more accurate and better performances of the PV design. After parameters optimization two programs are utilized for this design Helioscope and Design Builder program to compare and get a better simulation results. In addition, this design showed the affection of PV design on the used inverter and vice versa. 6-array of PV module showed an efficiency of 92% with 1.101043 kWh as an annual collected power. Moreover, design showed the affection of gathered power through year and the wasted power caused by inverter/Converter selection. As a future work applying this PV design array and according to gathered and optimized parameters with a high frequency switching topology as a power conversion/inversion circuit.

4

SINGLE & THREE PHASE TRANSFORMER STRUCTURE DESIGN

In order to obtain a good optimization method for the electrical transformer design with optimal parameters selection, performance evaluation of three evolutionary algorithms (Genetic Algorithm (GA), Differential Evolution Algorithm (DEA) and Non-dominated Sorting Genetic Algorithm (NSGA-II)) are carried out. The aim is to optimize transformer design parameters (core thicknesses, number of turns, conductor areas and some other related parameters) for minimization of total power losses (No-Load Losses (NLL) and Load Losses (LL)) in single & three phase transformer topology while maintaining high efficiency and low cost. The method used for this optimization scheme combines the Finite Element Method (FEM) and Evolutionary Algorithms (EAs) to provide an accurate selection of parameters together with the optimized magnetic flux density and decreased loss. Experimental results show that NSGA-II+FEM model successfully provides a global feasible solution by minimizing total loss and related cost while improving efficiency of single & three phase transformer, rendering it suitable for application in the industrial transformer design environment.

4.1 Introduction

Proper design of a transformer generally requires minimizing the manufacturing cost, satisfying the requirements and increasing the efficiency. In order to utilize an Evolutionary Algorithms (EAs) for the optimal design of an electrical transformer, an objective function has to be developed. These component costs, as well as the constraint functions must be expressed in terms of a basic set of design variables [104]. In [105], it is stated that the total cost of the transformer is dependent on primary turn and is also related with the magnetic flux density. Power losses minimization depending on transformer parameters is presented in [106-108]. In [109], transformer design optimization using GA for cost minimization is studied. Achieving the optimum balance

between the transformer cost and performance is a complicated task, and the techniques that are employed for the solution must be able to deal with the design considerations and constraints, while remaining cost-effective and flexible. Considering power loss minimization, NLL and LL are one of the main objectives in the transformer optimization. NLL are the continuous losses of the transformer regardless the load; it's also called iron or core losses. LL result from load currents following through transformer; it is also called copper or wire or winding losses [110]. Expressing NLL and LL as a function of transformer core's parameters are adopted by means of Artificial Neural Network (ANN) as in [111-112]. In [113], a hybrid structure consisting of a Decision Tree (DT), ANN and GA is presented. In [114], the application of one deterministic and three non-deterministic optimization algorithms is studied for global transformer design optimization. In [115], a bibliographical study and general backgrounds of research and developments in the field of transformer design and optimization using intelligent based techniques for the past 42 years, based on over 80 published articles is provided. Artificial Bee Colony algorithm (ABC), Bat algorithm, Cuckoo search algorithm and other algorithms have been suggested as a modern Bioinspired Artificial Intelligent technique for transformer design optimization as in [116]. It is also provided significant information about future work related to this type of design optimization. Four objective functions (total active part cost, total loss, percentage impedance and transformer tank volume) have been studied and optimized for 100 kVA three phase core type transformer as in [117]. In this paper, two MATLAB programs used: the first is unconstrained minimization for all the four objective functions and the second is just for the active part cost function using GA and conventional methods. Another researches taken into account other parameters like leakage inductance, phase shifted angle and voltage ampere rating as in [118]. In this paper, an optimization of a High Frequency Transformer (HFT) used in a bidirectional dual active bridge isolated Dc-Dc converter is presented. Moreover, it is showed that the Zero Voltage Switching (ZVS) can be achieved without used any extra inductor by specifying the required leakage inductance to achieve it. In [119], GA based searching technique is used to optimize the coil geometry of an Eddy Current non-destructive Testing Probe (ECTP) and the electromagnetic field is computed using Finite Element

Method Magnetic (FEMM). Numerical techniques as a mathematical function tool are extensively used and presented in many of transformer optimization design. One of the most common mathematical tools is Finite Element Method (FEM). The combination of Artificial Intelligence (AI) techniques with the numerical analysis methods have been also used to calculate and minimize core losses as in [120] where FEM is combined with Simulated Annealing (SA) to define transformer core variables. In [121-122], experimental results are presented by combining GA and FEM. DEA was also used for a complex and multiple objective optimizations, the design of recursive digital filter with 18 parameters with multiple constraints and objective one of these complex problems which it was solved in [123]. A novel Pareto-frontier DEA has been presented in [124] to solve multi objective optimization problems. DEA is also used to solve a transient stability problem which has been presented in [125-126]. In [127], it is used for reactive power and voltage control in power system operations as an optimization technique. A modified DEA has been studied for solving optimal power flow [128]. Optimum design of a single and three phase transformer using GA and FEM is presented in [129]. Three phase transformer design optimization is also studied in [130]. Another study of using FEM in calculating the flux paths in the transformer is carried out in [131] using a nonlinear high resolution magnetic equivalent circuit. Transformer loss optimization has many applications for electronic circuits design with isolated input/output power where total loss, soft switching approach and bidirectional power flow is of concern [132-133]. The main contributions of this section are: I) introduction of a new overall transformer optimization method (NSGA-II+FEM), minimizing both the overall transformer power losses and transformer cost. II) expansion of the solution space by EA techniques that define the variation of crucial design parameters such as the core thickness, number of turns and conductor areas, ensuring global optimum transformer design, III) study of EA own parameter effect on cost function minimization and IV) incorporation of FEM in order to validate the feasibility of the optimal designs. Following introduction part, single & three phase transformer model are explained in section 3.2. Proposed mathematical combinational model together with the details of EAs and FEM are explained in section 3.3 and section 3.4. Section 3.5 provides the experimental results of

EA+FEM based optimization of three phase transformer design. Finally, section 3.6 presents the Summary remarks and suggestions for future work.

4.2 Single & Three Phase Transformer Model

A commercial single & three phase transformer has been chosen for the EA based design; architecture and specifications of that are provided in Figure 4.1, 4.2, 4.3 and Table 4.1, respectively.

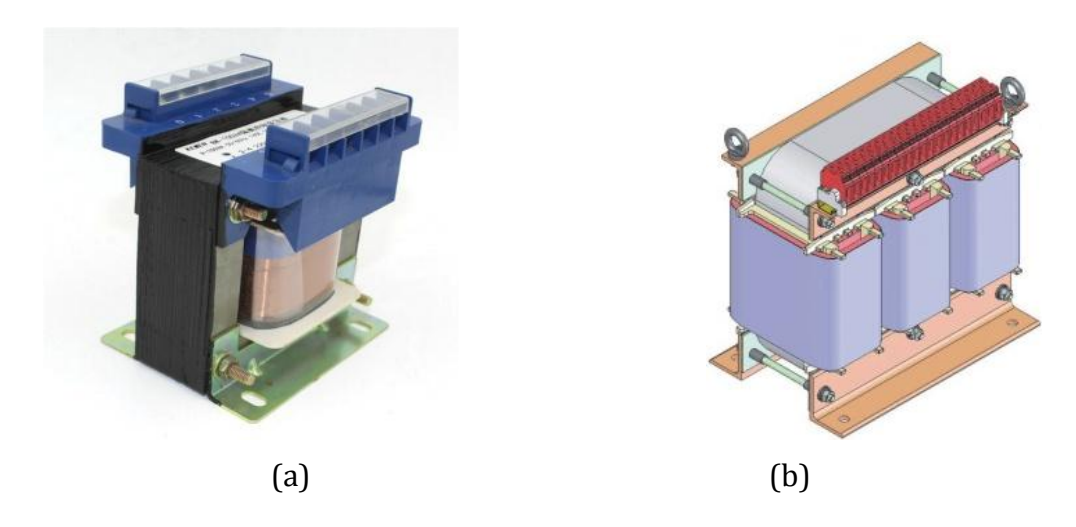


Figure 4.1 Commercial prototype transformers architecture of (a) single phase transformer (b) three phase transformer

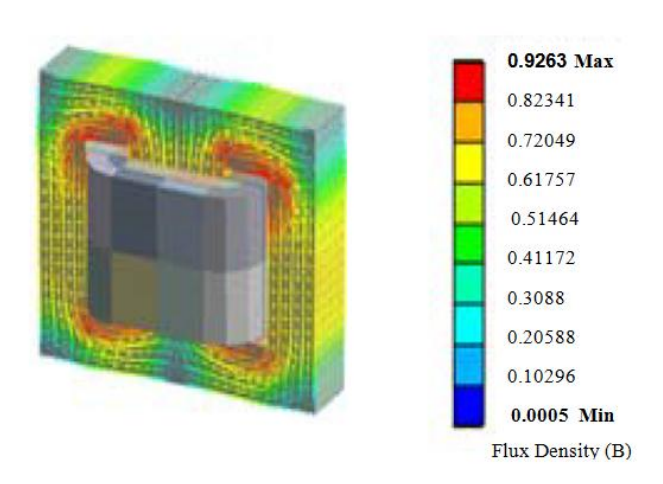


Figure 4.2 Flux density distributions of FEM calculations of single phase transformer

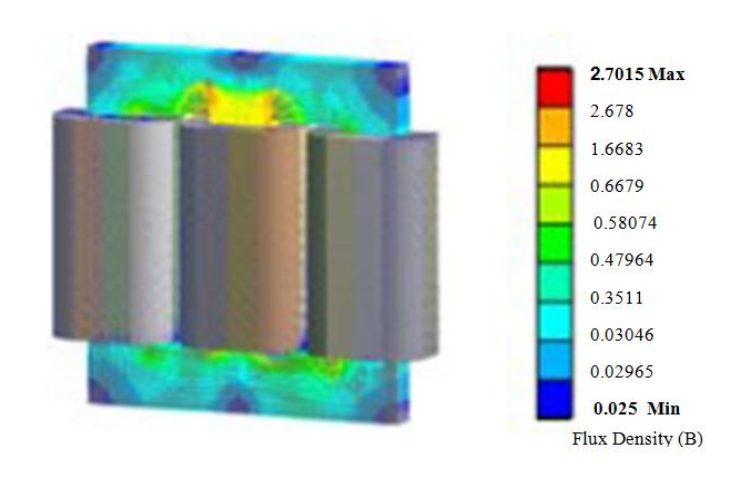


Figure 4.3 Flux density distributions of FEM calculations of three phase transformer

Table 4.1 Specifications of single and three phase transformer

Symbol	Quantity	Single Phase	Three Phase
V_{Tin}/V_{Tout}	Input /Output Voltage	220/12 V	6000/380 V
I _{Tout}	Output Current	1.25 A	1.52 A
P _{Tout}	Output Power	165 W	1 KW
X ₁	Core Thickness	20 mm	50 mm
X ₂	Primary Turn Number	950 Turn	8259 Turn
X ₃	Secondary Turn Number	80 Turn	31 Turn
X ₄	Primary Conductor Area	4.56*10 ⁻⁷ m ²	7.85*10 ⁻⁷ m ²
X ₅	Secondary Conductor Area	1.10*10 ⁻⁶ m ²	2.82*10 ⁻⁶ m ²

4.3 Optimization Tools

Optimization algorithms (GA, DEA and NSGA-II) with a mathematical tool (FEM) have been proposed for the minimization of LL, NLL and total losses (NLL+LL) of three phase transformer. GA modifies the population of individual solutions by selecting individuals from the current population to be parents and produce the next children (off-spring) population using two processes (cross-over and mutation) [134]. During search process,

the population evolves toward an optimal solution. DEA is a direct search algorithm has been selected for NLL and LL calculations [135]. It depends on the distance calculations by selecting three solutions and creates the new generations depending on these calculations. On the other hand, NSGA-II is a fast sorting and elite multi objective genetic algorithm [136]. First generation is implemented randomly; the selection of parents depends on the rank and the crowding distance for each individual. Parents and offsprings in NSGA-II are combined so that the non-dominated individuals get the optimal value while other individuals move to next set. These sets are called "Pareto Front" individuals. FEM is employed together with these EAs as a mathematical tool for analyzing these individuals for the transformer structure.

4.3.1 Genetic Algorithm

GA searches among a set of chromosomes for an appropriate solution of a fitness (objective) function to measure or calculate the value of the selected chromosomes. In other words, GA provides a score for these individual solutions. Selection from the initial chromosomes to reproduce new off-spring chromosomes is carried out using a selection, mechanism. New reproduction is done with cross-over operator. Following, mutation operator flips an arbitrary selective number of bits in chromosomes to another usable form. The new generations of chromosomes after these operators will be calculated by the GA using the same fitness function, repeating the steps from the selection [134]. GA model combined with FEM for transformer performance enhancement is given in Figure 4.4.

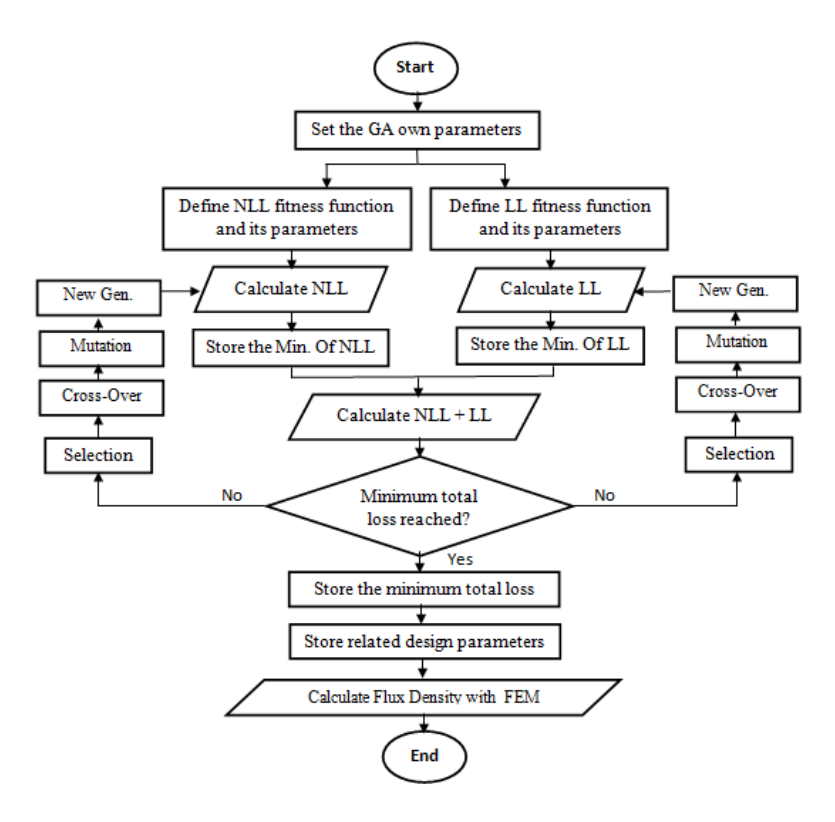


Figure 4.4 Detailed flow chart of GA+FEM optimization model

4.3.2 Differential Evolution Algorithm

DEA is a parallel direct search methods used also with multi objective functions, has been selected as one of the EAs algorithm to be applied on NLL and LL fitness functions. It requires a few controlling parameters with a good individuals diversity. DEA starts with a randomly initial population and generating testing (trial) individuals. It creates new individuals using two weighted different solutions, a comparison between these individuals will lead to a new generation if the objective functions (NLL+LL) are minimized. By calculating distance between two individuals and compare it to the third one DEA provides a convergence property as explained in [135]. A several variant of DEA formula has been tested and discussed, DEA1 has been selected to be applied on NLL+LL as in (4.1)

$$v_{i} = X_{i1,G} + F \cdot (X_{i2,G} - X_{i3,G})$$
(4.1)

where X_{i1} , $X_{i2,G}$, and $X_{i3,G}$ is [0, Npop-1], v is a new generated solution, G is generation number and F > 0. And for keeping and increasing diversity to a new generation with the

selected and required boundaries, a new vector of solutions should be considered as in (4.2).

$$Uj = \begin{cases} v_j & \text{if } X_i \text{ is } [X_{i,\min}, X_{i,\max}] \\ (X_{i,G})_j & \text{else where} \end{cases}$$
 (4.2)

Where U_j is a new solution, related tov_j , to satisfy the diversity and boundaries of selected parameters. According to these steps, DEA model for loss optimization is constructed. DEA combined with FEM for transformer performance enhancement is given in Figure 4.5.

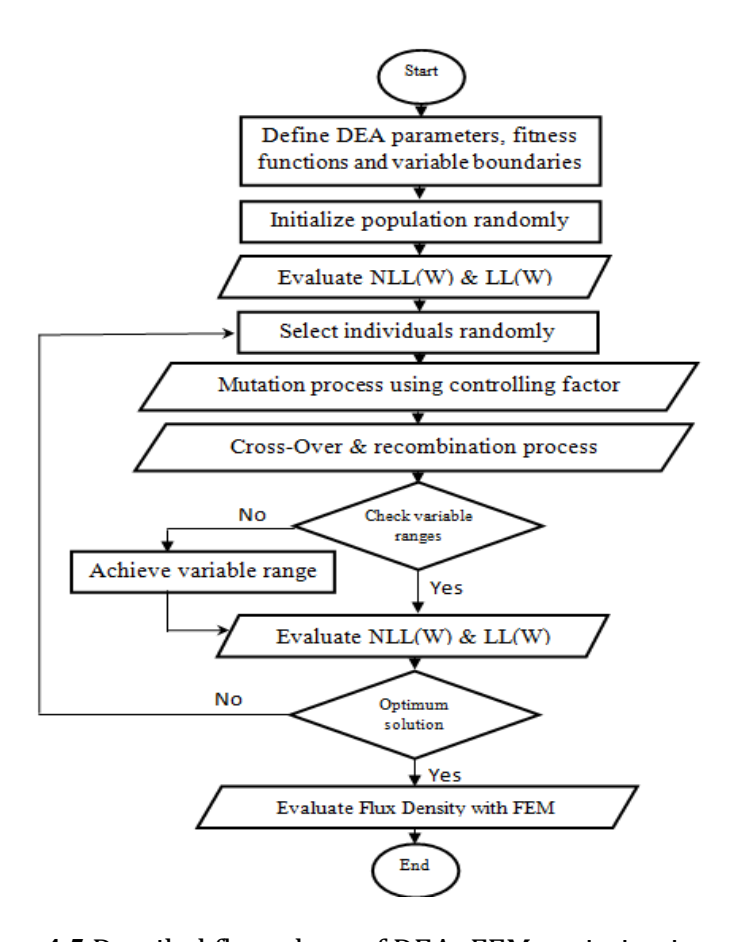


Figure 4.5 Detailed flow chart of DEA+FEM optimization model

4.3.3 Non-dominated Sorting Genetic Algorithm

Some of the Multi Objective (MO) problems' solutions need a set of optimal point (called as Pareto-Optimal points) instead of a single point of solution. GA gives a number of solutions for a MO problem simultaneously; however this requires a long execution time

to calculate such multiple objectives and it will be sensitive to the selected single objective problem. NSGA, a MO optimization algorithm, explores multiple Pareto-Points of solution instead of single as GA has [136]. The cross over and the mutation operator are the same as in GA. The selection in NSGA is applied after determination of non-domination individuals. In order to keep diversity, the population is then combined and shared with initial population to improve the reliability of NSGA [137-138]. Difficulties of computational calculations especially for MO problems, the population size, non-elitism approach, and the need to specify a sharing parameter are revised in NSGA-II [139-145]. The proposed NSGA-II model combined with FEM for transformer performance optimization is given in Figure 4.6.

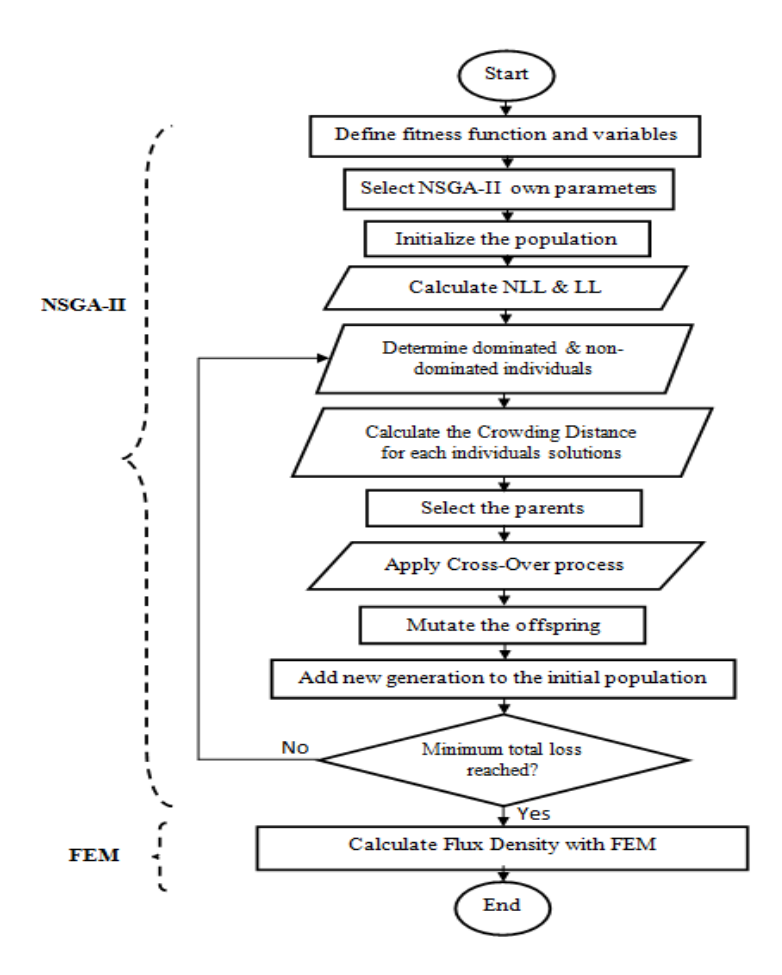


Figure 4.6 Detailed flow chart of NSGA-II+FEM optimization model

4.3.4 Finite Element Method

FEM has received wide popularity in numerical solution of the Maxwell set of equations which defines the magnetic flux density and electromagnetic field in every point of machine cross section. Method involves the discretization of the whole analyzed domain in small triangle surfaces, which are called FEM. FEM calculation can improve a design by means of performance and cost [146]. In this work, FEM is used to calculate the flux density according to the transformer design parameters. After obtaining the optimal parameters from the GA, DEA and NSGA-II, FEM is applied to calculate flux density as shown in following steps [147 - 148]:

Step 1: Calculate the flux density according to the core thickness (X_1) , assuming that flux is B_1 .

Step 2: Same calculation is applied according to the primary turn number (X_2) , secondary turn number (X_3) , primary area (X_4) and secondary area (X_5) separately to obtain $(B_2...B_5)$.

Step 3: The sum of two followed flux density values is calculated as (B_i+B_{i+1}) .

Step 4: Total flux density B is then calculated as the total sum of sub values.

4.4 Proposed Mathematical Combinational Model

Well-defined transformer parameters and equations are the key principles of the combinational optimization scheme proposed in this work. Specifying the best individuals' solution (a set of Pareto-Optimal points) using EAs and applying FEM model to those individuals aims to improve accuracy and reliability. NLL (which it is referred to iron/core losses) exists in the transformer core whenever the transformer is energized regardless of the load. Magnetization and demagnetization of the core lamination causes a Hysteresis loss, which mainly depends on the flux density and core material as given in (4.3).

$$H_{L} = k_{h} \cdot f \cdot (B_{Max})^{n} \tag{4.3}$$

where H_L is Hysteresis loss per unit volume, k_h is hysteresis constant, f is the transformer frequency, n is Steinmetz constant and is equal to 1.6 for iron. Magnetic

field variation and lamination eddy current generates a heat loss. It is also referred to eddy current losses and is also a part of NLL as well. It mainly depends on flux density and core thickness as given in (4.4).

$$E_L = k_e \cdot f^2 \cdot (B_{Max})^2 \cdot (X_1)^2$$
 (4.4)

Where E_L is the eddy current losses, k_e is eddy current constant. LL (which it is referred to copper/short circuit losses) occurs in the winding resistance when load is carried to the transformer. An ohmic heat loss (one of the main LL losses) depends on the winding resistance as given in (4.5).

$$O_L = (I_{TOut})^2 \cdot R_W. \tag{4.5}$$

Where O_L is the Ohmic losses, I_{TOut} is the transformer load current and RW is the winding resistance which depends mainly on the primary and secondary area (X_4 and X_5 , respectively). Various types of losses like harmonic, unbalanced and extra losses due to current or voltage distortion occur when nonlinear electrical devices are loaded [149]. The proposed mathematical model is used to minimize the losses at no load and load conditions for a single & three phase transformer in a way to be more compatible with the calculation of the transformer cost. Therefore; design steps of the proposed model are given as:

- 1. Set the algorithm own parameters for GA, DEA and NSGA-II, the objective parameters are bound in some constrained functions.
- 2. Calculate objective functions (NLL and LL) [23]. Objc₁= Min (NLL) = Min (F_1)

$$Objc_2 = Min (LL) = Min (F_2).$$

$$F_1 = K_1 \cdot X_1 \cdot B \tag{4.6}$$

$$F_2 = K_2 \cdot X_1 \cdot S_2 \tag{4.7}$$

Where X_1 is the core thickness, K_1 is the no load fitness coefficient and K_2 is the load fitness coefficient, theses fitness coefficients have to be larger than zero. In addition, they were designed and tested on single and three phase transformer before used. The differences between the selected five variables and B (the transformer flux density) in units made these coefficients so important to be chosen for the transformer design.

While B is related to all of the parameters and coefficients which are chosen to produce feasible solutions (C_1 - C_5) as in (4.8).

$$B = C_1 + \sum (C_{i+1} \cdot X_i) \tag{4.8}$$

 S_2 is the ratio of secondary turn number (X_3) to the secondary conductor area (X_5) as in (4.9).

$$S_2 = X_3 / X_5$$
 (4.9)

No-load and load coefficient ratio R refers to (4.10).

$$R = K_1 / K_2$$
 (4.10)

 S_1 is the ratio of primary turn number (X_2) to the primary conductor area (X_4) as in (4.11)

$$S_1 = X_2 / X_4$$
 (4.11)

- 3. Store the minima of each objective function (NLL and LL) for GA, DEA and NSGA-II.
- 4. Select the off-spring according to crossover probability, crowding distance and ranking, then for NSGA-II combine the initialized population and the offspring to recalculate the two objective functions and also to determine the Pareto front solution.
- 5. After determining the best individuals for each objective function, apply FEM on those best solutions for the optimized result.

4.5 Experimental Results

4.5.1 Single Phase Transformer Optimization Design using GA and NSGA-II with FEM

GA based calculations are carried out using MATLAB 2017 as shown in Figure 4.7 where the total loss of the prototype is decreased to 64.47 after NLL and LL calculations. In addition, the flux density of the single phase transformer is minimized to 0.95 using the FEM calculations as given in Table 4.2.

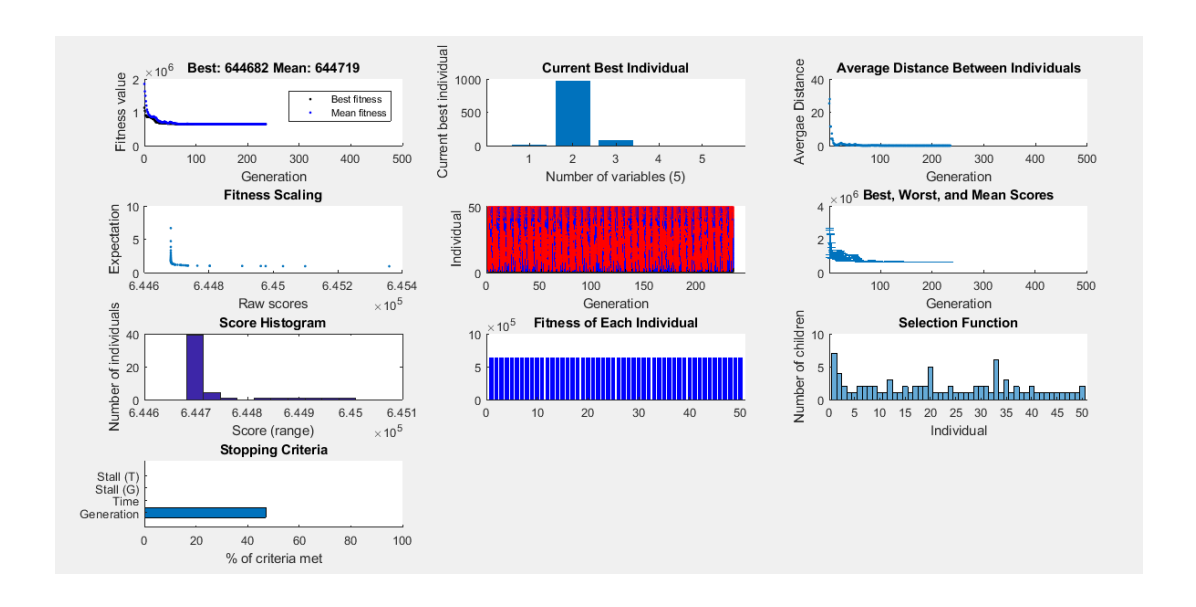


Figure 4.7 Computational results of GA for single phase transformer

Calculations of NSGA-II are shown in Figure 4.8 and Figure 4.9 for the fitness evaluations of NLL and LL, respectively. Those figures also demonstrate the relationship of loss calculations and transformer design parameters. Results show that the obtained losses in Figure 4.8 and Table 4.2 for NLL calculations are minimized when compared to the selected prototype single phase transformer; however it's close to the value obtained with GA. LL value obtained with NSGA-II is decreased to about half the value obtained with GA. Calculated parameters (for example, the primary turn number - X₂) affects both the LL loss and flux density. EAs minimized NLL and flux density almost the same amount. However, LL is minimized with NSGA-II leading to that the overall total losses and the efficiency are both enhanced and optimized with NSGA-II.

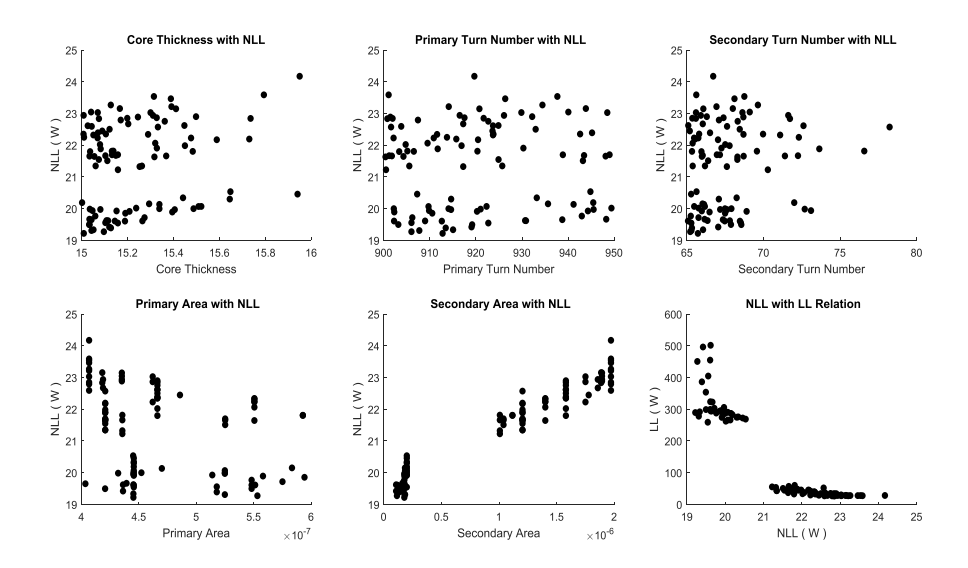


Figure 4.8 NSGA-II based results of NLL relationship with specific parameters of single phase transformer

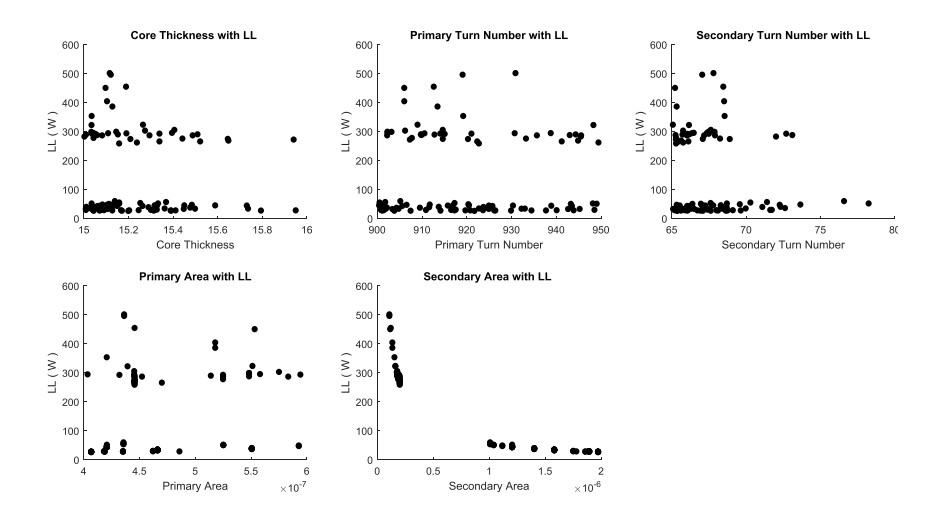


Figure 4.9 NSGA-II based results of LL relationship with specific parameters of single phase transformer

Resulting design parameter values and loss calculations of single phase transformer with the proposed EAs are given in Table 4.2. The results show that NSGA-II method outperforms GA for loss optimization.

Table 4.2 Design parameter and loss calculations of single phase transformer

Symbol	Quantity	Prototype	GA	NSGA-II
X ₁ (mm)	Core Thickness	20	15.662	15.199
X ₂ (Turn)	Primary Turn Number	950	905.12	921.66
X ₃ (Turn)	Secondary Turn Number	80	76.585	65.356
X ₄ (m ²)	Primary Area	4.56*10 ⁻⁷	4.355*10 ⁻⁷	4.06 *10 ⁻⁷
X ₅ (m ²)	Secondary Area	1.10*10 ⁻⁶	$1.007*10^{-6}$	1.971*10 ⁻⁶
B(T)	Flux Density	1.017	0.9506	0.989
NLL(W)	No-Load-Loss	3.092	2.2632	2.285
LL(W)	Load-Loss	75.971	62.207	26.319
NLL+LL	Total Loss	79.063	64.47	28.604

Table 4.3 provides other individual selections obtained with NSGA-II to produce another possible solution for different total loss values which are greater than optimized total loss. It can be seen that NSGA-II provides the optimum design parameters which can produce minimum amount of total loss and maximum transformer performance.

In order to evaluate the optimization performances of EAs, each algorithm is run 20 times with optimal own parameters. The resulting objective function values (NLL and LL) are used to produce box and whisker plots to show median performances as well as outliers as given in Figure 4.10.

Table 4.3 Total loss values for varying NSGA-II calculated design parameters of single phase transformer

X ₁ (mm)	X ₂ (Turn)	X ₃ (Turn)	X4(m²)	X ₅ (m ²)	В(Т)	Total Loss (W)
15.04	903.78	67.62	4.066 *10 ⁻⁷	1.97 *10 ⁻⁶	0.988	29.21
15.09	923.58	65.18	4.857 *10 ⁻⁷	1.77 *10 ⁻⁶	0.978	31.14
15.07	900.77	71.73	4.180 *10 ⁻⁷	1.88 *10 ⁻⁶	0.996	32.23
15.79	901.04	65.61	4.066 *10 ⁻⁷	1.97 *10 ⁻⁶	0.982	29.81
15.41	920.74	66.07	4.351 *10 ⁻⁷	1.89 *10 ⁻⁶	0.988	30.40

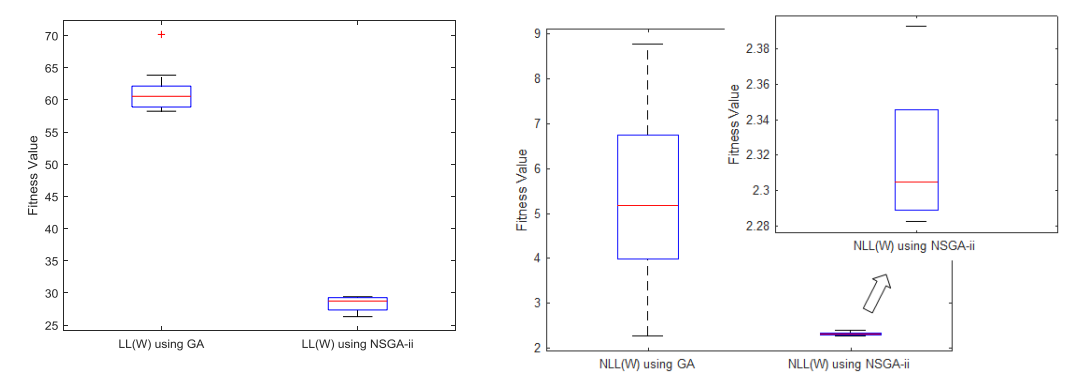


Figure 4.10 Results of (a) no-load-losses(NLL) and (b) load-losses(LL) box-and-whisker plot for GA and NSGA-II of single phase transformer design

Upper and lower ends of boxes represent 75th and 25th percentiles. Median is depicted by the red line. The whiskers are lines extending from each end of the boxes to show the extent of the rest of the data. Outliers are data with values beyond the ends of the whiskers. Box plot of the total losses obtained with EAs are given in Figure 4.11. According to that, NSGA-II based optimization results in higher performance than that of GA for the single phase transformer design. Figure 4.12 and 4.13 show that EA based methods calculate similar flux density amount using FEM.

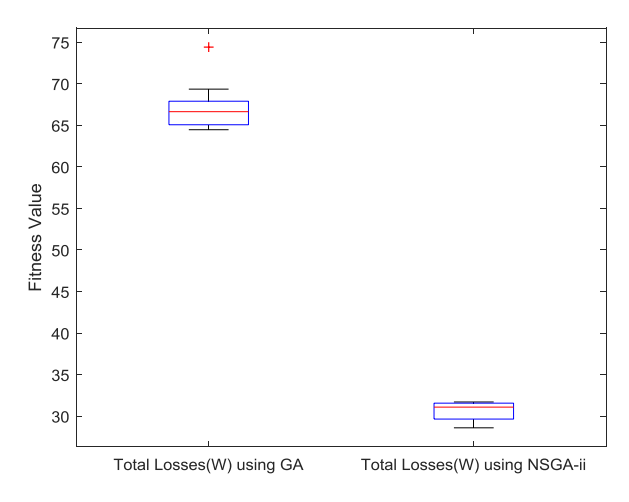


Figure 4.11 Results of total loss by using box-and-whisker plot for GA and NSGA-II of single phase transformer design

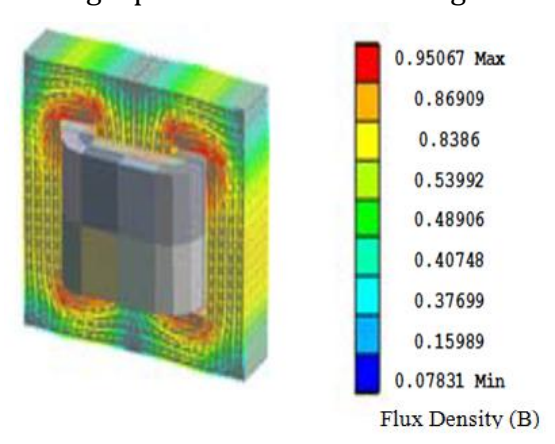


Figure 4.12 Flux density of GA for the FEM calculations

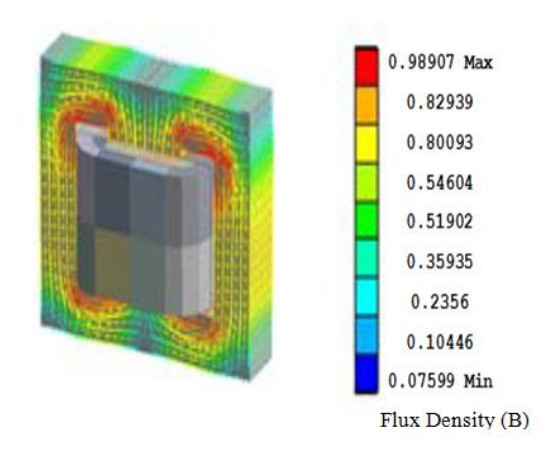


Figure 4.13 Flux density of NSGA-II for the FEM calculations

4.5.2 Three Phase Transformer Optimization Design using GA, DEA and NSGA-II with FEM

Calculations of GA, DEA and NSGA-II are carried out using MATLAB 2017 as shown in Figure 4.14, Figure 4.15 and Figure 4.16 for the fitness evaluations of NLL and LL, respectively. Results show that obtained parameters (i.e., the primary turn number - X2) affects both the LL loss and flux density. While the core thickness X1 is one of the most effective parameters on NLL calculation. Calculations of LL losses show that the primary and secondary transformer areas (X4 and X5, respectively) are the main effective parameters on the transformer design. Moreover, all of the selected parameters mainly affect the B, which is also related to NLL and LL. All EA methods calculated flux density and minimum NLL values at almost the same. But amongst all methods, NSGA-II significantly minimizes LL. Therefore the overall total losses are minimized and the efficiency is enhanced using NSGA-II with respect to other EA methods. Figure 4.14 shows NLL calculations using DEA and NSGA-II and its relationship to the selected parameters.

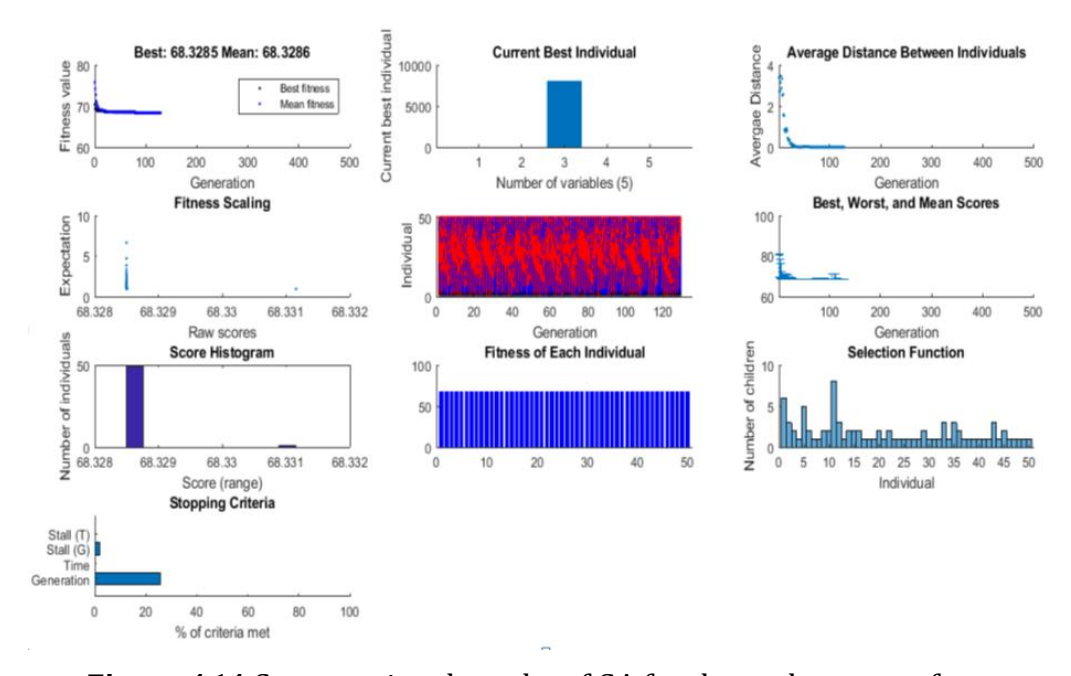


Figure 4.14 Computational results of GA for three phase transformer

In Figure 4.15 (a), DEA calculations showed that NLL searching functions for all parameters starts randomly with a large value of solutions, and then it needs a large number of iterations to get the minima. In addition, DEA sometimes failed to avoid local

minima because of the selecting procedure and boundary determination. NSGA-II calculations in Figure 4.15 (b) showed that it starts with a smaller value when compared to DEA calculations. Besides, NSGA-II moved towards to the desired/required minima faster than DEA with less iteration.

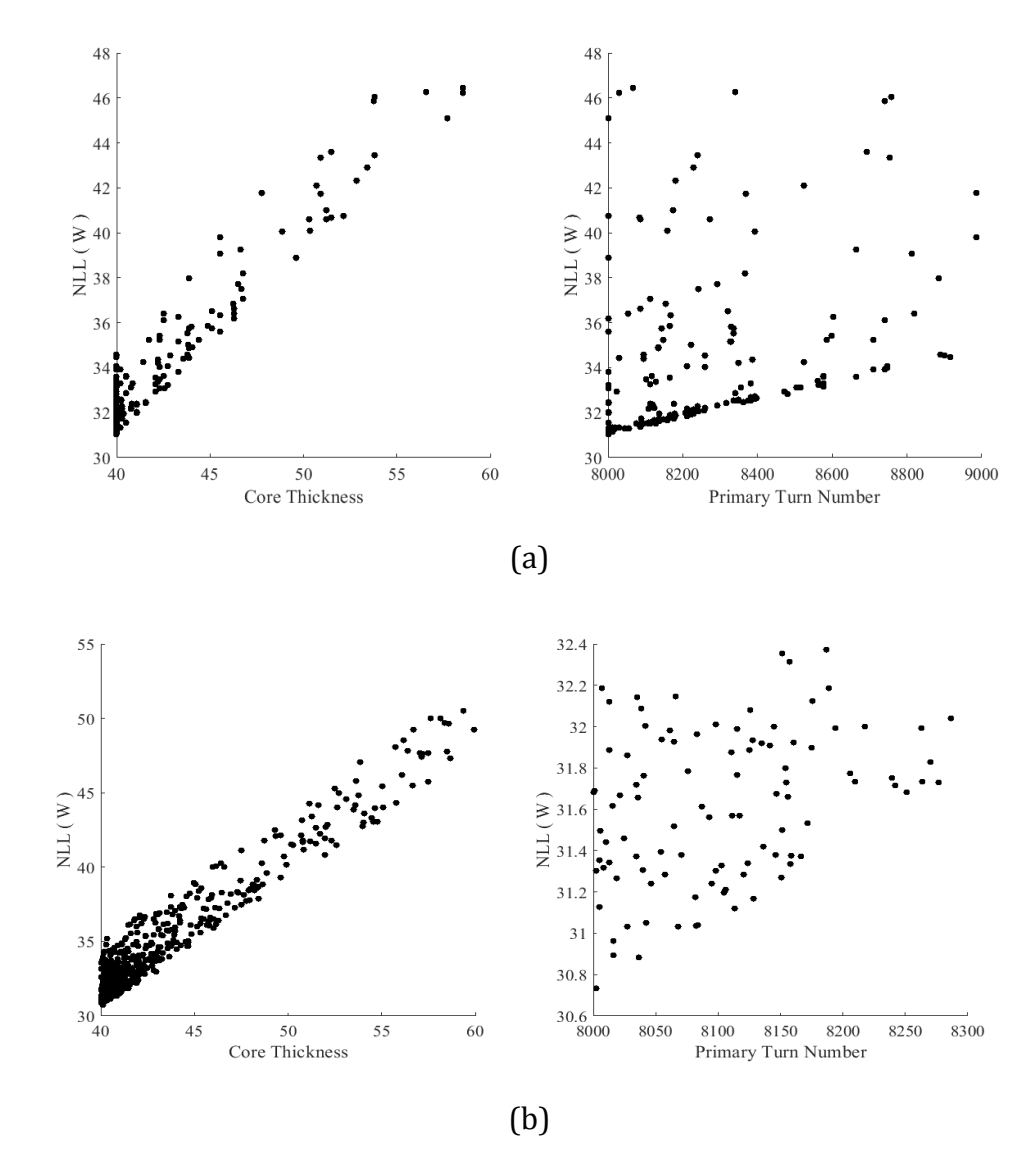


Figure 4.15 EA based results of NLL relationship with some specific parameters of three phase transformer (a) DEA and (b) NSGA-II

In Figure 4.16, the region of effective parameters to LL evaluation is shown for DEA and NSGA-II. The relationship between the first objective-NLL and the second objective-LL is provided in Figure 4.17. Here, DEA calculations showed that it reached the minima with more repeated solutions than that of NSGA-II. As a result, NSGA-II provides the best

individuals for the minimization of those two objectives when compared to GA, DEA and the prototype. Resulting design parameter values and loss calculations of three phase transformer with the evaluated EA methods are given in Table 4.4.

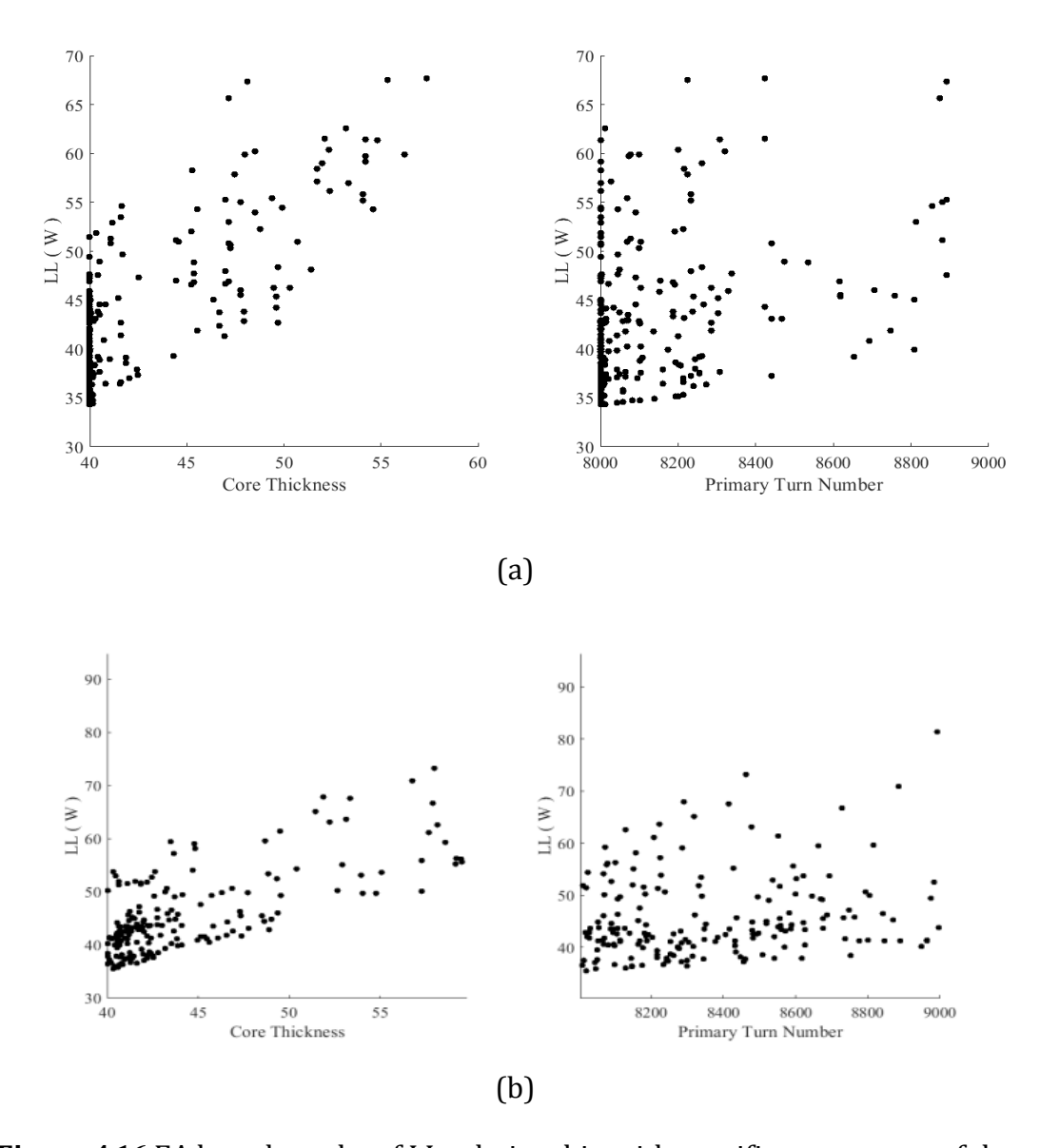


Figure 4.16 EA based results of LL relationship with specific parameters of three phase transformer (a) DEA and (b) NSGA-II

According to Table 4.4, overall loss is increased and transformer life is shortened when transformer is loaded. DEA and NSGA-II results is quite close values of X_2 and X_3 in the search space. X_2 parameter has an effect on LL and B calculations, while X_1 mainly effects on NLL calculations.

Table 4.4 EA based design parameter estimations and loss calculations

Quantity	Prototype	GA DEA		NSGA-II
X ₁ (mm)	50	42.061	40.063	40.156
X ₂ (Turn)	8259	8122.2	8098.4	8061.3
X ₃ (Turn)	31	32.185	26.395	31.282
X ₄ (m ²)	7.854 *10 ⁻⁷	7.264*10 ⁻⁷	7.3103*10-7	7.392*10-7
X ₅ (m ²)	2.835*10-6	2.703*10-6	2.947*10-6	2.988*10-6
B(T)	2.7015	1.2766	1.2726	1.2687
NLL(W)	30.13	31.802	31.647	31.631
LL(W)	37.62	36.407	35.411	34.842
NLL+LL	67.75	68.3286	67.058	66.473

600 400 200 100 30.5 31 31.5 NLL(W)

Figure 4.17 NLL and LL relationship using NSGA-II for the last iteration

Table 4.5 shows other individual selections obtained with NSGA-II to produce other possible solutions for different total loss values which are greater than optimized total loss.

Table 4.5 Optimized design parameter & total loss values obtained with NSGA-II

X ₁ (mm)	X ₂ (Turn)	X ₃ (Turn)	X ₄ (m ²)	X ₅ (m ²)	В(Т)	Total Loss (W)
40.01	8089.6	33.15	7.49*10 ⁻⁷	2.63*10 ⁻⁶	1.271	71.155
40.52	8040	35.16	7.02*10 ⁻⁷	2.83*10 ⁻⁶	1.2658	68.868
40.53	8075.2	22.01	7.02*10 ⁻⁷	2.83*10 ⁻⁶	1.2668	69.074
40.48	8114	27.82	7.18 *10 ⁻⁷	2.92*10 ⁻⁶	1.2753	68.23
40.32	8085.9	33.19	7.09 *10 ⁻⁷	2.38*10 ⁻⁶	1.2683	75.809

In order to evaluate the optimization performances of EAs, each algorithm is run 20 times with optimal own parameters. The resulting objective function values (NLL and LL) are used to produce box and whisker plots as given in Figure 4.18. Proposed NSGA-II provided better average solutions than GA and DEA, and by using NSGA-II model there is no outlier individuals in NLL and LL optimization unlike GA and DEA. Due to Paretofront calculations and depending on rank and crowding distance calculations, NSGA-II provides flexible and more reliable solutions. According to that, NSGA-II based optimization results in higher performance than that of GA and DEA model for the three phase transformer design. Figure 4.19, 4.20 and 4.21 show the flux density amount calculated with FEM according to GA, DEA and NSGA-II respectively.

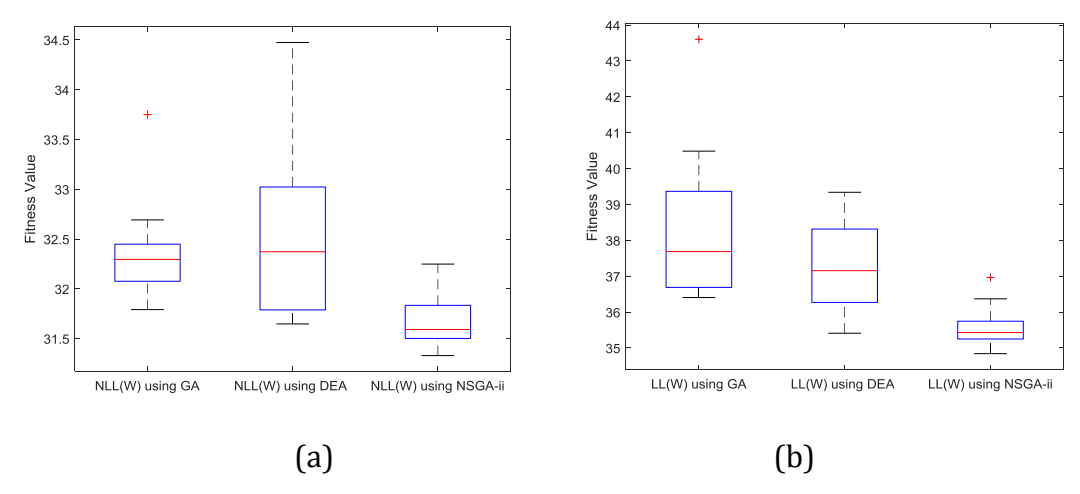


Figure 4.18 Box-and-whisker plots of (a) no-load-losses (NLL) and (b) load-losses (LL) using GA, DEA and NSGA-II

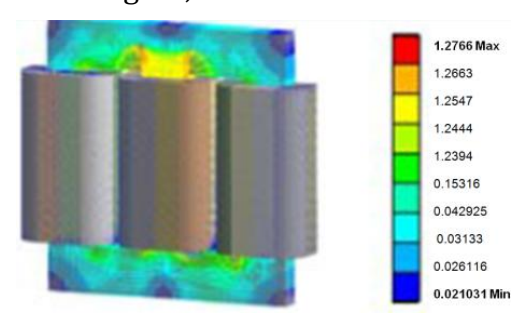


Figure 4.19 Flux density calculation with FEM for GA based design

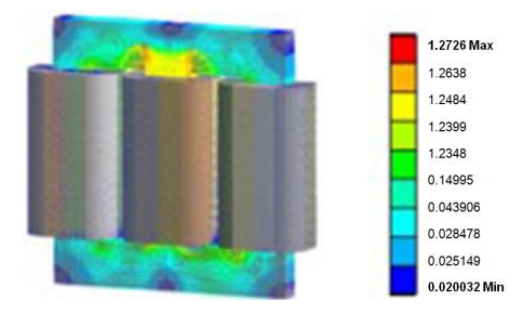


Figure 4.20 Flux density calculation with FEM for DEA based design

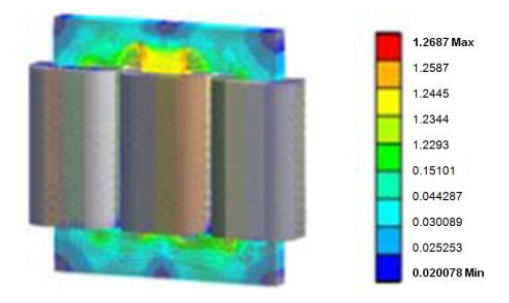


Figure 4.21 Flux density calculation with FEM for NSGA-II based design

Overall loss has been minimized using NSGA-II as shown in Table 4.4 and Figure 4.16, it is also demonstrated that, the value of X_1 and B are minimized comparing to the prototype example, which are the main parameters affected on both NLL and LL as well. NSGA-II provides a better solution divergence and wider search area when compared to GA and DEA.

4.5.3 Determination of EA Own Parameters

Population number, cross-over and mutation probability are the own parameters of GA and NSGA-II. In order to obtain optimized objective function value, designer should experiment the effects of own parameters by varying the values. Objective function values of GA and NSGA-II according to NLL and LL calculations for single and three phase transformer optimization are provided in Table 4.6 and Table 4.7. From Table 4.6 optimal own parameters for GA are set as the number of population is 50, mutation probability is 0.15 and cross over probability is 0.4 for single phase transformer design. Also optimal own parameters for NSGA-II are set as population number equal to 50, mutation probability equal to 0.15 and cross over probability equal to 0.4 for single phase transformer.

Table 4.6 Own parameter values of EA methods for single phase transformer design

Quantity	Npop	Cross-Over Prob.	Mutation Prob.	Execution Time (s)	Total Loss (W)
GA	50	0.4	0.15	16.83	64.47
DEA	200	0.6	0.2	37.55	55.87
NSGA-II	50	0.4	0.15	19.97	28.604

Npop= number of populations

Table 4.7 given that, the population number used for GA and NSGA-II are 50, which it was enough to find the global individuals solution. Considering DEA, that population number has to be increased because of its procedure selection of individuals to move to next generation. Moreover, EA own parameters have to be validated for more flexible and reliable solutions. It is also shows that using of NSGA-II with same GA own

parameters can achieve a good optimization when compared to other EAs. In addition, execution time of DEA is the longest amongst all methods.

Table 4.7 Own parameter values of EA methods for three phase transformer design

Quantity	Npop	Cross-Over Prob.	Mutation Prob.	Execution Time (s)	Total Loss (W)
GA	50	0.4	0.15	17.36	68.3286
DEA	200	0.6	0.2	39.62	67.058
NSGA-II	50	0.4	0.15	21.4	66.473

Npop= number of populations

4.5.4 Calculation of Total Efficiency and Cost

Efficiency of the transformer can be calculated basically using (4.12).

$$\eta_{T} = P_{Tout} / P_{Tin} = (P_{Tin} - P_{loss}) / P_{Tin}$$
(4.12)

The Total Owning Cost (TOC) is one of the evaluation and measurement test tools of a transformer taking into account the cost of no load and load losses during lifetime of the transformer [150]. TOC is expressed through using two evaluating coefficients namely A1 and A2 factors; where A_1 is the unit cost of no load losses coefficient and A_2 is the unit cost of load losses coefficient as in (4.13). In order to select the economical transformer in the long time, TOC should be considered and accounted as studied in [151]. Normally, the transformer life cycle is considered as its expected life before it fails or replaced [152].

$$TOC = (NLL \cdot A_1 + LL \cdot A_2) \tag{4.13}$$

The aim of this work is to minimize total loss and related cost for single & three phase transformer using EA methods together with FEM. Optimization performances of GA, NSGA-II and DEA are evaluated for minimization of TOC and total loss while maximizing the performance and the efficiency of the transformer under design. Table 4.8 shows that the total loss obtained with GA based model is decreased about 18.45% to the

proposed model, while DEA and NSGA-II results showed that the total loss has been more reduced of about 29.33% and 63.82% of the proposed model respectively. Also, the cost obtained with GA based model is decreased about 18.84% to the proposed model, while cost of DEA and NSGA-II based design was also more decreased of about 32.91% and 62.24% respectively. Total efficiency and total cost for the prototype model and EA based models of three phase transformer are given in Figure 4.22.

Table 4.8 Total efficiency and total cost calculated for single phase transformer under design

Quantity	Prototype	GA	DEA	NSGA-ii
Total Loss (W)	79.063	64.47	55.87	28.604
Efficiency (%)	52.08	60.927	66.139	82.664
Cost (USD)	6.516	5.288	4.371	2.46

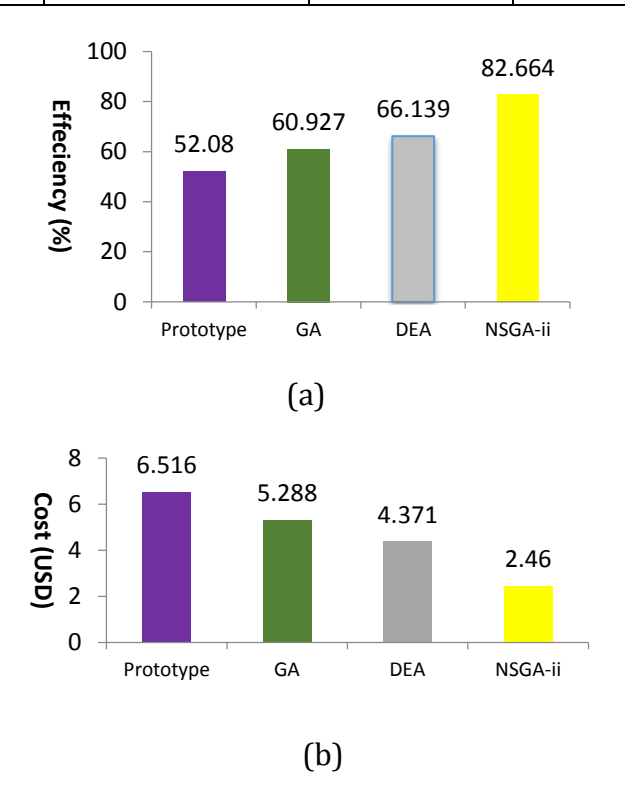


Figure 4.22 (a) Total efficiency and (b) cost for the prototype and EA based models of single phase transformer under design

Table 4.9 shows that the total loss obtained with GA based model is increased about 0.8% to the proposed model, while DEA and NSGA-II results showed that the total loss has been reduced about 1.02% and 1.88% respectively. Also, the cost obtained with GA based model is increased about 9.97%, while cost of DEA and NSGA-II based design was decreased about 0.76% and 1.99%, respectively. Total efficiency and total cost for the prototype model and EA based models are given in Figure 4.23.

Table 4.9 Total efficiency and total cost calculated for three phase transformer under design

Quantity	Prototype	GA	DEA	NSGA-II
Total Loss (W)	67.75	68.328	67.058	66.473
Efficiency (%)	92.2	91.1	93.29	94.02
Cost (USD)	184.04	202.44	182.61	180.36

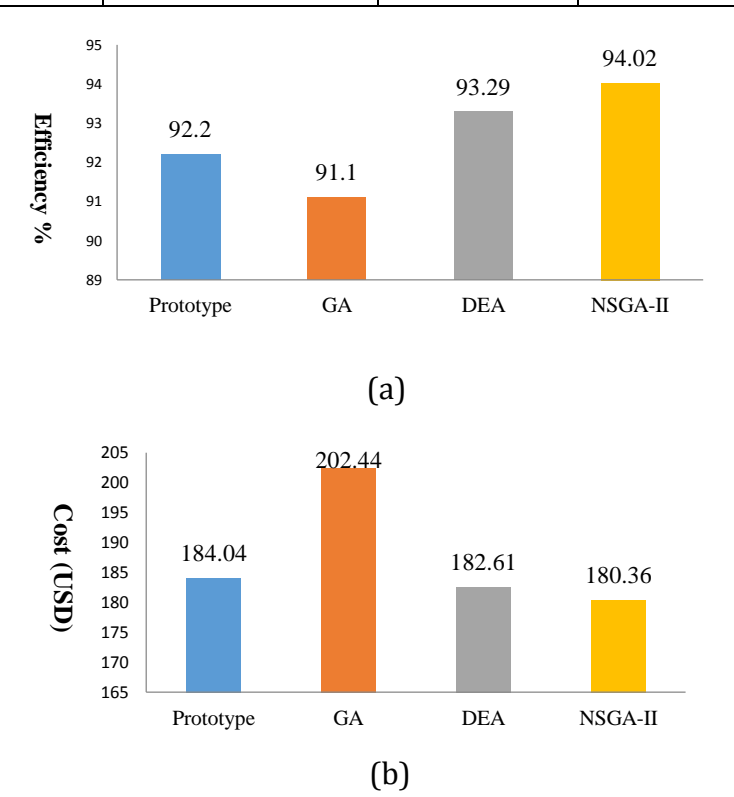


Figure 4.23 (a) Total efficiency and (b) cost for the prototype and EA based models of three phase transformer under design

4.6 Summary

In this chapter, an optimized single & three-phase transformer design is studied and presented by using multiple EAs method (GA, DEA and NSGA-II) with a mathematical tool FEM to make it more flexible and reliable. In the presented model, five parameters (core thickness, primary turn number, secondary turn number, primary conductor area and secondary conductor area) are selected for minimizing the total loss (NLL+LL) and TOC. In addition, the flux density calculations by determining the optimal five parameters are studied, while these calculations showed that some parameters like core thickness are more affected to the flux density. A comparison between EAs used and the prototype example showed that, NSGA-II provides a better optimal solution. It is also demonstrated that, the total loss (NLL+LL) and TOC are minimized with increasing in efficiency by using NSGA-II as compared to other presented model. This is due to the combination of parent generation with the off-spring generation in NSGA-II. The relation between NLL and LL is also studied and Pareto-optimal individuals are presented showing the region of effective parameter location which provides more flexibility for the transformer design. Transformer life cycle is considered by taking into account the cost of load and no load losses, which it is also related to the efficiency of the transformer for economical and longer time use. Simulation results showed that NSGA-II+FEM model provides more optimal individuals than GA, DEA and the prototype. In addition, running NSGA-II+FEM calculations for about 20 times, it's shown that NGSA-II is capable of searching near the optimal individuals which demonstrates the robustness of the proposed model. Transformer design optimization can be more reliable and cost effective using NSGA-II together with an effective mathematical tool like FEM. Execution time of NSGA-II algorithm is the shortest when compared to other EAs used in this work. As future work, this study can be utilized for design optimization of electronic circuits with isolated inputs and outputs where total loss minimization is of concern.

5 SERIES RESONANT CONVERTER AUTOMATED DESIGN

Series Resonant Converter (SRC) is one of the main parts which have to be designed carefully to be compatible with the general requirements of PV grid connected system. The extensive search space for design parameters of SRC such as resonant tank component values, transformer turn ratio, dead time and switching frequency requires an automated design framework. The proposed framework is developed using GA, DEA and NSGA-II for the multi-objective optimization of SRC circuit while accomplishing ZVS. Regulating the output voltage while minimizing the losses of MOSFET, diode and transformer are the design objectives. FEM is applied to subdivide the single phase transformer into simpler and finite parts to calculate flux density value according to the optimized design parameters. Amongst these evolutionary algorithms, NSGA-II achieved the best optimization performance considering various operation modes and required specifications. Simulation results are also provided to validate the efficient and robust automated design of SRC to be used in photovoltaic systems.

5.1 Introduction

Due to shortage of fossil fuels and the fast growing in energy demand unlatch away to notice renewable energy sources which has been changing to be imperative. Among all types of renewable energy sources, solar PV supplies have privilege as a result of clean and emission free aspects. However, irradiation and shading area has a remarkable impact on the solar power. Wide range of output voltage and varying current conditions require an adjustable and efficient design of a solar PV grid system. Putting PV panels in array with a series connection has several limitations in keeping with weather and shading. Moreover, conjunct constant current may not be provided. In order to achieve high performance power generation various studies are carried out. In [153], a loss optimization method is suggested for ZVS with two inductors as resonant parts. In [154],

Module Integrated Converter (MIC) and its cost balance effectiveness is pointed out. A control mechanism with Series Resonant Harmonic Compensator (SRHC) for minimizing voltage distortion is presented in [155]. PV grid connections are mainly implemented as series (where high output voltage is desired) or parallel (for special purposes of low output voltage requirement) as reviewed in [156]. A DC/DC converter design for PV system [157] achieved high accuracy for full load condition comparing to the traditional types. A different implementation [158] is used to retrieve losses due to weather conditions like shading and dust by using a resonant switched capacitor converter for mismatching purposes. In [159], voltage stress of low input voltage and its effect on reduction of power losses is studied. The resonant capacitor converter is implemented for managing the variation of power generated from PV system as in [160]. Two types of solar array are utilized to show that the current-voltage (IV) characteristics of PV generators are mainly affected by dynamic resistance and it needs a calibration due to differences in current-voltage region [161]. A wide range DC/DC converter operation required for specific PV applications like power conditioning system are analyzed in [162], [163].

The main advantages for the implementation of SRC for grid connected solar PV systems are to achieve high power density, high effectiveness, reduced losses and low cost. A fine-tuned switching frequency with a fine-tuned duty cycle is theoretically implemented for full bridge switching of SRC in [164]. Working with higher switching frequencies as in [165], [166] decreases the circuit size and increases efficiency with more frugal costs. In addition, a high voltage transformer design with core and copper loss calculations showed that the switching frequency and flux density are the paramount parameters for the evaluation of losses. In [167], a multilayered printed circuit board is designed for high frequency SRC and core losses are studied due to its frequency dependency. A control circuit design has been carried out to amend the SRC performance by determining the delay time of switching circuit signal regardless transmuting of wide range of input voltage, while Petri-nets showed that the transition between modes is depending on resonant current as in [168] and [169], respectively.

Mismatch of solar cells or even modules in series connection is an active research area for PV systems. The output power of a PV in general is determined by the solar cell/module having the lowest output power part amongst the rest of the solar cells/modules of the array. This occurs when cell/cells are shaded which in turn can cause power dissipation and eventually the total resultant PV power is reduced. This type of dissipation might damage the total module, and a reliable and accurate converter design is required which can handle the change in PV output voltage (50V - 240V) that is provided as an input to SRC. Output voltage of SRC is determined according to the demands. It is proposed that solar power systems can assemble adequate energy to macro base station at out range of a coverage area as in [170], [171]. Interference Cancellation System (ICS), radio frequency, frequency shift, fiber optic and digital repeaters are used as an essential parts of signal receiving and transmitting process to non or weak coverage area. It is shown that these devices can be preferred due to lower cost, lower complexity and reduced time instead of building a new Base Transceiver Station (BTS) to cover a wider distance area. Here, a minimum 96V DC voltage is required from the output of solar power system. Therefore, considering a practical application area, the target output voltage is set as 100V for this work. According to the voltage range of PV module, component values of the converter should be determined for various operation conditions and design requirements such as loss minimization and voltage regulation. Since the search space for optimal parameter values cannot be explored with conventional methods due to its complexity, an automated design methodology is required.

Parametric automation granted a pure identification of the popular base with the natural process between power electronics and automated circuit design. In addition, determining the boundary of the appropriate solution space for optimal circuit design considering design specifications and constraints turns out to be a rough issue with increasing number of design parameters. Besides, automated circuit design characterizes the upcoming needs and becomes a significant strategic method among power electronics community especially for multi object optimization and high frequency applications. Recently, employment of artificial intelligence for reliable measurements with parametric design is presented in [172] and [173]. The importance

of automated design in power electronics field especially in the combination of dispersed generation is discussed in [174]. The suggested model discovers more than one possible solution according to requirements. Automated design of SRC provides a proper evaluation for several design demands and explores the optimal solution in reasonable amount of time. This paper proposes DC/DC converter design automation and optimization based on loss analysis model and output voltage regulation. SRC provides a smooth transition among different operation modes in addition to its ability of operating in a discontinuous conduction mode with an adjustable dead time value. An automated design algorithm for SRC converter is developed depending on time domain waveforms as in [175], [176]. Complexity of time domain calculations, increasing number of parameters, application dependent requirements and constraints are challenging issues and the proposed methods provides effective solutions. In SRC circuit design automation, all parameters are initially set to random values and in the following steps these values are updated according to a mathematical model. In [177], design parameters are set theoretically and it is shown that utilizing of a snubber RC circuit is subsidiary for reducing switching losses and to avert overloading voltage across switching circuit. Due to the effect of duty cycle on switching losses, a pulse engendered circuit is studied in [178].

After selection of the appropriate PV module [179] maximum power points of 6-PV module are being tracked. The tracking process is carried out according to tilt and azimuth angle within the environmental condition of the selected area and simulated by using Helioscope software and Design Builder software [179]. A wide range of output voltage values delivered from these modules are collected during tracking which in turn, requires an accurate implementation of SRC to regulate this variation. In this work, automated design of SRC topology is developed using three EAs, GA [180], DEA [181] and NSGA-II [182] to optimize the design parameters of the converter for loss minimization and output voltage regulation for various loads. EAs were previously used for minimizing the loss of three phase transformer designed with 5 parameters [183]. In this work, four additional parameters are included to enhance the efficiency of the single phase transformer by providing more precise calculation of no-load and load losses of transformer. MOSFET switching loss, MOSFET & diode conduction losses and

transformer losses are defined by means of SRC design parameters. These loss expressions together with the output voltage variation expression are used as the cost function of evolutionary algorithms. In order to minimize the number of physical models and design parameters in the early stage of design process, Finite Element Method (FEM) is utilized [183]. In this work, FEM was applied to subdivide the single phase transformer into simpler and finite parts to calculate flux density value according to the optimized parameters. Following, these small parts are brought together to form single phase transformer parts which will be gathered into one model to calculate overall flux density with a sufficient knowledge of major affective elements on the design.

Reduction of overall losses of SRC, achieving ZVS condition with robust circuit performance and regulation of output voltage for various loads are the major challenges of this study. Multi-objective optimization of SRC design is carried out with EAs and FEM, where the evaluation performances of EAs are validated comprehensively. In addition, NLL and LL of single phase transformer are also optimized according to 9 parameter model to obtain lower loss values than that of 5 parameter model used in [183]. Other contributions of this study can be listed as the investigation of loss value dependency on particular SRC design parameters, selection of optimum operation mode for robust performance, and validation of optimization performances of EAs for different aspects and conditions.

Following introduction, the characteristics of selected PV module which has been optimized for shaded and non-shaded configuration are provided in section 5.2. In section 5.3 to section 5.8, loss analysis model of SRC is provided according to the selected optimization technique and SRC equivalent circuit with additional design parameters is given. Moreover, output voltage regulation and SRC operation modes are specified according to the SRC design parameter values. Section 5.9 presents simulation and optimization results comprehensively. Finally, concluding remarks and suggestions for future work is discussed in Section 5.10.

5.2 PV Module

PV system configuration mainly consists of PV module(s), unidirectional DC/DC converter or bidirectional DC/DC converter when conducting a storage unit. In this paper, a unidirectional DC/DC converter is designed with Pulse Width Modulation (PWM) as a controlling scheme for PV array as given in Figure 5.1. Maximum Power Point Tracking (MPPT) is used to optimize annual voltage variation delivered from PV array, due to climate conditions, shaded and non-shaded areas and other different reasons. A wide range of input voltages under these conditions requires a reliable DC/DC converter to respond efficiently to PV voltage variations. The selected PV module and electrical characteristics are provided in [179].

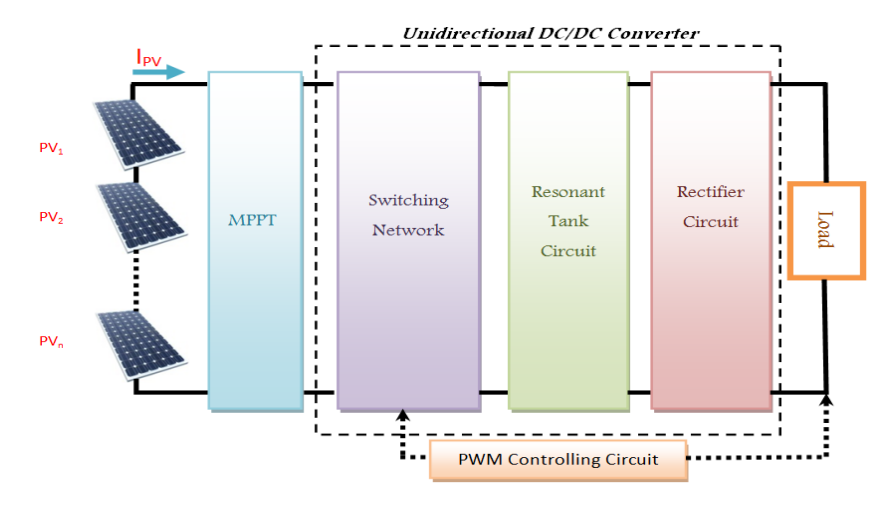


Figure 5.1 PV system configurations

5.3 Multi-objective Optimization of Overall Loss and Output Voltage Variation

The loss calculations and output voltage variation of SRC circuit according to load variation are carried out by indicating values of switching frequency, resonant inductor, resonant and output filter capacitors, transformer turn ratio, dead time and apparent load resistor which are the design parameters of SRC. For this purpose, optimal values of these parameters are determined using GA, DEA and NSGA-II and optimization performances of those are evaluated comprehensively.

In GA [180], first generation consists of random individuals called chromosomes. Each of them has the actual value and gene code. The quality of these solutions is measured by a metric called cost function. Selection of next generations depends on solutions' quality which is acquired after cost function calculation. The selected solutions are used as parents to generate different off-springs better than previous parents using cross-over. Following, some chromosomes are randomly selected from the current generation using a scaling factor to control the variety of solutions during mutation. The procedures are terminated when next generation cannot provide better solutions than the previous one. Unlike GA, DEA [181] starts with mutation process to obtain a target vector and then crossover is applied to generate a trial vector. Following, a stochastic decision is carried out to determine the next generations and tournament process is used to specify which vectors should remain for the next iterations. DEA operates with continuous and noisy parameters in a large search space of solutions and results in reasonable amount of computation time. GA requires long execution time for multi-objective problems and provides fewer solutions compared to NSGA. NSGA-II [182] reduces the computational complexity with crowding distance procedure. It provides solutions with better spread and closest to the optimal Pareto front line. Each solution is compared with previous generations to check the dominated sets of Pareto lines. Cost function is normalized for each solution before crowding distance calculation. Then, each edge parameter is assigned to be infinite distance value referring to the lowest and highest cost function values of each Pareto front lines. Intermediate solutions will be measured according to crowding distance procedure and ranked with their lines. Selection, cross-over and mutation processes are also used in overall optimization process as in GA and DEA. NSGA-II differs from the mentioned EAs such that the first and the second generations are combined together and separated by ranking and crowding distance procedures [183]. Following, FEM performed for flux density calculation of the single phase transformer design. Valuable information of the most effective parameters like transformer turn ratio which influences transformer loss calculation on the overall SRC design is gathered through FEM. Multi-objective optimization methodology for high efficient SRC circuit is presented in Figure 5.2. First of all, the own parameters of EAs and resonant tank component values, switching frequency, apparent load resistor and the input voltage of SRC which is provided from the PV panel are introduced to the algorithm. Meanwhile expressions for output voltage variation and overall loss (sum of conduction, switching and transformer losses) are defined as the cost function of EAs.

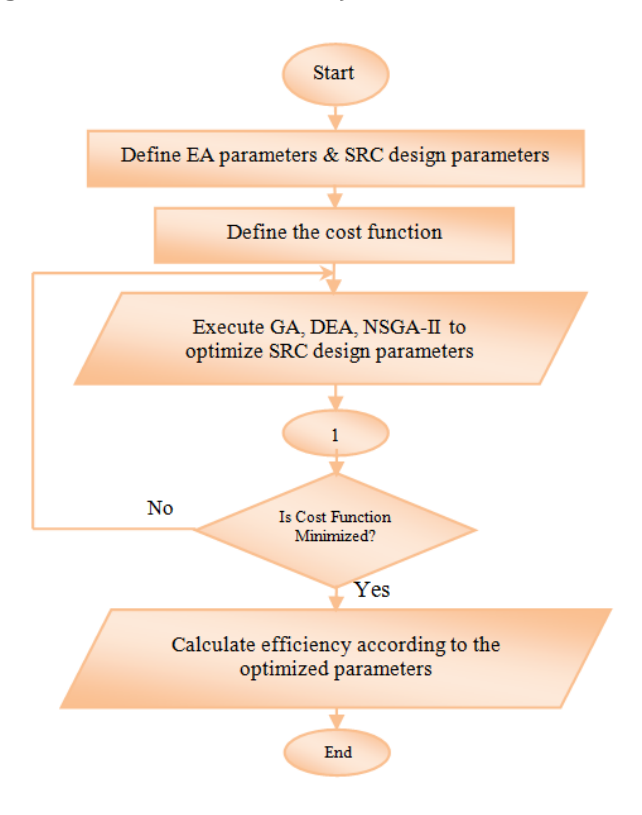


Figure 5.2 Multi-objective optimization methodology for SRC design

Setting the switching frequency value equal, higher or lower than the resonant frequency determines the region of operation as shown in Figure 5.3. Following, operating modes are analyzed through equivalent SRC circuit according to the input voltage range of SRC which is provided from the output of 6-PV module. Due to the different regions and modes of SRC, an automated design is required for the effective search of extensive possible solutions and accurate parameter value selection for loss minimization and output voltage regulation. For each operating mode of SRC equivalent circuit, loss values, actual output voltage and efficiency is calculated. FEM is used for validating the flux density change after NLL and LL evaluation to determine which design parameters are the most effective on transformer loss minimization.

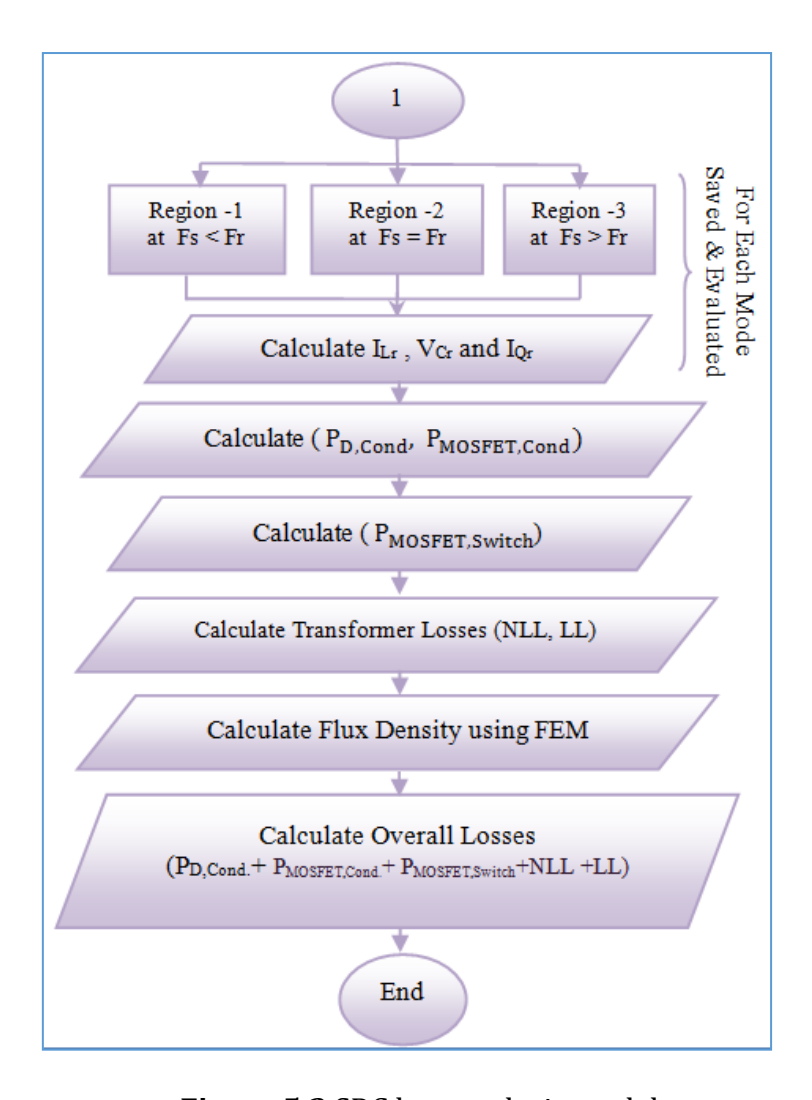


Figure 5.3 SRC loss analysis model

5.4 Equivalent SRC Circuit

SRC topology as shown in Figure 5.4 can be approximated to its fundamental equivalent circuit as given in Figure 5.5. Load resistor (R_{load}) in Figure 5.4 is affected by the charging process of the transformer primary side, therefore it is considered in the expression of apparent load resistance. In Figure 5.5, r_{eq} is the series connection of MOSFET drain-source resistance R_{ds} (only one switch will be ON) and photovoltaic cable resistance R_{pv} . The effect of diodes on primary side is neglected. Design equation for the apparent load resistance is given in (5.1). Electrical circuits and related waveforms are implemented and drawn using Multisim ver. 14.0.

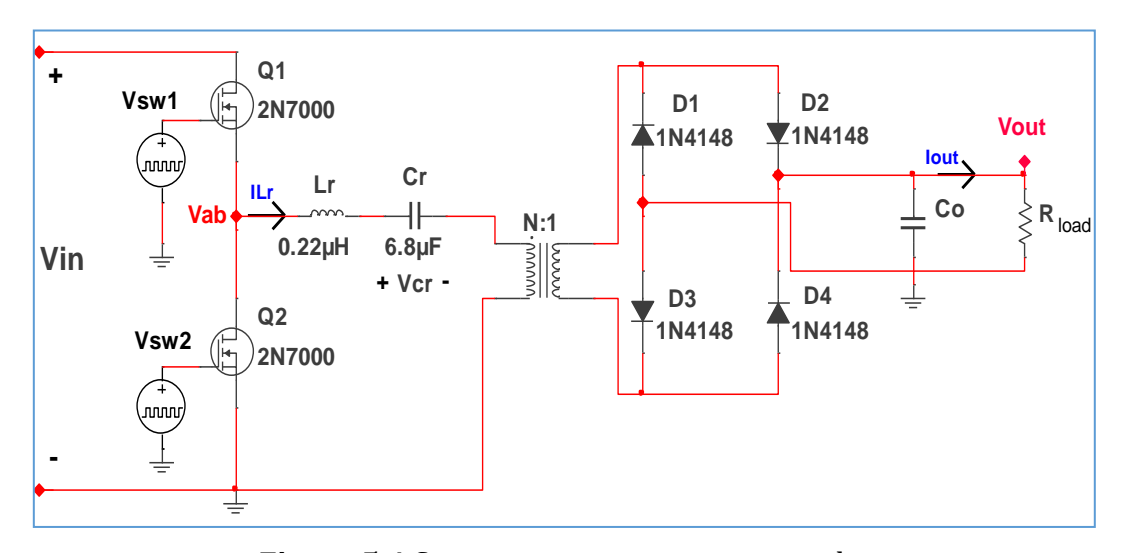


Figure 5.4 Series resonant converter topology

$$R'_{load} = \frac{8 N^2}{\pi^2} * R_{load} * D$$
 (5.1)

As shown in Fig. 5, the load connected in series with the resonant tank components made SRC operate as a voltage divider circuit. In [166] and [184], operating modes were explained based on capacitor charging time and influence by the primary side due to transformer turning ratio. While in this work, resistance of PV cable and MOSFET drainsource resistance are added to the equivalent circuit for more realistic results. Some of PV modules have large value of cable resistance and it should be considered in the optimization of losses. These additional elements may cause extra power consumption losses if ignored during design process, especially for applications that deals with delivering high currents. Also, the voltage on the primary side may be reduced due to the effect of these resistances which makes voltage regulation on the secondary side more difficult.

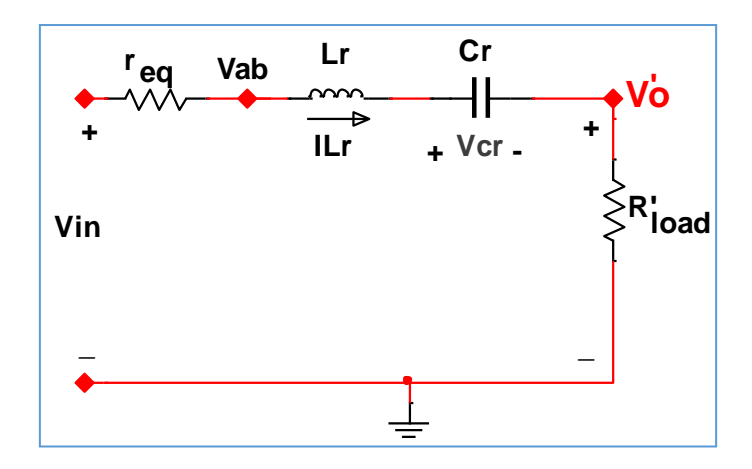


Figure 5.5 Series resonant converter equivalent circuit

5.5 Operating Modes

Resonant current and capacitor voltage waveforms for single switching period are plotted in Figure 5.6 according to the parameters shown in Figure 5.4 when ($f_s < 1/2f_r$). Equations for mode 1, mode 2 and mode 3 are given in (5.2, 5.3), (5.4, 5.5) and (5.6) respectively, [185].

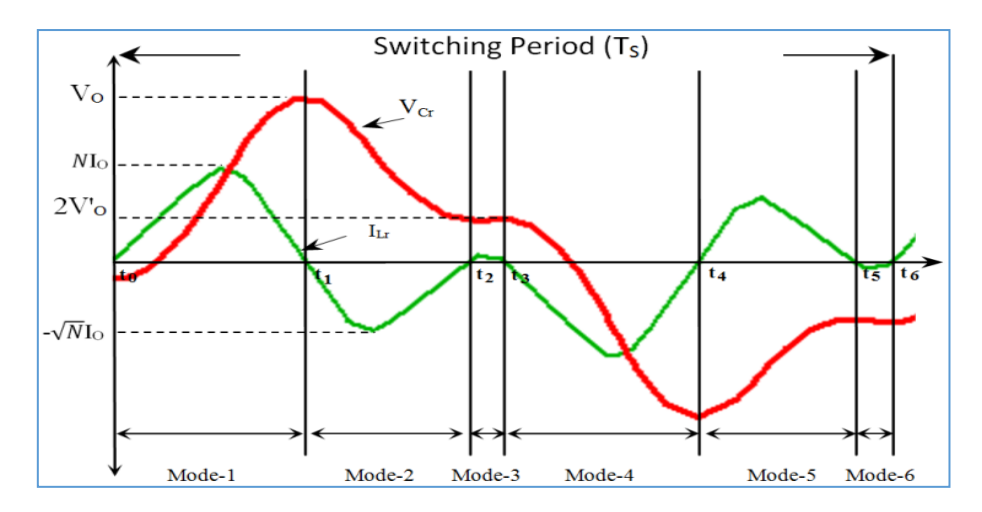


Figure 5.6 Waveforms of resonant inductor current and capacitor voltage

$$I_{Lr}(t) = \left[\left(V_{in} - V_{r_{eq}} - V_{Cr}(t_0) - V'_{O} \right) * \frac{C_r}{L_r} * Sin(\frac{t}{\sqrt{L_r C_r}}) \right]$$
 (5.2)

$$V_{Cr} = \left[\left(V_{in} - V_{r_{eq}} - V'_{0} \right) - \left(V_{in} - V_{r_{eq}} + V'_{0} - V_{Cr}(t_{0}) \right) * \sqrt{\frac{C_{r}}{L_{r}}} * Cos\left(\frac{t}{\sqrt{L_{r}C_{r}}}\right) \right]$$
 (5.3)

$$I_{Lr}(t) = \left[\left(-V_{in} + V_{req} + V_{Cr}(t_1) + V'_{O} \right) * \frac{C_r}{L_r} * Sin(\frac{t}{\sqrt{L_r C_r}}) \right]$$
 (5.4)

$$V_{Cr} = \left[\left(V_{in} - V_{r_{eq}} + V'_{O} \right) - \left(-V_{in} - V_{r_{eq}} + V'_{O} - V_{Cr}(t_{1}) \right) * \sqrt{\frac{C_{r}}{L_{r}}} * Cos\left(\frac{t}{\sqrt{L_{r}C_{r}}}\right) \right]$$
 (5.5)

$$V_{\rm Cr} = 2V_{\rm O}^{'}$$
 (5.6)

5.6 Calculation of SRC Overall Losses

The parameters of loss expressions that mainly affect the efficiency are investigated. The transformer turn ratio is the most influencing element on both transformer losses and diode conduction loss. Conduction losses of MOSFET & diode are more dependent on dead time, resonant frequency and resonant tank parameters. After calculating overall losses [185] using (5.7), cost function is derived with the inclusion of output voltage variation.

$$P_{\text{Overall_Losses}} = P_{\text{D,Cond.}} + P_{\text{MOSFET,Cond.}} + P_{\text{MOSFET,Switch.}} + \text{NLL} + \text{LL}$$
 (5.7)

$$P_{D,Cond.} = V_f * N * I_{Lr} * D$$
(5.8)

$$P_{\text{MOSFET.Cond.}} = I_{\text{av}}^2 * R_{\text{ds}} * D \tag{5.9}$$

$$P_{MOSFET,Switch.} = \frac{1}{2} (T_{SW_{on}} + T_{SW_{off}}) * V_{DS} * I_{Q} * f_{s}$$
 (5.10)

The transformer model in [146] utilizes 5 parameters, while in this work bobbin's height (X_6) , bobbin's depth (X_7) , core area (X_8) and window's width (X_9) are also included for more accurate NLL & LL calculations.

5.7 Calculation of Output Voltage Variation

Another objective towards robust SRC design is the output voltage regulation. Minimization of voltage variation (5.11) under different load resistor, input voltage and region conditions is evaluated. The desired output voltage is 100V as explained in introduction.

$$V_{\text{out var}} = |V_{\text{outDesired}} - V_{\text{outActual}}|$$
 (5.11)

5.8 Cost Function and Efficiency

Cost function is derived by taking into consideration of overall loss ($P_{Overall_Losses}$) and output voltage variation (V_{out_var}). The objectives are the minimization of these functions and optimization performances of EA methods are validated comprehensively. Following, efficiency of SRC circuit is calculated using (5.12).

$$\eta = \frac{P_{\text{in}} - P_{\text{Overall Losses}}}{P_{\text{in}}} \tag{5.12}$$

5.9 Simulation and Optimization Results

Table 5.1 shows the optimal own parameter values of each EA method which provides the minimum overall loss and output voltage regulation. The population number for GA and NSGA-II is equal and less than that of DEA. In order to achieve diversity in individuals' solutions for DEA, higher crossover probability value is applied. On the other hand, GA and NSGA-II provides more flexible solutions with crossover probability selected as '0.3'. Mutation probability is set to be low so as to keep diversity without moving towards primitive random searching process.

Table 5.1 Optimal own parameter values of EA methods

Proposed Methods	Population Number	Crossover probability	Mutation probability
GA	100	0.3	0.1
DEA	150-200	0.5	0.15
NSGA-II	100	0.3	0.1

Calculation of minimized overall losses, actual output voltage and efficiency after optimization process is shown in Tables 5.2, 5.3 and 5.4 considering a wide input voltage range with various conditions regarding switching frequency and load. Exact values of switching and resonant frequencies of three possible regions are calculated by EA methods. GA based optimization results are given in Table 5.3 and it is shown that working with high input voltage provides lower overall losses for all frequency conditions. Automated SRC design is proved to be more efficient on full load than other

conditions regardless of input voltage values. In addition, operating in regions 2 and 3 where f_s = f_r and f_s > f_r , respectively provided better performance due to fast switching operation than in region 1 where f_s < f_r . In region 1, hold-up time is increased which forces SRC circuit to keep regulating the output voltage. The best result of GA based optimization is obtained between 170V – 240V input voltage range on full load condition for regions 2 and 3. Using GA, dead time is optimized as 1.27 μ s which is considered to be a long hold-up period for SRC circuit to regulate output voltage.

Table 5.4 presents DEA based optimization results which are improved compared to GA based results; e.g. 10.9% efficiency increase is gained at full load condition when V_{in} =240V. Dead time is optimized as 0.31 μ s using DEA which is a shorter period than that of GA. The highest efficiency obtained with DEA is 96% when V_{in} =240 V with full load condition.

NSGA-II based optimization results are provided in Table 5.5. Dead time is optimized as 0.75 µs using NSGA-II which is a sufficient turning off and on time for the overall process. A proper optimization of dead time as well as other SRC design parameters is crucial to prevent high current absorption which may damage switching components of SRC circuitry. According to Table 5.5, output voltage is properly regulated to 100V for an input range of 170-240V when operating in region 2. Even when the input is decreased to 100V, output voltage is 98.4V at no load condition and 98.8V at full load condition. However output regulation is not preserved when input voltage is decreased in region 2. Moreover, NSGA-II provides lower transformer losses compared to GA and DEA with about 56% and 44%, respectively. Amongst them, NSGA-II obtained the smallest error between the desired output voltage and actual output voltage in region 2 with minimum overall losses and the highest efficiency.

Variation of losses according to the optimized parameter values of SRC circuit are given in Figure 5.7, 5.8 and 5.9, respectively. It can be observed that higher switching frequency leads to decreased MOSFET switching loss. On the other hand, dead time is one of the main effective parameters on diode conduction loss. Moreover, resonant current that depends on resonant inductor and capacitor has a significant impact on the overall losses.

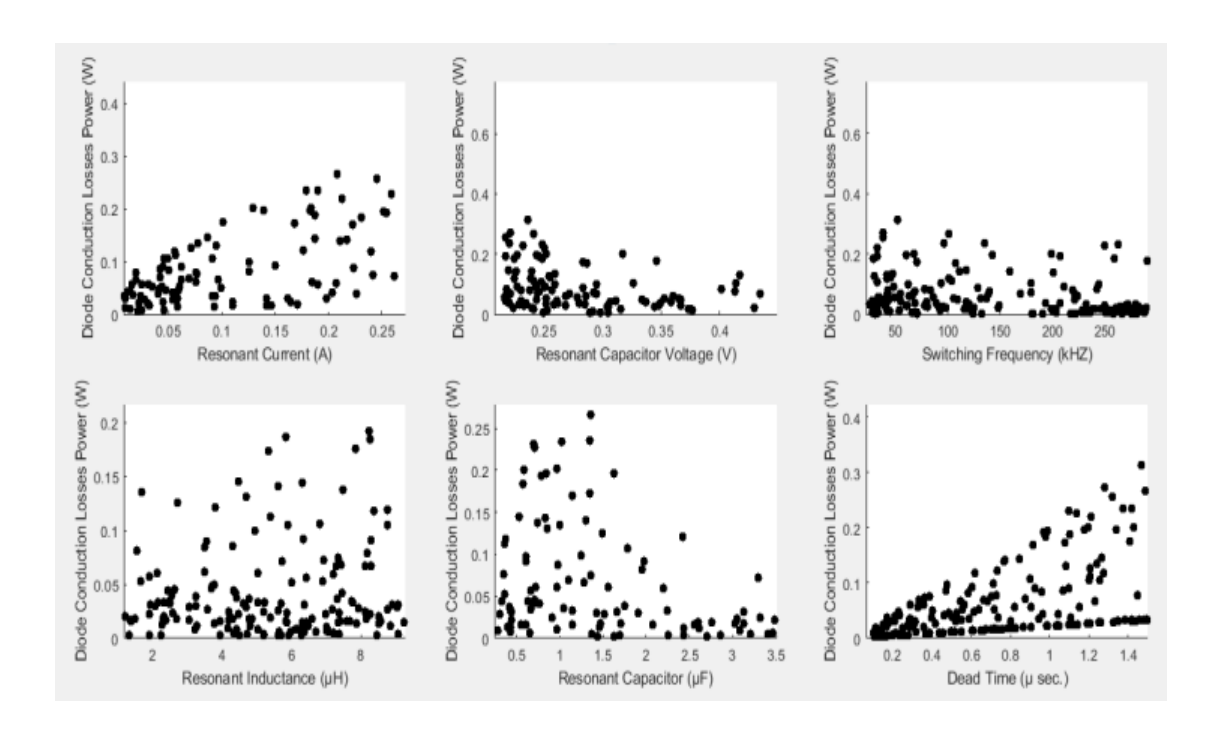


Figure 5.7 Diode conduction loss variations according to SRC design parameter variation

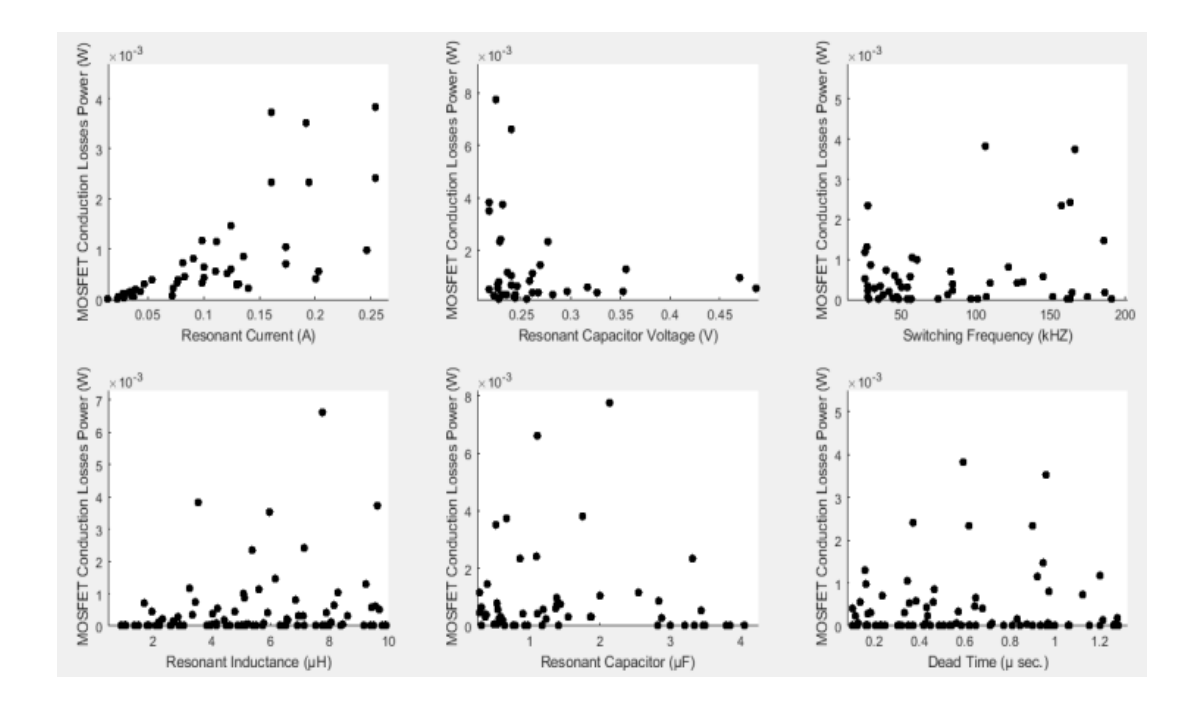


Figure 5.8 MOSFET conduction loss variations according to SRC design parameter variation

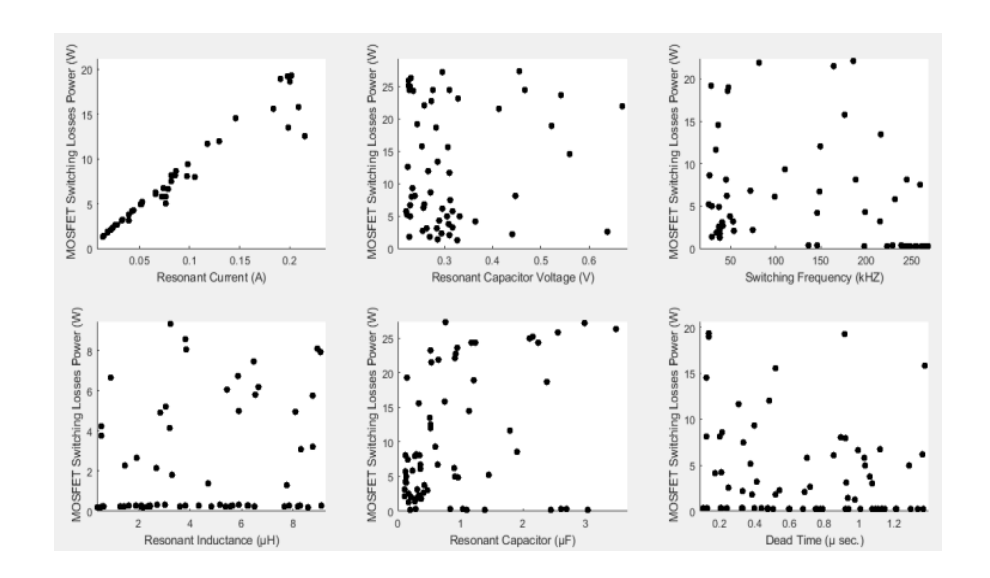


Figure 5.9 MOSFET switching loss variation according to SRC design parameter variation

Table 5.2 Optimization results for GA based method

Condition $f_s =$	f _r (Regio	12)							
Input Voltage	V _{in} = 240	0 V		V _{in} = 1'	70 V		V _{in} = 1	00 V	
External Load*	FL	HL	NL	FL	HL	NL	FL	HL	NL
V _{out} (V)	98.1	97.4	92.9	98	97.7	82.7	74.7	74.4	61.6
P _{D,Cond} (mW)	321	400	427.8	199.4	264.5	319.7	216	273.1	348.6
P _{MOSFET,Cond} (mW)	307.9	307.3	432.5	292.2	309.3	334.1	170	277.3	362.9
P _{MOSFET,Switch} (W)	11.3	13.4	13.5	11	11.4	11.7	8.4	10.7	12.2
NLL + LL (W)	4.8	4.2	2.7	4.8	3.9	2.7	4.3	3.4	2.7
Overall Loss (W)	16.7	18.3	17.1	16.3	15.9	15.1	13.1	14.7	15.6
Efficiency (%)	87.9	85.8	85.0	88.2	87.7	75.8	69.2	67.9	54.5
Condition $f_s > f$	r (Region	3)							
Input Voltage	V _{in} = 24	0 V		V _{in} = 17	0 V		V _{in} = 10	0 V	
External Load*	FL	HL	NL	FL	HL	NL	FL	HL	NL
V _{out} (V)	99.1	98.3	87.5	95.9	93.4	87.4	89.5	87.7	69.3
P _{D,Cond} (mW)	245.5	306.9	461.5	344.9	414.3	425.3	195.1	244.2	321

D (140)	4600	222	202.4	4600	404.0	200	1660	460.5	202.0
P _{MOSFET,Cond} (mW)	168.9	238.2	292.4	168.9	191.8	280	166.8	168.5	282.8
P _{MOSFET,Switch} (W)	8.3	9.9	11	8.4	8.8	10.7	8.3	8.9	10.8
NLL + LL (W)	6.4	5.6	3.5	5.2	4.3	3.5	4.7	3.8	3.5
Overall Loss (W)	15.1	16.0	15.3	14.1	13.7	14.9	13.5	13.2	14.9
Efficiency (%)	89.1	87.1	77.8	86.2	87.7	77.5	79.9	72.1	62.8
Condition $f_s < f$	r (Region	1)							
Input Voltage	V _{in} = 24	0 V		V _{in} = 17	0 V		V _{in} = 100	0 V	
External Load*	FL	HL	NL	FL	HL	NL	FL	HL	NL
V _{out} (V)	96.5	91.8	89.7	89.8	87	88.4	68.7	67.8	66.3
P _{D,Cond} (mW)	282.9	306.9	375	256.5	314.2	386.2	258.4	294.6	314.2
P _{MOSFET,Cond} (mW)	142.5	170	217.4	158.5	192.9	202.1	146.5	148.5	168.9
P _{MOSFET,Switch} (W)	8.2	8.4	9.5	8.1	8.9	9.1	8.1	8.5	8.7
NLL + LL (W)	4.3	3.9	2.5	4.2	3.8	2.5	4.1	4.1	2.5
Overall Loss (W)	13.0	12.8	12.6	12.7	13.2	12.2	12.6	13.0	11.6
Efficiency (%)	86.8	83.9	69.1	80.5	79.4	74.0	63.4	62.3	61.1

^{*} FL: Full Load = 750 Ω , HL: Half Load = 300 Ω , NL: No Load = 25 Ω .

 Table 5.3 Optimization results for DEA based method

Condition $f_s = f_r$ (Region 2)										
Input Voltage	Vin = 24	10 V		Vin = 170 V			Vin = 10	Vin = 100 V		
External Load*	FL	HL	NL	FL	HL	NL	FL	HL	NL	
V _{out} (V)	99.9	99.8	96.3	95	91.1	89.5	90.3	89.6	88.2	
P _{D,Cond} (mW)	613.8	1103.7	415.1	564.6	619.1	993.2	389.4	604.8	844.8	
P _{MOSFET,Cond} (mW)	87.3	89.2	78.6	77.8	77	73.7	80.3	80.7	70.4	
P _{MOSFET,Switch} (W)	5.3	4.9	5	5	4.9	4.8	5	5	4.7	
NLL + LL (W)	3.8	3.4	1.5	3.6	3.4	1.5	3.5	3.1	1.5	
Overall Loss (W)	9.8	9.5	7.0	9.2	9.0	7.4	9.0	8.8	7.1	

Efficiency (%)	96.0	91.9	89.2	90.3	87.5	86.1	86.6	86.0	85.0	
Condition $f_s >$	f _r (Regior	ı 3)								
Input Voltage	Vin = 24	40 V		Vin = 1	70 V		Vin = 1	00 V		
External Load*	FL	HL	NL	FL	HL	NL	FL	HL	NL	
V _{out} (V)	99.9	95.5	79.7	91.1	90.7	84.6	76.7	74.7	66.3	
P _{D,Cond} (mW)	352.6	569.1	686.3	349.3	624.9	745.4	248.8	392.8	708.6	
P _{MOSFET,Cond} (mW)	74.5	75.2	80.2	86.4	86.3	79.5	54	58.3	62.7	
P _{MOSFET,Switch} (W)	4.9	5	5.1	5.2	5.2	5	4.1	4.3	4.5	
NLL + LL (W)	5.2	4.8	2.4	4.9	4.4	2.4	4.8	4.2	2.4	
Overall Loss (W)	10.5	10.4	8.3	10.5	10.3	8.2	9.2	9.0	7.7	
Efficiency (%)	96.0	90.5	76.1	87.1	86.6	78.2	73.3	71.3	63.1	
Condition $f_s <$	f _r (Regior	n 1)		_						
Input Voltage	Vin = 24	40 V		Vin = 1	Vin = 170 V			Vin = 100 V		
External Load*	FL	HL	NL	FL	HL	NL	FL	HL	NL	
V _{out} (V)	99.9	95.8	73.4	92.9	91	89.9	84.4	82.6	69.1	
P _{D,Cond} (mW)	520	583.7	697.5	659.5	815.7	997	362.7	579.2	943	
P _{MOSFET,Cond} (mW)	82	121.1	141.7	87.3	122.1	223.2	38.6	65.7	82	
P _{MOSFET,Switch} (W)	5.1	6.2	6.7	5.3	6.2	8.4	3.5	4.6	5.1	
NLL + LL (W)	3.7	3.6	1.5	3.5	3.4	1.5	3.3	3.1	1.5	
Overall Loss (W)	9.4	10.5	9.0	9.5	10.5	11.1	7.2	8.3	7.6	
Efficiency (%)	96.1	87.5	69.3	89.0	83.6	80.7	81.6	79.2	65.7	

^{*} FL: Full Load = 750 Ω , HL: Half Load = 300 Ω , NL: No Load = 25 Ω .

Table 5.4 Optimization results for NSGA-II based method

Condition $f_s = f_r$ (Region 2)							
External Load* FL HL NL FL HL NL FL HL NL							

V _{out} (V)	99.9	99.8	99.8	99.9		99.6	99.6	98.8	}	98.6	98.4
P _{D,Cond} (mW)	159.9	277.7	65	9. 39	96.	21.7	157.4	556	.7	601.4	353.4
P _{MOSFET,Cond} (mW)	412.2	654.3	566	394.	2	415.8	390.7	66.9)	310.4	387.2
P _{MOSFET} ,Switch (W)	10.9	13.7	12.8	10.6	ı	10.9	10.6	8.4		9.4	10.5
NLL + LL (W)	2.1	2.0	1.3	2.0		1.9	1.3	2.0		1.8	1.3
Overall Loss (W)	13.6	16.6	15.3	13.4		13.2	12.4	11.0)	12.1	12.5
Efficiency (%)	96	95.2	95	96		94.8	94.8	95.6)	94.7	94.8
Condition $f_s > f_r$	(Region	3)					·				
Input Voltage	V _{in} = 24	0 V		V _{in} = 1	70 V	7		V _{in} = 1	00 \	V	
External Load*	FL	HL	NL	FL	Н	IL	NL	FL	ŀ	HL	NL
V _{out} (V)	99.9	77.6	64.8	99.9	8	2.5	61.5	98.9	7	77	58.2
P _{D,Cond} (mW)	151.2	269	705.5	324.8	2	8.00	487.3	321.1	4	153.8	820.8
P _{MOSFET,Cond} (mW)	568.1	570.3	563.4	566	5	67.1	561.6	406.8	4	102.7	388.9
P _{MOSFET,Switch} (W)	12.8	12.8	12.8	12.8	1	1.5	12	10.8	1	10.5	9.6
NLL + LL (W)	2.5	2.4	1.4	2.5	2	.2	1.4	2.4	2	2.3	1.4
Overall Loss (W)	16.0	16.0	15.5	16.2	1	4.7	14.4	13.9	1	13.7	12.2
Efficiency (%)	92.5	70.2	57.4	92.5	7	5.7	54.7	92.5	ϵ	67.8	52.5
Condition $f_s < f_r$	(Region	1)									
Input Voltage	V _{in} = 24	0 V		V _{in} = 1	70 V	V		V _{in} = 1	00 V	V	
External Load*	FL	HL	NL	FL	Н	IL	NL	FL	ŀ	HL	NL
V _{out} (V)	99.9	86	66.7	92.3	8	6	64.9	91.4	7	77.2	59.3
P _{D,Cond} (mW)	869.2	789.8	653.4	746.4	7	86.1	789.8	750.2	ç	908.9	1326
P _{MOSFET,Cond} (mW)	865.9	821.7	821.6	988.4	8	87.1	820.6	831.5	8	366	866.4
P _{MOSFET,Switch} (W)	15.8	15.4	15.4	16.9	1	6	16.1	16.8	1	16.7	16.8
NLL + LL (W)	2.0	1.9	1.2	1.8	1	.8	1.2	1.8	1	L.7	1.2
Overall Loss (W)	19.5	18.9	18.1	20.4	1	9.5	18.9	20.2	2	20.2	20.2

Efficiency (%)	90.6	77.1	58.0	82.6	76.7	55.8	81.8	67.5	49.6

^{*} FL: Full Load = 750Ω , HL: Half Load = 300Ω , NL: No Load = 25Ω .

In this study, NLL & LL optimization and flux density calculation are carried out with 9 parameters in order to increase accuracy. Table 5.5 provides a comprehensive insight for 5 parameters (5P) model and 9 parameters (9P) model considering single phase transformer design. As given in the table, GA results are not improved with 9P model due to premature convergence. DEA results are improved using 9P model. However, optimized results with 9P model are obtained with the usage of NSGA-II for both loss minimization and flux density calculation.

Figure 5.10 shows the comparison of efficiency values of EA based designs at varying input voltages at full load condition. NSGA-II provides more stable efficiency values for the provided input voltage range when compared to other EAs. Moreover, overall performance of EAs is reduced when input voltage is decreased except for NSGA-II.

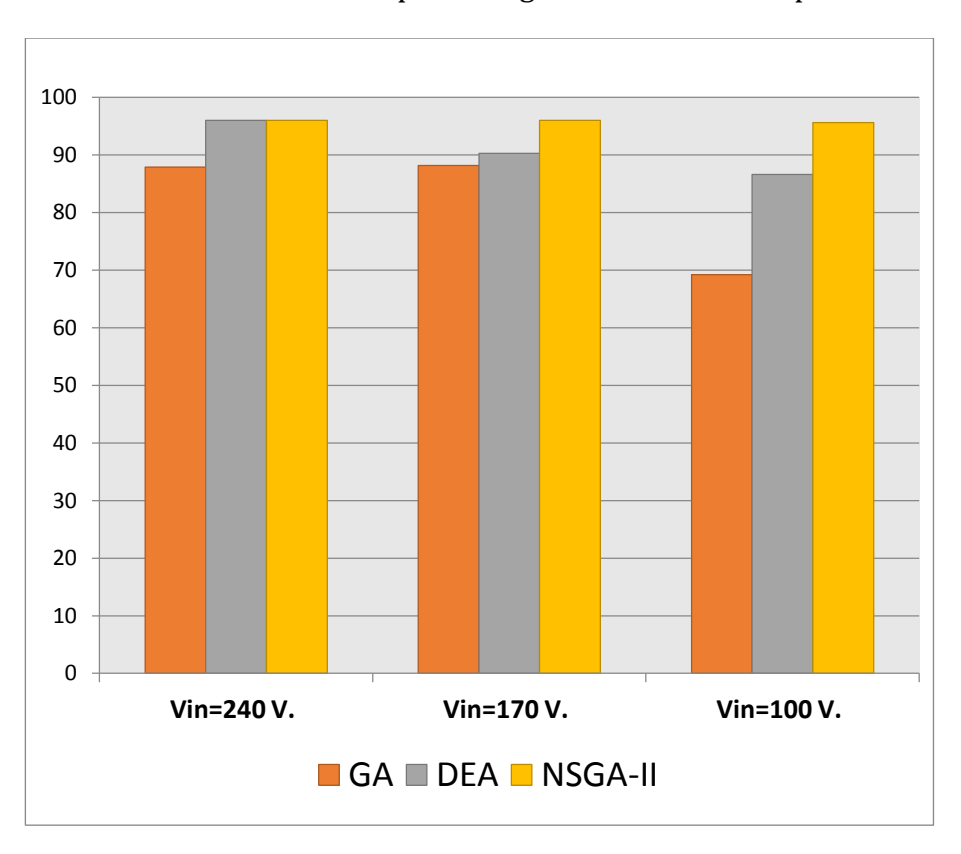


Figure 5.10 Efficiency of EA based designs at varying input voltages

Table 5.5 Transformer NLL&LL and flux density evaluation for 5P and 9P models

		GA			
6 11	NLL+L	L (W)	B (Wb	o/m²)	
Condition	5P Model	9P Model	5P Model	9P Model	
$f_s=f_r$	4.62	4.8	2.36	2.10	
$f_s > f_r$	6.98	6.4	2.388	2.23	
$f_s < f_r$	5.61	4.3	1.983	1.95	
		DEA			
0 11.1	NLL+L	L (W)	B (Wb/m²)		
Condition	5P Model	9P Model	5P Model	9P Model	
$f_s = f_r$	4.137	3.8	1.94	1.8	
$f_s > f_r$	5.35	5.2	2.217	1.88	
$f_s < f_r$	4.08	3.7	2.05	1.71	
		NSGA-II			
Condition	NLL+L	L (W)	B (Wb	o/m²)	
Condition	5P Model	9P Model	5P Model	9P Model	
$f_s=f_r$	3.272	2.1	1.712	1.20	
f _s >f _r	3.86	2.5	1.758	1.65	
$f_s < f_r$	2.54	2.0	1.624	1.20	

Table 5.6 presents a clear view of output voltage regulation using EA techniques considering varying input voltages. Algorithms were run for 25 times to provide the minimum output voltage, the maximum output voltage, the median and the Root Mean Square Error (RMSE) regarding each EA. As given in Table 5.6, GA delivered a large gap between minimum and maximum output voltages especially for lower input voltages. This is the prime reason of higher RMSE value of GA when compared to that of DEA and NSGA-II. The gap between maximum and minimum values of output voltages is still high

for DEA for lower input voltages, but improved when compared with GA. The lowest RMSE and best output voltage regulation is obtained with NSGA-II after 25 runs.

Table 5.6 Output voltage regulation using Ea techniques for 25 runs

	$GA (f_s=f_r)$								
Metric	V _{in} =240 V.	V _{in} =170 V.	V _{in} =100 V.						
Min. V _{out} (V)	90.20	79.67	55.423						
Max. V _{out} (V)	98.16	98.002	74.68						
Median (V)	93.621	86.964	66.113						
RMSE	0.06725	0.1291	0.360						
	DEA (fs	=f _r)							
Metric	V _{in} =240 V.	V _{in} =170 V.	V _{in} =100 V.						
Min. V _{out} (V)	95.005	87.042	82.005						
Max. V _{out} (V)	99.934	94.993	90.287						
Median (V)	97.497	90.887	86.409						
RMSE	0.0283	0.0932	0.1386						
	NSGA-II ($(f_s=f_r)$							
Metric	V _{in} =240 V.	V _{in} =170 V.	V _{in} =100 V.						
Min. V _{out} (V)	96.017	95.073	95.018						
Max. V _{out} (V)	99.990	99.987	98.806						
Median (V)	97.754	97.405	96.538						
RMSE	0.0242	0.0287	0.0357						

Depending on the best optimization result of NSGA-II amongst the EA methods, SRC design parameters together with the transformer design parameters are selected with NSGA-II for loss minimization and output voltage regulation. Providing the input voltage range and output load variation, the highest efficiency of SRC is obtained when the

design parameter values are set as given in Table 5.7. Apparent load resistor is calculated for full load condition where R_{load} =750 Ω .

Table 5.7 SRC design parameters optimized with NSGA-II

Transformer	Design Pa	arameters for	SRC Design Parameters for MOSFET & Diode Losses					
Definition	Unit	Values	Definition	Units	Values			
X_1	mm	6.12	f_s	kHZ	130.26			
X_2	-	55	$f_{\rm r}$	kHZ	130.02			
X ₃	-	320	Lr	μН	0.22			
X_4	mm ²	6.31	Cr	μF	6.81			
X ₅	mm ²	14.70	N	-	6			
X ₆	mm	7.28	$T_{ m dt}$	μs	0.75			
X ₇	mm	4.92	R' _{load}	kΩ	1.12			
X ₈	mm ²	53.67	Со	nF	9.67			
X 9	mm	5.78	-	-	-			

Table 5.8 shows the impact of each transformer design parameter for calculation of NLL & LL and flux density considering 5P model and 9P model using NSGA-II. It is evident that in 9P model, the impact of parameters are more distributed than in 5P model, so the sensitivity to transformer design parameters value is decreased. Especially, the impact of X_3 in 5P model is 78 % while it is decreased to 26% in 9P model for the calculation of flux density. Hence, focusing on adjusting the impact of transformer design parameters leads to minimizing transformer losses as well as flux density. It is also shown that FEM provides accurate calculation according to optimization of single phase transformer losses and clarify the effectiveness of transformer design parameters.

Table 5.8 Comparison of sensitivity to transformer design parameters between 5P-model and 9P-model using NSGA-II

Danamakana	NLL	+ LL	1	3
Parameters.	5P Model 9P Model		5P Model	9P Model
X ₁	3%	10%	1.7%	10.8%
X ₂	18%	12%	10.5%	18.25%
X ₃	30.9%	26%	78%	26%
X ₄	18.3%	9.1%	0.9%	8.1%
X ₅	29.8%	14%	8.9%	5%
X ₆	-	13.6%	-	10.3%
X ₇	-	12.1%	-	13.9%
X ₈	-	1.5%	-	4.35%
X ₉	-	1.7%	-	3.3%

According to Table 5.6, NSGA-II combined with a mathematical tool as FEM provided more suitable solutions than other EA techniques. Moreover, NSGA-II is able to search the closest optimal individuals to the desired Pareto-front line. Flux density calculation followed by NLL and LL optimization using NSGA-II and FEM is shown for each part of transformer in Figure 5.11.

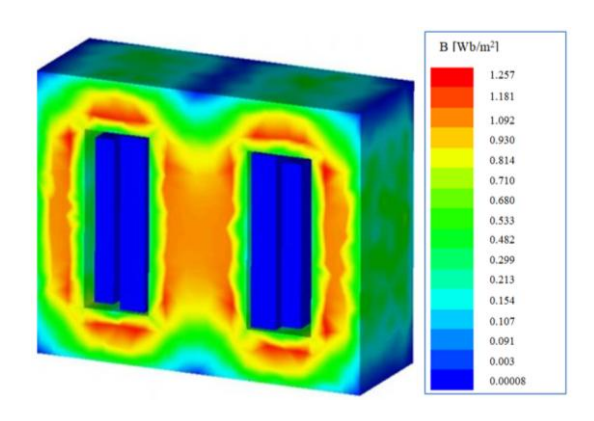


Figure 5.11 Single phase transformer flux density calculation using FEM method

The efficiency variation of NSGA-II based SRC design versus load current is provided in Figure 5.12 for input voltages of 100V, 170V and 240V. Operation in region 2 (f_s = f_r) is preferred because of the minimized losses when compared to that of regions 1 and 3. Higher input voltage improves circuit efficiency and output voltage is successfully regulated.

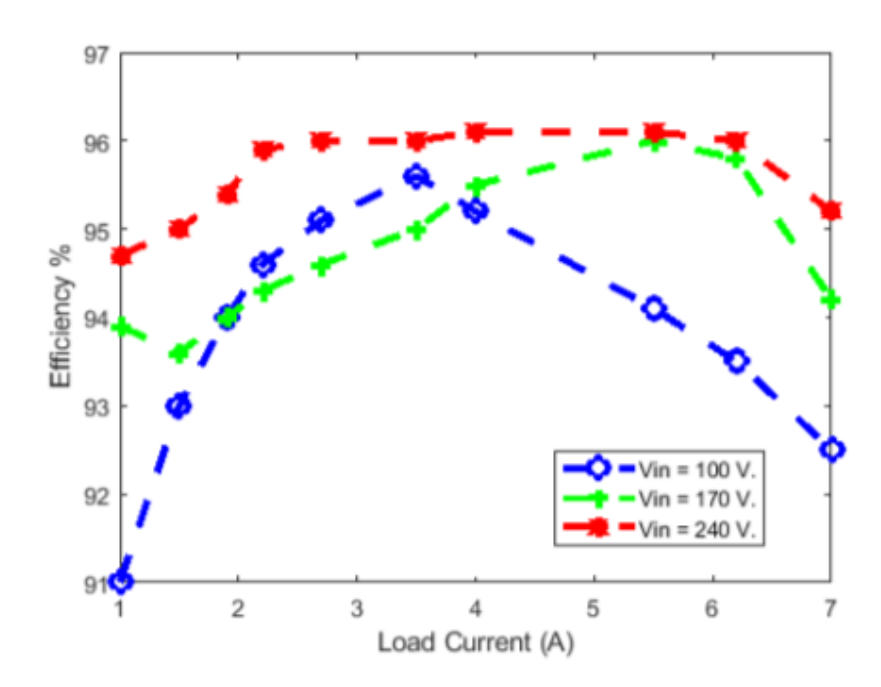


Figure 5.12 The efficiency variation of SRC versus load current for input voltages of 100V, 170V and 240V

Output voltage and resonant current waveforms of NSGA-II based SRC design are given in Figure 5.13 and Figure 5.14 for full load condition with 240V input voltage and 100V input voltage, respectively. The selection of region 2 depends on high efficiency and the achievement of regulated output voltage. According to the results in Table 5.6 and Figure 5.13 and Figure 5.14, NSGA-II based design results meets ZVS requirements. Therefore, ZVS can be applied at all regions for input voltage range of 100-240 V as shown in Figure 5.15.

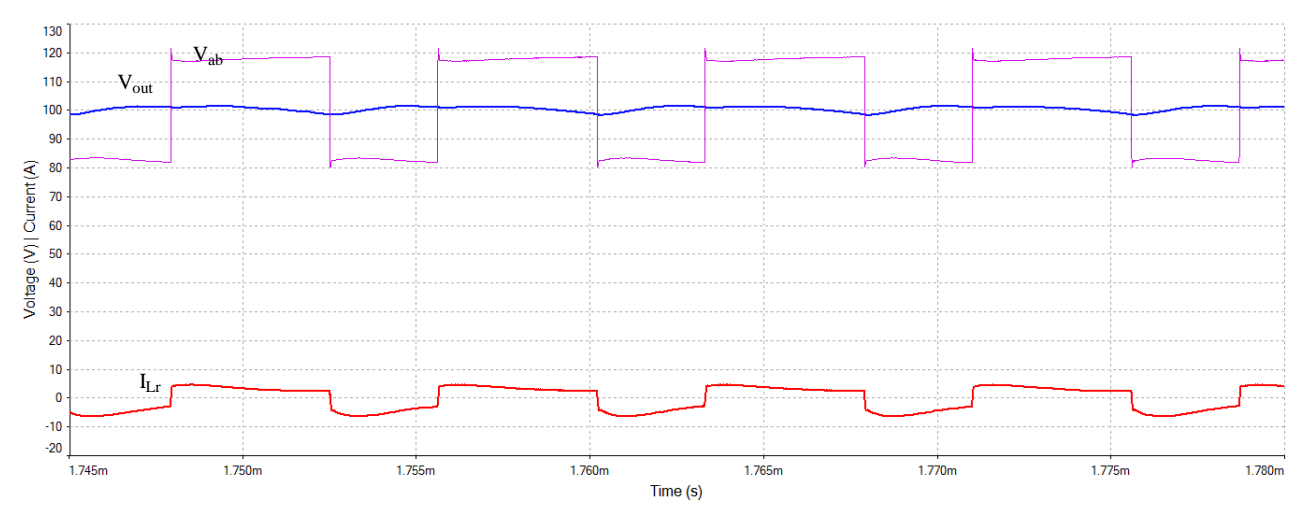


Figure 5.13 V_{ab} , V_{out} , I_{Lr} @ V_{in} = 240 V for full load condition

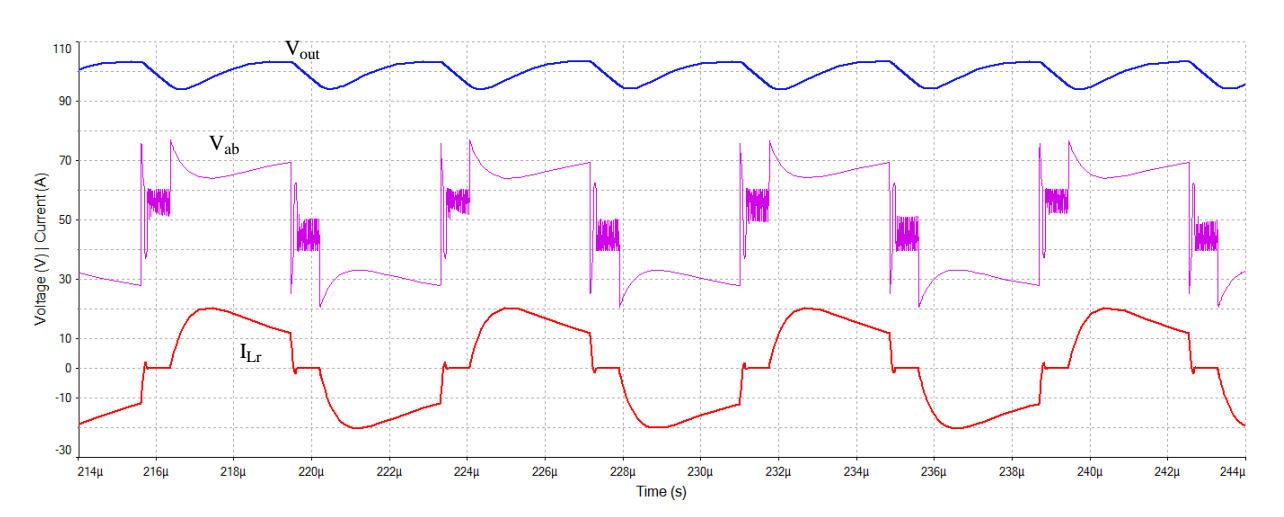


Figure 5.14 V_{ab} , V_{out} , I_{Lr} @ V_{in} = 100 V for full load condition

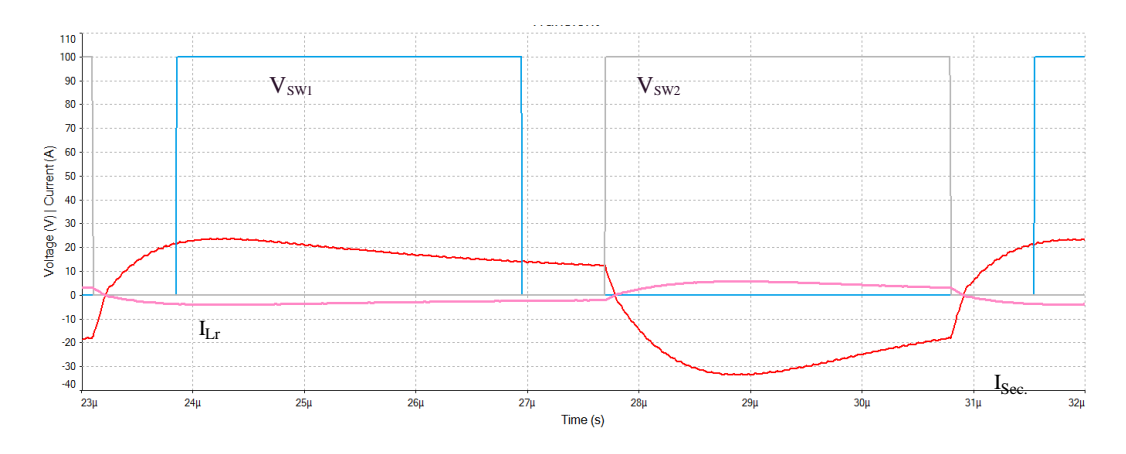


Figure 5.15 ZVS condition for NSGA-II based SRC design @ V_{in} = 240V, V_{out} = 100V

5.10 Summary

In this work, GA, DEA and NSGA-II are utilized to optimize SRC design parameters together with single phase transformer design parameters. In addition, operation modes of SRC are analyzed to determine the optimal operating conditions according to PV voltage and load variations. MOSFET & diode conduction losses, MOSFET switching losses, transformer NLL & LL and output voltage regulation are derived as the cost functions to be minimized. Flux density is calculated using FEM to demonstrate the effectiveness of the optimized parameters on transformer design. In this work, 8 parameters for MOSFET & diode losses and 9 parameters for single phase transformer losses are optimized. It is also proved that using 9P model for transformer design decreases sensitivity when compared to 5P model.

Considering optimization performances of EAs, GA sometimes diverges from optimal solutions. In early stages of iteration, GA may cause a premature convergence such that resonant frequency is determined far from the global solution as soon as lower switching losses are achieved regardless of output voltage regulation. DEA is very sensitive to population size, mutation and crossover probability. Increasing crossover probability leads to quicker convergence with a strong possibility of missing the optimal solutions. While smaller crossover probability is able to slow down the optimization process and thus DEA requires more iterations than GA and NSGA-II. A large population size ensures that solutions are adequate for mutation which is computationally long. NSGA-II selection process differs by means of ranking best solutions and crowding distance evaluation. Therefore solutions can be spread closer to the global minima value than that of GA and DEA as given in Tables 5.4, 5.5 and 5.6. Achieving better rank or higher crowding distance, individual solutions are to be proceeded further with a better chance to be reproduced.

The importance of AI based automated design in power electronics is growing as the design parameter selection for complicated circuits requires enormous search space. Moreover, parametric automation of circuit design provides faster optimization than trial and error methods. This study proves that NSGA-II, as one of the state-of-art EA techniques, is very suitable for multi-objective optimization of SRC circuit having a large

number of design parameters to be properly selected. It is also shown how to find the optimal balance between the robustness and loss minimization in SRC with respect to several design constraints and specifications.

As further work, the proposed methodology will be enhanced for more improvements in the challenging issues of power electronics circuit design.

RESULTS AND DISCUSSION

The importance of evolutionary algorithm (EA) based automated design in power electronics is growing as the design parameter selection for complicated circuits requires enormous search space. In this thesis, evolutionary optimization methodology for SRC design is proposed as a flexible and reliable solution. SRC design parameters are calculated by evaluating circuit characteristics of resonant tank circuit, transformer and rectifier circuit that constructs SRC.

The first stage of this work is to select a renewable energy source as the input of SRC. Photovoltaic (PV) is a widespread renewable energy system which requires accurate calculations of the annual generated power according to a specific region. In this study, NSGA-II has successfully optimized the shaded and non-shaded configuration for 6-array of Trina Solar PV module (TSM-PC05) connected in series. Two simulator tools are used for the annual PV generated power calculation: Helioscope online application and Design Builder program. In addition, weather conditions are considered to provide more accurate calculations according to the selected region for this PV installation. Climate online data has been downloaded from the internet for the selected region. For nonshading and shading configuration, several parameters are optimized which are azimuth angle, tilt angle and spaces between two plates of the model. Moreover, racking type and the height of the selected building are indicated more reliable calculations. Amongst the EA methods, the highest performance for PV optimization process is obtained with NSGA-II having 92% accuracy with 207° and 10° as azimuth angle and tilt angle, respectively. A wide range of output voltage values delivered from these modules are collected during tracking which in turn, requires an accurate implementation of SRC to regulate this variation.

In the second stage of this work, transformer design optimization is considered because optimal design of transformer is an important aspect for constructing an accurate and reliable SRC. For this purpose, single and three phase transformers are used for the minimization

of transformer losses (NLL and LL) and optimization of design parameters where 5-parameter and 9-parameter models are evaluated. 5-parameter (5P) model includes core thickness, primary conducting area, secondary conducting area and the number of coil turns in the primary and secondary windings. The results show that some parameters for this model can be more effective on both NLL & LL optimization. For example, core thickness is the main affective parameter on NLL optimization while primary and secondary conducting areas are the prime effective parameters on LL optimization.

NLL & LL optimization and flux density calculation are carried out also with 9parameter model (9P) in order to increase accuracy. Results provided a comprehensive insight for 5 parameters (5P) model and 9 parameters (9P) model considering single phase transformer design for SRC topology. Same optimization techniques for (5P) model utilized for (9P) model as well. GA results are not improved with 9P model due to premature convergence. DEA results are improved using 9P model. However, optimized results with 9P model are obtained with the usage of NSGA-II for both loss minimization and flux density calculation. Results also show the impact of each transformer design parameter for calculation of NLL & LL and flux density considering 5P model and 9P model using NSGA-II. It is evident that in 9P model, the impact of parameters are more distributed than in 5P model, so the sensitivity to transformer design parameters value is decreased. Especially, the impact of transformer secondary turn value in 5P model is 78 % while it is decreased to 26% in 9P model for the calculation of flux density. Hence, focusing on adjusting the impact of transformer design parameters leads to minimizing transformer losses as well as flux density. It is also shown that FEM provides accurate calculation according to optimization of single phase transformer losses and clarify the effectiveness of transformer design parameters.

Validation and enhancement of EA own parameters are also studied to evaluate optimization performances. Population number for GA and NSGA-II are less than DEA for single and three phase transformer parameters optimization. The long selection process of DEA which depends on the distance between each different generated solutions requires larger population number compared to GA and NSGA-II. This is also

the main reason of longer execution time of DEA compared to other EAs. Total Owning Cost (TOC) model is used for evaluation of cost considering NLL & LL values.

The aim of single and three phase transformer parameters optimization process was to minimize the transformer total losses and therefore cost reduction is ensured. According to TOC model, a cost reduction is obtained of about 1.99% than the prototype model.

Final stage of this study is to propose an evolutionary optimization methodology for SRC design to be convenient with PV requirements. Same EAs are used also to conjugate the total design of transformer, PV module and resonant converter. EAs own parameters are also determined first like population number, cross over and mutation probability. GA and NSGA-II population number are lower than DEA, which was sufficient to obtain better individual solutions. While DEA requires larger population number to achieve individual's diversity. GA, DEA and NSGA-II are applied to optimize SRC according to several conditions: - wide input voltage range, different mode operations and different load conditions. GA provided better performances only when input voltage was high for all mode operations. While DEA provided better accomplishment compared to GA with a lower output voltage regulation. NSGA-II was the best applied EAs to optimize resonant converter design with preferable performances and superior output voltage regulation. Automated SRC design is demonstrated that working under full load condition can provide more efficient direction among other load conditions. Furthermore, operating at resonant frequency or above resonant frequency supplied better performances. The main reason of considering these regions is because of soft switching process and moving towards ZVS condition which is preferred for MOSFET switching process. At region-1 (when switching frequency is less than resonant frequency), hold up time is increased which force SRC to attempt regulating output voltage at higher switching frequencies. Delay time optimization using GA considered as a high value compared to switching frequency value. While DEA based optimization results are improved compared to GA, for example at full load condition 10.9% efficiency increment occurred compared to GA. Delay time optimization using DEA was more convenient compared to the delay time that optimized using GA and more compatible with switching frequency value. Also highest efficiency using DEA was under higher input voltage and full load conditions. Delay time is substantial for turning on and off process which is better optimized using NSGA-II. Proper value of delay time prevents high currents absorption that may damage switching circuit.

Also output voltage regulation is more accurate using NSGA-II due to favorable optimization parameters compared to GA and DEA. NSGA-II was able to reduce outlier solutions for both NLL & LL single phase transformer losses optimization. After FEM combination with EAs methods, it's provided appropriate solutions and especially with NSGA-II. In fact, NSGA-II inspect the nearest optimal individuals to more suitable solutions. This is also led to assist FEM to provide accurate evaluations of flux density for single and three phase transformer which can clarify the effectiveness of transformer optimization parameters. Flux density calculation was after NLL & LL optimization which helps to minimize overall losses as well as accurate calculation for each physical parts of single and three phase transformer. Load variation is also clarified for three conditions: full, half and no load cases. EAs applied techniques provided minimization for overall SRC losses types at full load conditions especially for high input voltage. This is due to the ability of SRC to regulate the output voltage more adjacent to the desired value at high input voltage cases.

In general, GA required less defining parameters than DEA and NSGA-II about the optimized problem. While implementing an objective cost function to get the closest representation and reach the right operation is difficult as much as optimization parameters are increased. For this study, 8 parameters for SRC losses minimization and 9 parameters for single phase transformer losses minimization are proposed to be optimized at the same time. GA is weak and not easily paralleled for these two optimization design. In addition, GA sometimes diverges from optimal solutions that related to one objective function than another like NLL+LL and MOSFET switching loss. Some of optimized parameters are close to optimal solutions and fit to the fitness requirement characteristics. For example, working with higher switching frequency is achieved by GA as clarified in results section. But, at the same time in early stages of iteration may bring a premature convergence. For example: resonant frequency moving

far from the optimal one regardless the losses optimization and output voltage regulation. Another example is the average ratio of switching to resonant frequency value is about 1.769 when repeating this model about 25 times. This is mean that GA moving far away from the global minima solutions with a huge range between resonant and switching frequency of about 50 kHZ. The main reason for this optimization issues that GA tried to rank some of objective function higher than the rest. While DEA is very sensitive to population size, mutation and crossover probability and lead to be a disadvantage for some cost function optimizations particularly with a high optimization parameters. DEA compared to GA is able to discover closest solutions regardless of the initial population size. It is also convergence to the required solutions and keeps it on to be saved for upcoming iteration process. DEA compared to other EA techniques need more computation time to optimize the objective function due to in between distance calculation. A higher rang and population size is needed for DEA to be sure that there is adequate and convenient solution for mutation process. In the other hand, larger value of cross over lead to quicker convergence close the global minima solutions but with a high chance of missing it. While lower cross over value is able to slow down the optimization process and need further iteration number than GA and NSGA-II. For example, the average value of resonant and switching frequency ratio of DEA optimization is less than GA of about 1.638 with a less rang than GA with about 20 kHZ. NSGA-II selection process is differing than GA and DEA by rank and crowding distance evaluation. This is lead to more spread of solutions closer to the global minima value. In NSGA-II, individuals retain and continue if achieving either better rank or higher crowding distance. This property make NSGA-II save these solutions to the next generation so better solutions are able to be reproduced again and again. Its mean that NSGA-II does not neglected any pareto front closest solution like GA or even DEA. For example, the average ratio between switching to resonant frequency is about 1.312 closer to the center region compared to other EA used techniques with a less range of 10 kHZ between switching and resonant frequency. In this thesis, automated design of series resonant converter is covered with the aid of EA methods combined with mathematical tool like FEM. As a future work, combining optimization techniques with a different mathematical tools to improve deign performances and emplyed it for other

different resonant converter topologies. More investigation can be also done focusing on operating modes according to different related conditions. In addition, automated design can be applied as well for different modern power electronics such as electric veicle system and capacitor charging applications. Furthermore, different transformer structure can be investigated according to various issues such us aging factor, overloading, winding leakage inductance,....., etc.

- [1] V. Vodovozov, Introduction To Power Electronics. Bookboon, 2010.
- [2] B. W. Williams, Power Electronics: Devices, Drivers, Applications, and Passive Components. Palgrave, 2006.
- [3] M. Prabhakar and V. Kamaraj, "Optimal design and implementation of LCC resonant converter for automotive application," PEOCO 2010 4th Int. Power Eng. Optim. Conf. Progr. Abstr., no. June, pp. 507–510, 2010, doi: 10.1109/PEOCO.2010.5559158.
- [4] M. Pinto, H. Ribeiro, B. Borges, and M. Santos, "A resonant, frequency Tracking, step-down piezoelectric transformer based converter," 2010 IEEE Energy Convers. Congr. Expo. ECCE 2010 Proc., pp. 2004–2010, 2010, doi: 10.1109/ECCE.2010.5618112.
- [5] D. Thenathayalan, C. G. Lee, and J. H. Park, "High-order resonant converter topology with extremely low-coupling contactless transformers," IEEE Trans. Power Electron., vol. 31, no. 3, pp. 2347–2361, 2016, doi: 10.1109/TPEL.2015.2435254.
- [6] Y. E. Bouvier et al., "DC/DC fixed frequency resonant LLC full-bridge converter with Series-Parallel transformers for 10kw high efficiency aircraft application," 2017 IEEE Energy Convers. Congr. Expo. ECCE 2017, vol. 2017–Janua, no. Dcm, pp. 3788–3795, 2017, doi: 10.1109/ECCE.2017.8096669.
- [7] S. H. Ahn, H. J. Ryoo, J. W. Gong, and S. R. Jang, "Design and Test of a 35-kJ/s high-voltage capacitor charger based on a delta-connected three-phase resonant converter," IEEE Trans. Power Electron., vol. 29, no. 8, pp. 4039–4048, 2014, doi: 10.1109/TPEL.2013.2287709.
- [8] G. Rubino, L. Rubino, N. Serbia, P. Ladoux, and P. Marino, "LLC resonant converters in PV applications comparison of topologies considering the transformer design," in 013 International Conference on Clean Electrical Power (ICCEP), pp. 37–41.
- [9] W. Chen, X. Hong, S. Wang, Z. Lu, and S. Ye, "High efficiency soft-switched step-up DC-DC converter with hybrid mode LLC+C resonant tank," Conf. Proc. IEEE Appl. Power Electron. Conf. Expo. APEC, vol. 1, pp. 1358–1364, 2010, doi: 10.1109/APEC.2010.5433406.
- [10] R. Beiranvand, M. R. Zolghadri, B. Rashidian, and S. M. H. Alavi, "Optimizing the LLC-LC resonant converter topology for wide-output-voltage and wide-output-load applications," IEEE Trans. Power Electron., vol. 26, no. 11, pp. 3192–3204, 2011, doi: 10.1109/TPEL.2011.2143429.
- [11] M. Y. Kim, B. C. Kim, K. B. Park, and G. W. Moon, "LLC series resonant converter with auxiliary hold-up time compensation circuit," 8th Int. Conf. Power Electron. -

- ECCE Asia "Green World with Power Electron. ICPE 2011-ECCE Asia, pp. 628–633, 2011, doi: 10.1109/ICPE.2011.5944623.
- [12] L. Hang, B. Li, S. Liu, Y. Gu, W. Yao, and Z. Lu, "Asymmetrical secondary structure of LLC series resonant DC/DC converter for multi-output applications," IET Power Electron., vol. 4, no. 9, pp. 993–1001, 2011, doi: 10.1049/iet-pel.2010.0146.
- [13] W. Inam, K. K. Afridi, and D. J. Perreault, "High efficiency resonant DC/DC converter utilizing a resistance compression network," IEEE Trans. Power Electron., vol. 29, no. 8, pp. 4126–4135, 2014, doi: 10.1109/TPEL.2013.2282626.
- [14] N. C. D. Pont, D. G. Bandeira, T. B. Lazzarin, and I. Barbi, "A ZVS APWM half-bridge parallel resonant DC-DC converter with capacitive output," IEEE Trans. Ind. Electron., vol. 66, no. 7, pp. 5231–5241, 2019, doi: 10.1109/TIE.2018.2868270.
- [15] B. R. Lin, W. R. Yang, J. J. Chen, C. L. Huang, and M. H. Yu, "Interleaved LLC series converter with output voltage doubler," 2010 Int. Power Electron. Conf. ECCE Asia -, IPEC 2010, pp. 92–98, 2010, doi: 10.1109/IPEC.2010.5543842.
- [16] S. Miyawaki, J. I. Itoh, and K. Iwaya, "Optimization design of an isolated DC/DC converter using series compensation on the secondary side," 2010 IEEE Energy Convers. Congr. Expo. ECCE 2010 Proc., pp. 1428–1435, 2010, doi: 10.1109/ECCE.2010.5618261.
- [17] G. Pledl, M. Tauer, and D. Buecherl, "Theory of operation, design procedure and simulation of a bidirectional LLC resonant converter for vehicular applications," 2010 IEEE Veh. Power Propuls. Conf. VPPC 2010, pp. 1–5, 2010, doi: 10.1109/VPPC.2010.5728978.
- [18] J. J. Sandoval, S. Essakiappan, and P. Enjeti, "A bidirectional series resonant matrix converter topology for electric vehicle DC fast charging," Conf. Proc. IEEE Appl. Power Electron. Conf. Expo. APEC, vol. 2015–May, no. May, pp. 3109–3116, 2015, doi: 10.1109/APEC.2015.7104795.
- [19] B. R. Lin, Y. S. Zhuang, and H. S. Syu, "Parallel soft switching converters: Analysis, design and implementation," Proc. 13th IEEE Conf. Ind. Electron. Appl. ICIEA 2018, pp. 1016–1021, 2018, doi: 10.1109/ICIEA.2018.8397860.
- [20] X. Tan and X. Ruan, "Equivalence Relations of Resonant Tanks: A New Perspective for Selection and Design of Resonant Converters," IEEE Trans. Ind. Electron., vol. 63, no. 4, pp. 2111–2123, 2016, doi: 10.1109/TIE.2015.2506151.
- [21] Q. Cao, Z. Li, and H. Wang, "Wide Voltage Gain Range LLC DC/DC Topologies: State-of-the-Art," 2018 Int. Power Electron. Conf. IPEC-Niigata ECCE Asia 2018, vol. 201210, pp. 100–107, 2018, doi: 10.23919/IPEC.2018.8507899.
- [22] F. Shi, R. Li, J. Yang, and W. Yu, "High Efficiency Bidirectional DC-DC Converter with Wide Gain Range for Photovoltaic Energy Storage System Utilization," Proc. 2018 IEEE Int. Power Electron. Appl. Conf. Expo. PEAC 2018, pp. 1–6, 2018, doi: 10.1109/PEAC.2018.8590308.

- [23] X. Jin, X. Zhou, W. Wang, Z. Ma, J. Xu, and Z. Lu, "A Half-Bridge LLC Converter for Wide Input Voltage Range Applications," Proc. 2018 IEEE Int. Power Electron. Appl. Conf. Expo. PEAC 2018, pp. 1–5, 2018, doi: 10.1109/PEAC.2018.8590334.
- [24] Y. Chen, X. Wu, Z. Qian, and W. Zhang, "Design and optimization of a wide output voltage range LED driver based on LLC resonant topology," 8th Int. Conf. Power Electron. ECCE Asia "Green World with Power Electron. ICPE 2011-ECCE Asia, pp. 2831–2837, 2011, doi: 10.1109/ICPE.2011.5944780.
- [25] R. Beiranvand, B. Rashidian, M. R. Zolghadri, and S. M. H. Alavi, "A design procedure for optimizing the LLC resonant converter as a wide output range voltage source," IEEE Trans. Power Electron., vol. 27, no. 8, pp. 3749–3763, 2012, doi: 10.1109/TPEL.2012.2187801.
- [26] T. Labella, W. Yu, J. S. Lai, M. Senesky, and D. Anderson, "A bidirectional-switch-based wide-input range high-efficiency isolated resonant converter for photovoltaic applications," IEEE Trans. Power Electron., vol. 29, no. 7, pp. 3473–3484, 2014, doi: 10.1109/TPEL.2013.2282258.
- [27] X. Zhao, L. Zhang, R. Born, and J. S. Lai, "A High-Efficiency Hybrid Resonant Converter with Wide-Input Regulation for Photovoltaic Applications," IEEE Trans. Ind. Electron., vol. 64, no. 5, pp. 3684–3695, 2017, doi: 10.1109/TIE.2017.2652340.
- [28] Z. Li and H. Wang, "Comparative analysis of high step-down ratio isolated DC/DC topologies in PEV applications," Conf. Proc. IEEE Appl. Power Electron. Conf. Expo. APEC, vol. 2016–May, pp. 1329–1335, 2016, doi: 10.1109/APEC.2016.7468040.
- [29] Y. Shen, H. Wang, A. Al-Durra, Z. Qin, and F. Blaabjerg, "A Bidirectional Resonant DC-DC Converter Suitable for Wide Voltage Gain Range," IEEE Trans. Power Electron., vol. 33, no. 4, pp. 2957–2975, 2018, doi: 10.1109/TPEL.2017.2710162.
- [30] N. Swaminathan and N. Lakshminarasamma, "The Steady-State DC Gain Loss Model, Efficiency Model, and the Design Guidelines for High-Power, High-Gain, Low-Input Voltage DC-DC Converter," IEEE Trans. Ind. Appl., vol. 54, no. 2, pp. 1542–1554, 2018, doi: 10.1109/TIA.2017.2779099.
- [31] M. Shang and H. Wang, "A Voltage Quadrupler Rectifier Based Pulsewidth Modulated LLC Converter with Wide Output Range," IEEE Trans. Ind. Appl., vol. 54, no. 6, pp. 6159–6168, 2018, doi: 10.1109/TIA.2018.2850033.
- [32] Y. Shen, H. Wang, A. Al-Durra, Z. Qin, and F. Blaabjerg, "A Structure-Reconfigurable Series Resonant DC-DC Converter with Wide-Input and Configurable-Output Voltages," IEEE Trans. Ind. Appl., vol. 55, no. 2, pp. 1752–1764, 2019, doi: 10.1109/TIA.2018.2883263.
- [33] X. Fang et al., "Efficiency-oriented optimal design of the LLC resonant converter based on peak gain placement," IEEE Trans. Power Electron., vol. 28, no. 5, pp. 2285–2296, 2013, doi: 10.1109/TPEL.2012.2211895.

- [34] X. Fang, H. Hu, J. Shen, and I. Batarseh, "An optimal design of the LLC resonant converter based on peak gain estimation," Conf. Proc. IEEE Appl. Power Electron. Conf. Expo. APEC, pp. 1286–1291, 2012, doi: 10.1109/APEC.2012.6165984.
- [35] L. Sahaya Senthamil, P. Ponvasanth, and V. Rajasekaran, "Design and implementation of LLC resonant half bridge converter," IEEE-International Conf. Adv. Eng. Sci. Manag. ICAESM-2012, pp. 84–87, 2012.
- [36] Nam, R. Dougal, and E. Santi, "Optimal design method for series LCLC resonant converter based on analytical solutions for voltage gain resonant peaks," in 2013 Twenty-Eighth Annual IEEE Applied Power Electronics Conference and Exposition.
- [37] W. S. Lee, J. H. Kim, J. Y. Lee, and I. O. Lee, "Design of an Isolated DC/DC Topology with High Efficiency of over 97% for EV Fast Chargers," IEEE Trans. Veh. Technol., vol. 68, no. 12, pp. 11725–11737, 2019, doi: 10.1109/TVT.2019.2949080.
- [38] H. Wang and A. Khaligh, "Comprehensive topological analyses of isolated resonant converters in PEV battery charging applications," in 2013 IEEE Transportation Electrification Conference and Expo (ITEC), 2013, pp. 1–7.
- [39] S. Hu, J. Deng, C. Mi, and M. Zhang, "Optimal design of line level control resonant converters in plug-in hybrid electric vehicle battery chargers," IET Electr. Syst. Transp., vol. 4, no. 1, pp. 21–28, 2014, doi: 10.1049/iet-est.2013.0016.
- [40] P. He and A. Khaligh, "Comprehensive Analyses and Comparison of 1 kW Isolated DC-DC Converters for Bidirectional EV Charging Systems," IEEE Trans. Transp. Electrif., vol. 3, no. 1, pp. 147–156, 2017, doi: 10.1109/TTE.2016.2630927.
- [41] F. Shang, G. Niu, and M. Krishnamurthy, "Design and Analysis of a High-Voltage-Gain Step-Up Resonant DC-DC Converter for Transportation Applications," IEEE Trans. Transp. Electrif., vol. 3, no. 1, pp. 157–167, 2017, doi: 10.1109/TTE.2017.2656145.
- [42] F. Costa, G. Buticchi, and M. Liserre, "Highly Efficient and Reliable SiC-Based DC-DC Converter for Smart Transformer," IEEE Trans. Ind. Electron., vol. 64, no. 10, pp. 8383–8392, 2017, doi: 10.1109/TIE.2017.2696481.
- [43] T. Outeiro and A. Carvalho, "Design, implementation and experimental validation of a DC-DC resonant converter for PEM fuel cell applications," IECON Proc. (Industrial Electron. Conf., pp. 619–624, 2013, doi: 10.1109/IECON.2013.6699206.
- [44] J. M. Jo, Y. J. Han, C. Y. Lee, A. J. H. Lee, and H. S. Jeong, "Analysis on the half bridge resonant DC to DC converter for electrical multiple units train set," Int. Conf. Control. Autom. Syst., no. Iccas, pp. 424–426, 2013, doi: 10.1109/ICCAS.2013.6704006.
- [45] V. Suel and S. Kizir, "A Comprehensive Loss Analysis of Half-Bridge LLC Resonant Converter used in LED Street Lights," 2019 IEEE 1st Glob. Power, Energy Commun. Conf. GPECOM 2019, pp. 146–151, 2019, doi:10.1109GPECOM.2019.8778526.
- [46] J. Yu, "Application of Series Resonant Converters in Laser Power Supply," in 2010 International Conference on Electrical and Control Engineering, pp. 3377–3380.

- [47] T. Outeiro, H. Suryawanshi, and G. Buja, "Resonant power converters applications: LsCsLpCp circuit for renewable energy sources as case study," IECON Proc. (Industrial Electron. Conf., pp. 5651–5656, 2016, do:10.1109/IECON.2016.7793416.
- [48] S. M. Tayebi, H. Hu, O. Abdel-Rahman, and I. Batarseh, "Design and analysis of a dual-input single-resonant tank LLC converter for PV applications," Conf. Proc. IEEE Appl. Power Electron. Conf. Expo. APEC, vol. 2018–March, pp. 476–483, 2018, doi: 10.1109/APEC.2018.8341054.
- [49] C. G. Dincan et al., "Design of a High-Power Resonant Converter for DC Wind Turbines," IEEE Trans. Power Electron., vol. 34, no. 7, pp. 6136–6154, 2019, doi: 10.1109/TPEL.2018.2876320.
- [50] G. Healy and T. Wang, "A novel design for a 3.6kW LLC transformer with tight tolerance, primary side concentrated leakage inductance to replace a discrete resonant inductor for improved EV/HEV on board charger performance," PCIM Eur. Conf. Proc., no. May, pp. 1346–1350, 2019.
- [51] Z. Hu, L. Wang, H. Wang, Y. Liu and P. C. Sen, "An Accurate Design Algorithm for LLC Resonant Converters—Part I," in *IEEE Transactions on Power Electronics*, vol. 31, no. 8, pp. 5435-5447, Aug. 2016.
- [52] Z. Hu, L. Wang, Y. Qiu, Y. Liu and P. C. Sen, "An Accurate Design Algorithm for LLC Resonant Converters—Part II," in *IEEE Transactions on Power Electronics*, vol. 31, no. 8, pp. 5448-5460, Aug. 2016
- [53] Moradewicz, A & Kazmierkowski, M.P.. (2009). High efficiency contactless energy transfer system with power electronic resonant converter. Bulletin of the Polish Academy of Sciences: Technical Sciences. 57. 10.2478/v10175-010-0141-0
- [54] Wenjin, Sun & Wu, Hongfei & Hu, Haibing & Xing, Yan. (2015). Resonant Tank Design Considerations and Implementation of a LLC Resonant Converter with a Wide Battery Voltage Range. Journal of power electronics. 15. 1446-1455. 10.6113/JPE.2015.15.6.1446.
- [55] T. Dragicevic, P. Wheeler, and F. Blaabjerg, "Artificial intelligence aided automated design for reliability of power electronic systems," IEEE Trans. Power Electron., vol. 34, no. 8, pp. 7161–7171, 2019.
- [56] N. Srinivas and K. Deb, "Multi objective optimization using no dominated sorting in genetic algorithms," Evol. Comput., vol. 2, no. 3, pp. 221–248, 1994.
- [57] M. S. Mohammed and R. A. Vural, "NSGA-II + FEM based loss optimization of three phase transformer," IEEE Trans. Ind. Electron., vol. 66, no. 9, pp.7417-7425, 2019.
- [58] B. Lee and H. Cha, "Comparative Analysis of Charging Modes of Series-Resonant Converter for an Energy Storage Capacitor," in IEEE Transactions on Plasma Science, vol. 41, no. 3, pp. 570-577, 2013.
- [59] H. B. Kotte, R. Ambatipudi and K. Bertilsson, "High speed series resonant converter (SRC) using multilayered coreless printed circuit board (PCB) step-down power

- transformer," IEEE 33rd International Telecommunications Energy Conference, Amsterdam, pp. 1-9, 2011.
- [60] Q. Li and P. Wolfs, "The power loss optimization of a current fed ZVS two-inductor boost converter with a resonant transition gate drive," IEEE Trans. Power Electron., vol. 21, no. 5, pp. 1253–1263, 2006.
- [61] M. S. Mohammed, R. A. Vural, "A high efficiency design of PV-array dimension optimization for shaded and non-shaded configuration," 2019 IEEE GCAT, 2019 IEEE Global Conference for Advancement in Technology, Bangalore, India, 2019
- [62] H. A. Cabral and M. T. De Melo, "Using genetic algorithms for device modeling," IEEE Trans. Magn., vol. 47, no. 5, pp. 1322–1325, 2011, doi: 10.1109/TMAG.2010.2099107.
- [63] T. Bendib and F. Djeffal, "Electrical performance optimization of nanoscale double-gate MOSFETs using multiobjective genetic algorithms," IEEE Trans. Electron Devices, vol. 58, no. 11, pp. 3743–3750, 2011, doi: 10.1109/TED.2011.2163820.
- [64] Z. Q. Jiang, J. X. Jin, L. H. Zheng, and Z. H. Wu, "HTS Field Coil Optimization for Large Capacity Generators," IEEE Trans. Appl. Supercond., vol. 26, no. 7, pp. 1–5, 2016, doi: 10.1109/TASC.2016.2594947.
- [65] J. Gao, L. Dai, and W. Zhang, "Improved Genetic Optimization Algorithm with Subdomain Model for Multi-objective Optimal Design of SPMSM," CES Trans. Electr. Mach. Syst., vol. 2, no. 1, pp. 160–165, 2018.
- [66] J. Yan et al., "Output current optimization for multibrick parallel discharge drivers based on genetic algorithm," IEEE Trans. Plasma Sci., vol. 47, no. 6, pp. 3015–3025, 2019, doi: 10.1109/TPS.2019.2899031.
- [67] K. C. Wong, "Evolutionary algorithms: Concepts, designs, and applications in bioinformatics," Nature-Inspired Comput. Concepts, Methodol. Tools, Appl., vol. 1–3, pp. 111–137, 2016, doi: 10.4018/978-1-5225-0788-8.ch006.
- [68] A. E. Eiben and J. E. Smith, Natural Computing Series Introduction to Evolutionary Computing. 2015.
- [69] S. Editors et al., Differential Evolution APractical Approach to Global Optimization. Germany: Leiden Center for Natural Computing C N C Advisory, 2005.
- [70] I. Guerra-Gómez, E. Tlelo-Cuautle, T. McConaghy, and G. Gielen, "Optimizing current conveyors by evolutionary algorithms including differential evolution," 2009 16th IEEE Int. Conf. Electron. Circuits Syst. ICECS 2009, pp. 259–262, 2009, doi: 10.1109/ICECS.2009.5410989.
- [71] Z. H. Zhan and J. Zhang, "Differential evolution for power electronic circuit optimization," TAAI 2015 2015 Conf. Technol. Appl. Artif. Intell., pp. 158–163, 2016, doi: 10.1109/TAAI.2015.7407129.
- [72] L. M. Zheng, S. X. Zhang, S. Y. Zheng, and Y. M. Pan, "Differential Evolution Algorithm with Two-Step Subpopulation Strategy and Its Application in Microwave Circuit

- Designs," IEEE Trans. Ind. Informatics, vol. 12, no. 3, pp. 911–923, 2016, doi: 10.1109/TII.2016.2535347.
- [73] M. O. Akinsolu, B. Liu, V. Grout, P. I. Lazaridis, M. E. Mognaschi, and P. Di Barba, "A Parallel Surrogate Model Assisted Evolutionary Algorithm for Electromagnetic Design Optimization," IEEE Trans. Emerg. Top. Comput. Intell., vol. 3, no. 2, pp. 93–105, 2019, doi: 10.1109/tetci.2018.2864747.
- [74] B. N. Thakkar and V. H. Nayak, "Automatic design of low power CMOS buffer-chain circuit using differential evolutionary algorithm and particle swarm optimization," 2017 Int. Conf. Algorithms, Methodol. Model. Appl. Emerg. Technol. ICAMMAET 2017, vol. 2017–Janua, pp. 1–5, 2017, doi: 10.1109/ICAMMAET.2017.8186702.
- [75] Y. Yusoff, M. S. Ngadiman, and A. M. Zain, "Overview of NSGA-II for optimizing machining process parameters," Procedia Eng., vol. 15, pp. 3978–3983, 2011, doi: 10.1016/j.proeng.2011.08.745.
- [76] K. Deb, S. Agrawal, A. Pratap, and T. Meyarivan, "A fast elitist non-dominated sorting genetic algorithm for multi-objective optimization: NSGA-II," Lect. Notes Comput. Sci. (including Subser. Lect. Notes Artif. Intell. Lect. Notes Bioinformatics), vol. 1917, pp. 849–858, 2000, doi: 10.1007/3-540-45356-3_83.
- [77] V. S. Ghomsheh, M. A. Khanehsar, and M. Teshnehlab, "Improving the non-dominate sorting genetic algorithm for multi-objective optimization," Proc. CIS Work. 2007, 2007 Int. Conf. Comput. Intell. Secur. Work., pp. 89–92, 2007, doi: 10.1109/cisw.2007.4425453.
- [78] T. C. Bora, L. Lebensztajn, and L. D. S. Coelho, "Non-Dominated sorting genetic algorithm based on reinforcement learning to optimization of broad-band reflector antennas satellite," IEEE Trans. Magn., vol. 48, no. 2, pp. 767–770, 2012, doi: 10.1109/TMAG.2011.2177076.
- [79] O. B. Kchaou, A. Sallem, P. Pereira, M. Fakhfakh, and M. H. Fino, "Multi-objective sensitivity-based optimization of analog circuits exploiting NSGA-II front ranking," 2015 Int. Conf. Synth. Model. Anal. Simul. Methods Appl. to Circuit Des. SMACD 2015, pp. 1–4, 2015, doi: 10.1109/SMACD.2015.7301696.
- [80] M. T. Jensen, "Reducing the run-time complexity of multiobjective EAs: The NSGA-II and other algorithms," IEEE Trans. Evol. Comput., vol. 7, pp. 502–515, 2003.
- [81] J. López-Arredondo, E. Tlelo-Cuautle, and F. V. Fernández, "Optimization of LDO voltage regulators by NSGA-II," 2016 13th Int. Conf. Synth. Model. Anal. Simul. Methods Appl. to Circuit Des. SMACD 2016, pp. 4–7, 2016, doi: 10.1109/SMACD.2016.7520743.
- [82] K. J. Bathe, Finite Element Procedures. 1996.
- [83] Q. Yu and T. W. Holmes, "A study on stray capacitance modeling of inductors by using the finite element method," IEEE Trans. Electromagn. Compat., vol. 43, no. 1, pp. 88–93, 2001, doi: 10.1109/15.917948.

- [84] T. Tsuchiya, Y. Kagawa, N. Wakatsuki, and H. Okamura, "Finite element simulation of piezoelectric transformers," IEEE Trans. Ultrason. Ferroelectr. Freq. Control, vol. 48, no. 4, pp. 872–878, 2001, doi: 10.1109/58.935703.
- [85] M. Zhu, E. Worthington, and J. Njuguna, "Analyses of power output of piezoelectric energy-harvesting devices directly connected to a load resistor using a coupled piezoelectric-circuit finite element method," IEEE Trans. Ultrason. Ferroelectr. Freq. Control, vol. 56, no. 7, pp. 1309–1318, 2009, doi: 10.1109/TUFFC.2009.1187.
- [86] M. A. Tsili, A. G. Kladas, P. S. Georgilakis, A. T. Souflaris, and D. G. Paparigas, "Geometry optimization of magnetic shunts in power transformers based on a particular hybrid finite-element boundary-element model and sensitivity analysis," IEEE Trans. Magn., vol. 41, no. 5, pp. 1776–1779, 2005, doi: 10.1109/TMAG.2005.846075.
- [87] H. Zhang et al., "Dynamic deformation analysis of power transformer windings in short-circuit fault by FEM," IEEE Trans. Appl. Supercond., vol. 24, no. 3, pp. 1–4, 2014, doi: 10.1109/TASC.2013.2285335.
- [88] S. V. Kulkarni and G. B. Kumbhar, "Analysis of short circuit performance of splitwinding transformer using coupled field-circuit approach," 2007 IEEE Power Eng. Soc. Gen. Meet. PES, vol. 22, no. 2, pp. 936–943, 2007, doi: 10.1109/PES.2007.385827.
- [89] C. Deline, N. Renewable, and S. Janzou, "A simplified model of uniform shading in large photovoltaic arrays," Solar Energy/Elsevier, vol. 96, pp.274–282, October 2013.
- [90] J. R. P. Gallardo, "Ecodesign of large-scale photovoltaic (PV) systems with multiobjective optimization and Life-Cycle Assessment (LCA) ",PhD. Thesis, France, 2013.
- [91] H. Hassanzadehfard, S. M. Moghaddas-tafreshi, and S. M. Hakimi, "Optimization of grid-connected microgrid consisting of PV / FC / UC with," Turkish Journal of Electrical Engineering and Computer Sciences, vol. 23(1), pp. 1–16, 2015.
- [92] V. Dabra, K. K. Paliwal, P. Sharma, and N. Kumar, "Optimization of photovoltaic power system: a comparative study," Protection and Control of Modern Power Systems, vol. 2:3, pp. 1–11, 2017.
- [93] E. Lodhi, R. N. Shafqat, and K. D. E. Kerrouche, "Application of Particle Swarm Optimization for Extracting Global Maximum Power Point in PV System under Partial Shadow Conditions," International Journal of Electronics and Electrical Engineering, vol. 5, no. 3, pp. 223–229, 2017.
- [94] J. C. Teo, R. H. G. Tan, V. H. Mok, and V. K. Ramachandaramurthy, "Effects of bypass diode configurations to the maximum power of photovoltaic module," International Journal of Smart Grid and Clean Energy, vol. 6, no. 4, pp. 225–232, 2017.

- [95] J. C. Teo, R. H. G. Tan, and C. Tan, "Impact of Partial Shading on the P-V Characteristics and the Maximum Power of a Photovoltaic String," Energies, vol. 11, pp. 1-22, 2018.
- [96] E. O. Shaughnessy, D. Cutler, K. Ardani, and R. Margolis, "Solar plus: Optimization of distributed solar PV through battery storage and dispatchable load in residential buildings," Applied Energy/Elsevier, vol. 213, December 2017, pp. 11–21, 2018.
- [97] A. S. Aziz, M. Faridun, N. Tajuddin, M. R. Adzman, M. A. M. Ramli, and S. Mekhilef, "Energy Management and Optimization of a PV / Diesel / Battery Hybrid Energy System Using a Combined Dispatch Strategy," Sustainability, MDPI, Open Access Journal, vol. 11(3), pp. 1-26, 2019.
- [98] M. H. Shams, M. Kia, A. Heidari, and D. Zhang, "Optimal design of photovoltaic solar systems considering shading effect and hourly radiation using a modified PSO algorithm," Simulation: Transactions of the Society for Modeling and Simulation International, no. March, pp. 1-9, 2019.
- [99] "Trinasolar PV Panel." [Online]. Available: https://static.trinasolar.com/sites/default/files/PC05_05_Datasheet_35mm_EN.pd f.
- [100] "Weather Conditions." [Online]. Available: http://www.energy-designtools.aud.ucla.edu/climate-consultant/.
- [101] K. Deb, S. Agrawal, A. Pratap, and T. Meyarivan, "A Fast Elitist Non-Dominated Sorting Genetic Algorithm for Multi-Objective Optimization: NSGA-II," Parallel Problem Solving from Nature PPSN VI. PPSN 2000. Lecture Notes in Computer Science, vol. 1917, pp.849-858, 2000.
- [102] M. S. Mohammed and R. A. Vural, "NSGA-II + FEM Based Loss Optimization of Three Phase Transformer," IEEE Transactions on Industrial Electronics, vol. 66, no. 9, pp.7417-7425, 2019.
- [103] K. Lamamra, K. Belarbi, A. Belhani, and S. Boukhtini, "NSGA2 based of multicriteria decision analysis for multi-objective optimization of fuzzy logic controller for non linear system," Journal of Next Generation Information Technology •, vol. 5(1), no. December 2015, pp.57-64, 2014.
- [104] E. I. Amoiralis, M. A. Tsili and A. G. Kladas, "Transformer design and optimization: a literature survey," IEEE Transactions on Power Delivery, vol. 24, no. 4, pp. 1999-2024, Oct. 2009.
- [105] L. J. Rivera and D. J. Tylavsky, "Acceptability of four transformer top-oil thermal models—Part II: Comparing metrics," IEEE Transactions on Power Delivery, vol. 23, no. 2, pp. 866–872, Apr. 2008.
- [106] N. D. Doulamis, A. D. Doulamis, P. S. Georgilakis, S. D. Kollias, and N. D. Hatziargyriou" A synergetic neural network-genetic scheme for optimal transformer construction," Integrated Computer-Aided Engineering, vol. 9, no. 1, pp. 37-56, Dec. 2002.

- [107] N. D. Doulamis and A. D. Doulamis, "Optimal distribution transformers assembly using an adaptable neural network-genetic algorithm scheme," Proc. IEEE Int. Conf. Systems, Man Cybernetics, vol. 5, pp. 6, 2002.
- [108] T. H. Pham, S. J. Salon, and S. R. H. Hoole, "Shape optimization of windings for minimum losses," IEEE Transactions on Magnetics, vol. 32, no. 5, pp. 4287–4289, Sept. 1996.
- [109] L. Hui, H. Li, H. Bei, and Y. Shunchang, "Application research based on improved genetic algorithm for optimum design of power transformers," 5th Int. Conf. Electrical Machines and Systems, pp. 242–245, 2001.
- [110] J. H. Harlow, Electric power transformer engineering, ser. the electric power engineering, Boca Raton, FL: CRC, ch. 2, pp. 28-29, 2004.
- [111] C. Nussbaum, H. Pfützner, T. Booth, N. Baumgartinger, A. Ilo, and M.Clabian, "Neural networks for the prediction of magnetic transformer core characteristics," IEEE Transactions on Magnetics, vol. 36, no. 1, pp. 313–329, Jan. 2000.
- [112] P. S. Georgilakis, N. D. Hatziargyriou, N. D. Doulamis, A. D. Doulamis, and S. D. Kollias, "Prediction of iron losses of wound core distribution transformers based on artificial neural networks," Neurocomput., vol. 23, pp. 15–29, Dec. 1998.
- [113] P. S. Georgilakis, "Spotlight on modern transformer design," London, U.K., Springer, 2009.
- [114] E. I. Amoiralis, M. A. Tsili and A. G. Kladas, "Global transformer design optimization using deterministic and non-deterministic algorithms," Electrical and Computer Engineering, National Technical University of Athens, : IEEE Industry Applications Society, vol. 50, no. 1, pp. 383-394, Jan.-Feb. 2014.
- [115] O. Eseosa and S.O. Oboma, "Review of intelligent based optimization techniques in power transformer design," Nigeria Applied Research Journal, vol. 1, no. 2, pp.80-90, ISSN: 2423-4796, April, 2015.
- [116] H. D. Mehta and R. M. Patel, "A review on transformer design optimization and performance analysis using artificial intelligence techniques," International Journal of Science and Research (IJSR), vol. 3, no. 9, pp. 2319-7064, Sept. 2014.
- [117] H. D. Mehta and R. M. Patel, "Optimal design of transformer using tournament selection based elitist genetic algorithms," Indian Journal of Science and Technology, vol. 8, no. 12, pp. 0974-5645, Jun. 2015.
- [118] K. D. Hoang and J. Wang, "Design optimization of high frequency transformer for dual active bridge DC-DC converter," XXth International Conference on Electrical Machines (ICEM), Marseille, France. IEEE, pp. 2311-2317, 02–05 Sept. 2012.
- [119] I. Dolapchiev , K. Brandisky and P. Ivanov," Eddy current testing probe optimization using a parallel genetic algorithm," Serbian Journal Of Electrical Engineering, vol. 5, no. 1, pp. 39-48, May 2008.

- [120] T. D. Kefalas, P. S. Georgilakis, A. G. Kladas, A. T. Souflaris, and D. G. Paparigas, "Multiple grade lamination wound core: A novel technique for transformer iron loss minimization using simulated annealing with restarts and an anisotropy model," IEEE Transactions on Magnetics, vol. 44, no. 6, pp. 1082–1085, Jun. 2008.
- [121] E. I. Amoiralis, M.A. Tsili, P.S. Georgilakis, A.G. Kladas, and A.T. Souflaris, "A parallel mixed integer programming-finite element method technique for global design optimization of power transformers," IEEE Transactions on magnetics, vol. 44, no. 6, pp. 1022-1025, June 2008.
- [122] E. I. Amoiralis, P. S. Georgilakis, M. A. Tsili, and A.G. Kladas, "Global transformer optimization method using evolutionary design and numerical field computation," IEEE Transactions on Magnetic, vol. 45, no. 3, pp. 1720-1723, Marh 2009.
- [123] R. Storn, "Differential evolution design of an IIR-filter", IEEE International Conference on Evolutionary Computation, Japan, 1996.
- [124] H. A. Abbass, R. Sarker and C. Newton ,"PDE: a Pareto-frontier differential evolution approach for multi-objective optimization problems", Congress on evolutionary computation IEEE, n. 01TH8546, Seoul, South Korea , 27-30 May 2001.
- [125] H. R. Cai, C. Y. Chung and K. P. Wong ,"Application of differential evolution algorithm for transient stability constrained optimal power flow", IEEE Transactions on Power Systems, vol. 23, no. 2, pp. 719-728, May 2008.
- [126] A. K. Qin, V. L. Huang and P. N. Suganthan ,"Differential evolution algorithm with strategy adaptation for global numerical optimization", IEEE Transactions on Evolutionary Computation, vol. 13, no. 2, pp. 398-417, Apr. 2009.
- [127] M. Varadarajan and K. S. Swarup, "Differential evolutionary algorithm for optimal reactive power dispatch", International Journal of Electrical Power & Energy Systems, vol. 30, no. 8, pp. 435-441, Oct. 2008.
- [128] S. Sayah and K. Zehar, "Modified differential evolution algorithm for optimal power flow with non-smooth cost functions", Energy Conversion and Management, vol. 49, no. 11, pp. 3036-3042, 2008.
- [129] D. Phaengkieo and S. Ruangsinchaiwanich, "Design optimization of electrical transformer using genetic algorithm," 2014 17th International Conference on Electrical Machines and Systems (ICEMS), electronic ISBN: 978-1-4799-5162-8, 22-25 Oct., Thailand, 2014.
- [130] R. Escarela-Perez, S. V. Kulkarni, N. K. Kodela, and J. C. Olivares-Galvan, "Asymmetry during load-loss measurement of three-phase three-limb transformers," IEEE Transactions on Power Delivery, vol. 22, no. 3, pp. 1566–1574, Jul. 2007.
- [131] J. Liu and V. Dinavahi ,"Detailed magnetic equivalent circuit based real-time nonlinear power transformer model on FPGA for electromagnetic transient

- studies ".IEEE Transactions on Industrial Electronics, vol. 63, no. 2, pp. 1191-1202, Feb. 2016.
- [132] H. S. Kim, J.H. Jung, J.W. Baek, and H.J. Kim, "Analysis and design of a multioutput converter using asymmetrical PWM half-bridge flyback converter employing a parallel-series transformer", IEEE Transactions on Industrial Electronics, vol. 60, no. 8, 2013.
- [133] H. Keyhani, H. A. Toliyat, M. Harfman-Todorovic, R. Lai, and R. Datta,"An isolated resonant AC-link three-phase AC-AC converter using a single HF transformer", IEEE Transactions on Industrial Electronics, vol. 61, no. 10, pp. 5174 5183, Oct. 2014.
- [134] D. E. Goldberg, "Genetic Algorithms in search, optimization and machine learning," Reading, MA: Addison-Wesley, 1989.
- [135] R. Storn and K. Price," Differential evolution a simple and efficient heuristic for global optimization over continuous spaces", vol. 11, no. 4, pp. 341–359, Dec. 1997.
- [136] N. Srinivas and K. Deb, "Multi objective optimization using non-dominated sorting in genetic algorithms," Evolutionary Computation, vol. 2, no. 3, pp. 221-248, 1994.
- [137] K. Deb, "Genetic algorithms in multimodal function optimization," MS Thesis and TCGA Report No. 89002, Tuscaloosa: University of Alabama, The Clearinghouse for Genetic Algorithms, 1989.
- [138] D. E. Goldberg and J. Richardson, "Genetic algorithms with sharing for multimodal function optimization," in Proc. of the Second International Conference on Genetic Algorithms and Their Application. Hillsdale, NJ, USA: L. Erlbaum Associates Inc., pp. 41–49, July 28-31, 1987.
- [139] K. Deb, S. Agrawal and A. Pratap and T. Meyarivan, "A fast elitist non-dominated sorting genetic algorithm for multi-objective optimization: NSGA-II," PPSN VI Proceedings of the 6th International Conference on Parallel Problem Solving from Nature, pp. 849-858, Sep. 18 20, 2000.
- [140] K. Deb and A. Pratap and S. Agarwal and T. Meyarivan, "A fast and elitist multi objective genetic algorithm: NSGA–II," IEEE Transactions on Evolutionary Computation, vol. 6, no. 2, pp. 182-197, Apr. 2002.
- [141] X. Guan, "Multi-objective PID Controller Based on NSGA-II algorithm with application to main stream temperature control", International Conference on Artificial Intelligence and Computational Intelligence, Shanghai, China, 7-8 Nov. 2009.
- [142] S. Chaine, M. Tripathy and S. Satpathy, "NSGA-II based optimal control scheme of wind thermal power system for improvement of frequency regulation characteristics," Ain Shams Engineering Journal, vol. 6, no. 3, pp. 851-863, Egypt, Sep. 2015.
- [143] B. Tomoiagă, M. Chindriş, A. Sumper, A. Sudria-Andreu and R. Villafafila-Robles, "Pareto optimal reconfiguration of power distribution systems using a genetic

- algorithm based on NSGA-II," Electrical Power Distribution Networks Conference (EPDC), Conference on Energies, pp. 1439-1455, March 2013.
- [144] S. De, S. Bhattacharyya and S. Chakraborty "Application of pixel intensity based medical image segmentation using NSGA-II based OPTI MUSIG activation function," Int. Conference on Computational Intelligence and Communication Networks (ICCICN), 2014.
- [145] N. J. da S. Lima, C. J. A. Bastos-Filho, D. R. B. Araújo, "Boolean operators to improve multi-objective evolutionary algorithms for designing optical networks," Journal of Microwaves, Optoelectronics and Electromagnetic Applications, vol. 15, no. 4, pp.319-332, 2016.
- [146] V. Sarac and G.Galvincev "Application of numerical methods in calculation of electromagnetic in electrical machines," Scientific Proceedings XI International Congress "Machine, Technologies, Materials", vol. 1, pp.33-36, 2014.
- [147] O. C. Zienkiewicz, The finite element method in structural and continuum mechanics, 5th ed., vol. 2, Butterworth-Heinemann, London 2000.
- [148] I. Babuska and A. K. Aziz, "Survey lectures on the mathematical foundations of the finite element method," Academic Press, pp. 3-636, New York, 1972.
- [149] T. K. Bhattacharya," Basic electrical technology", EE IIT, Kharagpur, 2nd ed., ch. 7, lesson 23, INDIA, 2008. [Online]. Available: http://www.nptel.ac.in.
- [150] P. S. Georgilakis, "Environmental cost of distribution transformer losses", Applied Energy, Elsevier, vol. 88, no. 9, pp. 3146-3155, 2011.
- [151] B. W. McConnell, "Increasing distribution transformer efficiency: potential for energy savings," Proc. IEEE Power Engineering Review, vol. 18, no. 7, pp. 8–10, 1998.
- [152] W.D.A.S. Wijayapala, S.R.K. Gamage and H.M.S.L.G. Bandara, "Determination of capitalization values for no load loss and load loss in distribution transformers," Journal of the Institution of Engineers, Sri Lanka, vol. 49, no. 03, pp. 11-20, Aug. 2016.
- [153] T. Labella et al., "A bidirectional-switch-based wide-input range high-efficiency isolated resonant converter for photovoltaic applications," IEEE Trans. Power Electron., vol. 29, no. 7, pp. 3473–3484, 2014.
- [154] A. Soto, J. Cortes, and F. Pascual, "Dynamic modeling of the series resonant converter operating in discontinuous conduction mode and its application in space," 11th European Space Power Conference, 2017.
- [155] Y. Nour, A. Knott and L. P. Petersen, "High frequency soft switching half bridge series-resonant dc-dc converter utilizing gallium nitride FETs," 2017 19th European Conference on Power Electronics and Applications (EPE'17 ECCE Europe), Warsaw, pp. 1-7, 2017.
- [156] S. R. Jang, H. J. Ryoo, J. S. Kim and S. H. Ahn, "Design and analysis of series resonant converter for 30kW industrial magnetron," IECON 36th Annual

- Conference on IEEE Industrial Electronics Society, Glendale, AZ, USA, pp. 415-420, 2010.
- [157] C. Tai and C. Chen, "The design of a half-bridge series-resonant type heating system for magnetic nanoparticle thermotherapy," Piers Online, vol. 4, no. 2, pp. 276–280, 2008.
- [158] Y. Jang, M. M. Jovanovi, J. M. Ruiz, and G. Liu, "Series-Resonant converter with reduced- frequency-range control," IEEE Applied Power Electronics Conference and Exposition, pp. 1453–1460, 2015.
- [159] B. Amghar, A. Darcherif, J. Barbot, and D. Boukhetala, "Modeling and control of series resonant converter for high voltage applications," 2014 IEEE International Energy Conference (ENERGYCON), Cavtat, Croatia, p. pp.216-221, 2014.
- [160] D. U. Ike, A. U. Adoghe, and A. Abdulkareem, "Analysis of telecom base stations powered by solar energy," International Journal of Scientific & Technology Research, vol. 3, no. 4, pp. 369–374, 2014.
- [161] M. H. Alsharif and J. Kim, "Optimal solar power system for remote telecommunication base stations: a case study based on the characteristics of South Korea Solar Radiation Exposure," Sustainability, vol. 8, pp. 1–21, 2016.
- [162] T. Dragicevic, P. Wheeler, and F. Blaabjerg, "Artificial intelligence aided automated design for reliability of power electronic systems," IEEE Trans. Power Electron., vol. 34, no. 8, pp. 7161–7171, 2019.
- [163] A.R. Yilmaz and B. Erkmen,"FPGA Based Space Vector PWM and Closed Loop Controllers Design for Z Source Inverter" IEEE Access, vol.7, pp. 130865-130873, 2019.
- [164] F. Blaabjerg, Z. Chen, and S. Kjaer, "Power electronics as efficient interface in dispersed power generation systems," IEEE Trans. Power Electron., vol. 19, no. 5, pp. 1184–1194, 2004.
- [165] Z. Hu, L. Wang, H. Wang, Y. Liu, P. C. Sen, and L. Fellow, "An accurate design algorithm for llc resonant converters Part I," IEEE Trans. Power Electron., vol. 31, no. 8, pp. 5435–5447, 2016.
- [166] Z. Hu, L. Wang, Y. Qiu, and S. Member, "An accurate design algorithm for llc resonant converters Part II," IEEE Trans. Power Electron., vol. 31, no. 8, pp. 5448–5460, 2016.
- [167] X. Qi, Y. Peng, and Y. Li, "Parameters design of series resonant inverter circuit," International Conference on Applied Physics and Industrial Engineering, Physics Procedia, vol. 24, pp. 133–138, 2012.
- [168] G. Alpa, S. M.T., and P. Vinod, "Topology selection, design and simulation of 300W resonant dc-dc converter," International Journal on Emerging Technologies, vol. 1, no. 1, pp. 57–60, 2010.

- [169] M. S. Mohammed, R. A. Vural, "A high efficiency design of PV-array dimension optimization for shaded and non-shaded configuration," 2019 IEEE GCAT, 2019 IEEE Global Conference for Advancement in Technology, Bangalore, India, 2019
- [170] D. E. Goldberg, "Genetic Algorithms in Search, Optimization and Machine Learning," Reading, MA, USA: Addison-Wesley, 1989.
- [171] R. Storn and K. Price, "Differential evolution a simple and efficient heuristic for global optimization over continuous spaces," J.Global Optim., vol. 11, no. 4, pp. 341–359, Dec. 1997.
- [172] N. Srinivas and K. Deb, "Multi objective optimization using no dominated sorting in genetic algorithms," Evol. Comput., vol. 2, no. 3, pp. 221–248, 1994.
- [173] M. S. Mohammed and R. A. Vural, "NSGA-II + FEM based loss optimization of three phase transformer," IEEE Trans. Ind. Electron., vol. 66, no. 9, pp.7417-7425, 2019.
- [174] B. Lee and H. Cha, "Comparative Analysis of Charging Modes of Series-Resonant Converter for an Energy Storage Capacitor," in IEEE Transactions on Plasma Science, vol. 41, no. 3, pp. 570-577, 2013.
- [175] H. B. Kotte, R. Ambatipudi and K. Bertilsson, "High speed series resonant converter (SRC) using multilayered coreless printed circuit board (PCB) stepdown power transformer," IEEE 33rd International Telecommunications Energy Conference, Amsterdam, pp. 1-9, 2011.
- [176] Q. Li and P. Wolfs, "The power loss optimization of a current fed ZVS two-inductor boost converter with a resonant transition gate drive," IEEE Trans. Power Electron., vol. 21, no. 5, pp. 1253–1263, 2006.
- [177] D. Dc, Q. Li, and P. Wolfs, "A review of the single phase photovoltaic module integrated converter topologies with three different dc link configuration," IEEE Trans. Power Electron., vol. 23, no. 3, pp. 1320–1333, 2008.
- [178] M. Castilla et al., "Linear current control scheme with series resonant harmonic compensator for single-phase grid-connected photovoltaic inverters," IEEE Trans. Ind. Electron., vol. 55, pp. 2724–2733, 2008.
- [179] W. Li and X. He, "Review of nonisolated high-step-up dc / dc converters in photovoltaic grid-connected applications," IEEE Trans. Ind. Electron., vol. 58, no. 4, pp. 1239–1250, 2011.
- [180] D. Jung, Y. Ji, S. Park, Y. Jung, and C. Won, "Interleaved soft-switching boost converter for photovoltaic power-generation system," IEEE Trans. Power Electron., vol. 26, no. 4, pp. 1137–1145, 2011.
- [181] J. T. Stauth, M. D. Seeman, and K. Kesarwani, "A resonant switched-capacitor ic and embedded system for sub-module photovoltaic power management," IEEE J. Solid-State Circuits, vol. 47, no. 12, pp. 3043–3054, 2012.
- [182] W. Choi, "High-Efficiency dc dc converter with fast dynamic response for low-voltage photovoltaic sources," IEEE Trans. Power Electron., vol. 28, no. 2, pp. 706–716, 2013.

- [183] J. T. Stauth, M. D. Seeman, and K. Kesarwani, "Resonant switched-capacitor converters for sub-module distributed photovoltaic power management," IEEE Trans. Power Electron., vol. 28, no. 3, pp. 1189–1198, 2013.
- [184] L. Nousiainen et al., "Photovoltaic generator as an input source for power electronic converters," IEEE Trans. Power Electron., vol. 28, no. 6, pp. 3028–3038, 2013.
- [185] Y. Chuang, Y. Ke, H.-S. Chuang, and Y.-S. Wang, "A novel single-switch resonant power converter for renewable energy generation applications," IEEE Trans. Ind. Appl., vol. 50, pp. 1322–1330, 2014.

PUBLICATIONS FROM THE THESIS

Contact Information: Mohammed_sami9@yahoo.com

Papers

- 1. M. S. Mohammed and R. A. Vural, "NSGA-II+FEM Based Loss Optimization of Three-Phase Transformer," in *IEEE Transactions on Industrial Electronics*, vol. 66, no. 9, pp. 7417-7425, Sept. 2019, doi: 10.1109/TIE.2018.2881935. Published
- 2. M. S. Mohammed and R. Acar Vural, "Evolutionary Design Automation of High Efficiency Series Resonant Converter for Photovoltaic Systems," in *IEEE Transactions on Power Electronics*, doi: 10.1109/TPEL.2020.2987086. <u>Published</u>

Conference Papers

1. Mohammed Sami Mohammed, Revna Acar Vural, "A High Efficiency Design of PV-Array Dimension Optimization for Shaded and Non-Shaded configuration", Advancement in Technology (GCAT) 2019 Global Conference for, pp. 1-5, 2019. <u>Published</u>